

Log End Image Databases: Biometric Tracking & Image Analysis

Magisterarbeit

Zur Erlangung des Titels

Magister

an der Naturwissenschaftlichen Fakultät der
Paris-Lodron-Universität Salzburg

Eingereicht von

Dipl. Ing. Rudolf Schraml

Gutachter:

Univ.-Prof. Dr. Andreas Uhl

Fachbereich:

Computerwissenschaften

Salzburg, April, 2016

Rudolf Schraml
Halleiner Landesstraße 40a
A-5061 Elsbethen

Hiermit versichere ich, dass ich die von mir vorgelegte Arbeit selbstständig verfasst habe, dass ich die verwendeten Quellen, Internet-Quellen und Hilfsmittel vollständig angegeben habe und dass ich die Stellen der Arbeit – einschließlich Tabellen, Karten und Abbildungen –, die anderen Werken oder dem Internet im Wortlaut oder dem Sinn nach entnommen sind, auf jeden Fall unter Angabe der Quelle als Entlehnung kenntlich gemacht habe.

Salzburg, 20.April 2016

Rudolf Schraml

Acknowledgement

Thanks to my girlfriend Tanja, without i would have lost the motivation for writing this thesis. I also want to thank the Austrian and German railway. The majority of this work was written in trains, probably because due to the lack of an internet connection that would have kept my attention away for senseless internet surfing.

Abstract

This diploma thesis is based on the need for testset data in the TreeBio project funded by the FWF. For this reason, a final project at the higher technical college HTL Kuchl was initialized and accompanied by me. Three pupils from the HTL Kuchl successfully processed the project in the school year 2013/14. Within this project log end images of 172 logs were captured at two different sawmills. All log end images were annotated using an annotation tool which was especially developed for this project and within this thesis. In the practical part of the project the pupils performed a statistical analysis of relationships between log end face measurements and log shape measurements. The results provide interesting insights which are valuable for log quality estimation considerations. The acquired testset data already served as basis for two scientific publications. Furthermore, the developed annotation tool has also been utilized for the annotation of further testsets and the acquired groundtruth database was utilized in most of the experiments within the TreeBio project.

keywords Biometric Log End Recognition, Cross-Section Image Analysis, Wood Log Tracking, Performance Evaluation Databases

Zusammenfassung

Ausgangspunkt für diese Diplomarbeit war das fehlen von geeigneten Testdaten für das FWF geförderte Projekt "TreeBio". Aus diesem Grund wurde an der Höheren Technischen Lehranstalt (HTL) Kuchl ein Abschlussprojekt für Schüler/innen initiiert und später als Kooperationspartner begleitet. Das Abschlussprojekt wurde von drei Schülern der HTL Kuchl im Schuljahr 2013/2014 erfolgreich durchgeführt und mit einer Abschlussarbeit sowie einer Abschlusspräsentation beendet. In diesem Abschlussprojekt wurden Stammendbilder von 172 Baumstämmen in zwei unterschiedlichen Sägewerken aufgenommen. Alle Stammendbilder wurden, mit einem eigens für das Abschlussprojekt entwickelten Annotierungstool, annotiert. Die statistische Auswertung der Zusammenhänge zwischen Stammend- und Stammformmerkmalen führt zu neuen und für die Stammqualitätsbeurteilung wertvollen Ergebnissen. Die entwickelte Annotationssoftware wurde auch für die Annotation weiterer Datensätze verwendet und die daraus resultierende Datenbank, mit Grundwahrheiten der Stammendmerkmale, wurde in fast allen Experimenten des TreeBio Projektes verwendet.

Contents

1	Introduction	1
1.1	Project - HTL Kuchl	2
I	Theoretical Background	4
2	CS-Image Analysis	6
2.1	Wood Basics	6
2.1.1	Wood Anatomy	7
2.2	CS Analysis Applications and Research	9
2.2.1	Pith estimation	10
2.2.1.1	Literature Overview	11
2.2.2	Annual ring analysis	16
2.2.2.1	Literature Overview	17
2.2.3	Further Literature on CS Analysis	22
2.2.3.1	Log Defect Detection and Analysis	22
2.2.3.1.1	Further Defects: Detection and Analysis	25
2.2.3.2	Further Wood Properties: Detection and Analysis	26
2.2.4	CS Segmentation	27

<i>CONTENTS</i>	IV
3 Traceability of Wood Logs	31
3.1 Traceability Definition	31
3.2 Log Supply Chain - LSC	31
3.3 Traceability Methods	32
3.3.1 Manual Labels	32
3.3.2 Badge Labels	33
3.3.3 Transponders	33
4 Biometric Wood Log Traceability	36
4.1 Biometric Systems	36
4.1.1 System Characteristics and Classification Categories	37
4.1.2 System Performance Evaluation	39
4.2 Research on Biometric Log Recognition	42
4.2.1 Log Shape Recognition	42
4.2.2 Log to Board Recognition	44
4.2.3 Log End Recognition	45
4.2.3.1 Literature Review	46
4.2.4 Wood Board Recognition	52
II Log End Image Analysis Project	54
5 Project Report	55
5.1 Databases for Performance Evaluation	55
5.1.1 Log End Image Database Requirements	56
5.2 Project Goals	57

<i>CONTENTS</i>	V
5.3 Project Implementation	58
5.3.1 Workpackages	58
5.4 Database Acquisition	59
5.4.1 Testset Entacher	59
5.4.2 Testset Mayr-Melnhof	60
5.5 Database Annotation	61
5.5.1 Annotated CS Properties	62
5.5.2 Annotation Software/ CrossSection Editor	62
5.5.2.1 Database	63
5.5.2.2 CS-Editor Workflow and Features	66
5.6 Statistical Analysis	75
5.6.1 Results	76
5.6.1.1 Correlation Analysis	76
5.6.1.2 Regression Analysis	78
5.6.1.2.1 RW-Length Regression Analysis	79
6 Conclusions	80
III Appendix	81
.1 Project Application HTL Kuchl	82
.2 Project Timeline	86
.3 Project Meeting Report Example	87
.4 Project Progress Report Example	89

Chapter 1

Introduction

Wood log traceability is a constraint to solve economical, ecological, social and legal issues. From an economic point of view tracking of wood logs is required to map the ownership of each log. Furthermore, in the past two decades social aspects have become more important and sustainability certificates like Pan European Forest Certification (PEFC) and Forest Stewardship Council (FSC) are a must have for all end-sellers. Regarding ecological issues, illegal logging and deforestation are driving forces of the climate change. Actions against illegal logging led to regulations like the European Timber Regulation, the U.S. Lacey Act and the Australia Illegal Logging Prohibition Act (see www.forestlegality.com).

Currently, various wood log tracking approaches exist which all show up different pros and cons for different fields of applications in the timber based industries. Such approaches range from simple methods like punching, colouring or applying batches to more sophisticated methods like DNA fingerprinting and the usage of Radio Frequency Identification Transponders (RFID) Tzoulis and Andreopoulou (2013). In the industry just approaches which rely on physically marking each log are utilized. Another approach assumes that wood logs are separable identities based on their intrinsic biometric characteristics. Investigations on the hypothesis that logs are separate entities on the basis of biometric log characteristics were presented in the works of Chiorescu and Grönlund (2003, 2004); Flodin et al. (2007, 2008a,b), which show up the high potential of biometric log recognition. The approaches presented in Chiorescu and Grönlund (2003, 2004); Flodin et al. (2008a) utilized 2D and 3D scanners to extract geometric wood properties.

On account of the fact, that wood logs offer features on their end faces in terms of annual rings, pith position, shape and dimension images log end faces can be used as biometric

characteristic for log recognition. Images containing a cross-section (CS) of a wood log are denoted as CS-Images throughout this thesis. A biometric log recognition system based on log end images could be used to track the ownership from the forest based industries to further processing companies. Another application is to discover illegally harvested tree logs based on CS-Images of their stumps Barrett (2008).

This thesis is based on the need for log end image datasets which are suited to perform investigations on the identification performance of a biometric log end recognition system. Based on that need a final project for pupils of the higher technical college HTL Kuchl was initialized and accompanied.

1.1 Project - HTL Kuchl

As graduate of the HTL Kuchl, who also had the great opportunity to conduct such a project within the last year of my secondary school education (2002-2003), we had the idea to initialize a project within the FWF project entitled *Traceability of Logs by Means of Digital Images* (FWF TRP project 254). Thanks to DI Erwin Tremml and Dr. Karl Entacher three motivated pupils confirmed to work on this project.



Figure 1.1: Project Team: Alexander Sampl, Michael Geistlinger and Michael Schober

The project officially started at the end of the school year 2012/2013 and was finished by a final presentation in Kuchl in May 2014. Based on our need for a testset database and the input/ ideas of the two project advisor's (Erwin Tremml, Karl Entacher) the goals for the project were defined:

- Create a representative database of wood log end images from different wood logs suited for research purposes.
- Annotate wood features which are visible on wood log ends.
- Elaborate dependencies between log end features and wood log anomalies which are relevant for log and wood quality assessment.

This thesis is subdivided in two parts: Part I introduces topics relevant for log end image analysis and biometric log tracking and summarizes related scientific literature. In Part II the schedule and foregoing of the conducted project as well as the gathered results are presented.

Part I

Theoretical Background

The majority of the theoretical part of this thesis was already published by myself in my master thesis (Schraml, 2013). I declare that this content is my own intellectual property (for comparison I refer to Schraml (2013)). Where appropriate, content was added, deleted, restructured and revised so that the content presents the theoretical background related to the topic of this diploma thesis.

The first part of this thesis contains a theoretical work-up related to cross-section image (CS-Image) analysis and biometric wood log tracking. First, Chapter 2 introduces different CS-Image analysis tasks and for each task a literature overview is provided. Subsequently, in Chapter 3 a possible definition for log traceability (Section 3.1 and 3.2) is introduced first and second an overview on common and state-of-the-art traceability methods (3.3) is presented. Finally, Chapter 4 introduces biometric systems (Section 4.1) and provides a structured review on research related to biometric log tracking (Section 4.2).

Chapter 2

CS-Image Analysis

The increasing industrialization of sawmills in the 1990's presented new challenges to existing processes. Requirements such as higher process speeds, better yields and lower costs contributed significantly to the development of new wood log scanning devices and algorithms for further processing the acquired data. For example, the first fast (120m/min with 190 rpm) and robust industrial CT-Scanner was developed recently within the CT Pro Project in 2010 Giudiceandrea et al. (2011, 2012). Within the project, among other things, investigations on knot detection Johansson et al. (2013); Breinig et al. (2012, 2013) and log positioning Berglund et al. (2013); Fredriksson et al. (2014b,a) were presented. Actually, a few of these scanners were produced and are already installed in sawmills, i.e. in Germany, France and Chile. Research showed that CT scanning in combination with an exact log positioning at the saw intake increases the value of each log up to about 20% Berglund et al. (2013). It can be expected that the number of sawmills equipped with a CT-Scanner increases rapidly.

CSs in log end images or CS-Images captured with a CT scanner show features which provide valuable information for log processing. First, Section 2.1 presents wood basics and introduces features visible in CS-Images. Subsequently, in Section 2.2 applications and research related to CS-Image analysis are presented.

2.1 Wood Basics

This section presents facts on wood as raw material and introduces features shown in wood log CS-Images. Although European and Austrian tree species share some basic anatomic features,

their CS surfaces can look completely different. These differences have to be considered for the development of CS-Image analysis applications.

2.1.1 Wood Anatomy

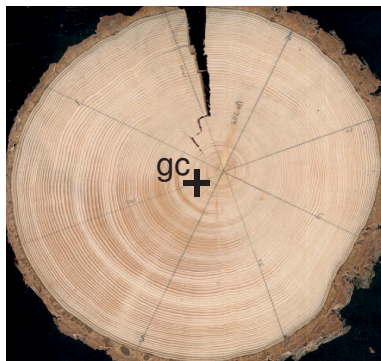
Worldwide more than thousand tree species are known. In Austria, about twenty-five tree species are of economic interest. Generally, Austrian and European tree species are subdivided into softwood and hardwood tree species. Macroscopic and microscopic features identify each tree species. Microscopically there are major differences between the anatomy of hardwood and softwood. Following, some macroscopic features and related basic information will be presented.

Standing trees can be easily classified according to their leaves. Hardwood trees typical wear broad leaves and softwood trees scale-like leaves also known as needles. These leaves are essential for the tree to grow, as they collect sunlight and carbon dioxide which are necessary for photosynthesis.

Annual Rings/ Growth Rings Each year a tree, independent of its species, produces new sap conducting tissue in shape of an annual ring. These annual rings record the age of a tree. Due to our climate and the seasons, an annual ring consists of two ring-like bands. Earlywood/ springwood is produced at the beginning of the growing season and is mostly light-coloured, -weight and soft tissue. The dark coloured, stronger and harder tissue is formed in the period from summer to the end of the growing season and is called latewood/ summerwood. In most tree species annual rings and the two different tissue bands are clearly visible. In regions without major climatic changes and seasons there are less differences between earlywood and latewood. Especially in subtropical/ tropical regions trees form several rings each year, which are called growing rings. The number of growing rings depends on wet and dry periods. The growing of annual rings and growing rings depends on weather and other environmental conditions. Dendrochronology uses annual ring patterns for tree dating (Crossdating) in order to draw conclusions about ecological conditions in the past (ProHolz, 2007).

Pith The pith represents the innermost point of of a tree stem. As a tree starts growing or grows higher the first annual ring is formed around the pith. The thickness of a single annual ring varies within itself due to different influences, like wind or pressure. As a result the annual ring pattern is not a real circular concentric pattern. So the pith is not the geometric center

(gc) of a tree stem. A pith which is located wide outside of the geometric center acts as an indicator for reaction wood.



(a) The pith is located slightly outside due to compression wood in the bottom left of the CS. (Image source: http://commons.wikimedia.org/wiki/File:Reaction_Wood_of_Picea_Abies.jpg)



(b) The pith is located near to the geometric center (gc). (Image source: Rudolf Schraml)

Figure 2.1: Examples for different pith locations

Heartwood/Sapwood As a tree grows and becomes older only the outer zones transport water and nutrients (sap) stem-upwards. This causes the inner zone dying and it gets embalmed in tannins and resins. The resulting heartwood is commonly darker than sapwood and has different mechanical properties.

Tracheids/ Pores and Vessels Sap transport differs in soft- and hardwood. In softwood tracheids are responsible to transport sap upwards and can only be seen microscopically. Hardwood is often referred to as porous wood. Huge vessels appearing as holes or pores conduct sap upwards. Depending on the hardwood species, these pores are distributed differently and can be recognized macroscopically on sanded log end faces or CSs. The distribution of the pores is used to subdivide hardwood species into three different categories (further reading - Fellner et al. (2006)).

Vascular/ Medular Rays To transport sap in horizontal direction so-called vascular or medular rays are formed. For some tree species these rays are very distinctive and visible. Maple is well known for its distinct texture caused by these rays leading to a mirror effect at the tangential surface.

Bark Bark is the outermost layer of a tree stem. At the inner side of the bark there is a special layer called xylem. Xylem is supported by vascular rays with sap and produces fresh wood cells. Phloem is the outer side of the bark and protects the tree stem from environmental damages.

Knots Each tree develops branches laterally from the tree trunk. Branches accommodate leaves and needles which collect sunlight. In the wood stem and on the wood surface branches can be seen as knots. Generally it can be distinguished between inter-grown and encased or loosed knots. Inter-grown knots are formed by healthy branches and get encased when branches die and fresh wood is surrounding them. Encased knots are not disturbing the wood texture/ grain as much as inter-grown knots (Wiedenhoeft, 2010).

Reaction Wood When a tree is physically (eg. by wind, snow, slate subsoil) stressed he tends to form reaction wood to counteract these influences. Softwood tree species react by producing compression wood on the inner side of the load while hardwood species produce tension wood on the rear side of the load. Macroscopically reaction wood can be identified by narrower and darker annual rings in contrast to their surrounding. Branches always cause mechanical stress at the tree trunk and so lead to the production of reaction wood. Unfortunately, reaction wood has a strong negative impact on the mechanical and physical properties of wood. Consequently reaction wood is evaluated very negatively and mostly restricted by grading rules.

Diseases and Vulnerabilities Trees can be affected by diseases or attacked/ injured by animals and micro-organisms. Some of them cause colour changes or wood structure damages.

2.2 CS Analysis Applications and Research

CS analysis refers to the analysis of RGB CS-Images or CT-CS-Images. RGB CS-Images are captured from the log end face or from CS slices. Mobile or industrial devices are utilized and RGB CS-Images can be captured using visible light or near infra-red sensors. So far, just visible light RGB CS-Images were utilized for CS-Image analysis. For the rest of this work the term CS-Images refers to RGB CS-Images captured with a visible light sensor. CT-CS-Images are captured with a CT scanner. CT scanners are utilized for wood log research since

almost two decades and now an industrial CT scanner is available too. Thus, CT log scanning and CT-CS-Image analysis is becoming increasingly important. In general, CT-CS-Images are prevented from disturbances due to cutting or dirt. Compared to RGB CS-Images, analysis of CT-CS-Images shows several advantages and in addition information from the total log CT-CS-Image stack can be utilized.

Since the middle of the 19th century CS analysis is used in the field of dendrochronology for tree dating (ProHolz, 2007). The first known approach which uses computers for CS analysis was presented by McMillin (1982). The author presented a semi-automatic image analysis system which requires an operator who mainly performs image or camera enhancement. A scanner unit was used to produce an analogue video signal from sanded pine samples. This signal was then displayed to the operator who adjusted the region of interest, gray levels and threshold values before the signal could be binarized and processed. 13 basic measurements including annual ring measurements like growth rate per inch or late and early wood measurements have been implemented. Therefore, the current feature that should be measured had to be emphasized by setting the threshold adequately. He also presented measurements of microscopic features like the fibre length or some cell measurements of specially prepared pine samples. Finally geometric measurements of a CT scanned CS slice were shown. McMillin (1982) already proposed the advantages of internal log scanning regarding the sawing of a log.

In the next subsections an overview on present research until 2015 is provided. The present literature on CS-Image analysis can be subdivided depending on the analysed macroscopic feature. Pith estimation and annual ring analysis tasks are the most common CS-Image analysis tasks. For both tasks a literature overview and selected state-of-the-art algorithms will be presented in detail in Section 2.2.1 and 2.2.2, respectively. Furthermore, an overview on literature treating further CS-Image analysis tasks is presented in Section 2.2.3 and finally CS segmentation is treated in Section 2.2.4.

2.2.1 Pith estimation

Pith detection/ estimation is very important for CS imaging. Anatomically the pith is the growth centre of a tree stem. At the CS of the tree stem the pith is the innermost point surrounded by annual rings. Annual rings and the pith are the only features that are always present. Thus, the pith is a unique point on a CS. In determining the wood quality the pith position has two main functions: First, it is an indicator for the presence of other wood properties like compression or reaction wood. Second, it represents a reference point for further

analysis like annual ring measurements. Pith estimation is fundamental for CS analysis.

In some cases it can be impossible to determine a ground truth for the pith location, whether by visual inspection or an image analysis application. In combination with the fact that all pith detection/ estimation approaches rely on a probability match it is appropriate to speak of pith estimation rather than pith detection.

2.2.1.1 Literature Overview

The existing literature can be subdivided into approaches based on annual ring analysis or local orientation estimation. Both rely on the assumption that annual rings are concentric circles the center point of which is the pith position. Annual ring analysis focuses on finding and identifying annual rings or arcs. The detected annual rings or arcs are then used to compute orthogonal vectors pointing towards to the pith or to compute annual ring/ arc centre points representing votes for the pith position. Local Orientation estimation utilizes the fact that small annual ring sections represent an oriented texture. Equal as orthogonal vectors from annual rings/arcs local orientation estimates from annual sections point towards the pith. With intersection of the local orientations the pith position can be determined.

Regarding the capturing device, the most approaches were developed for images from polished/sanded CSs or CT-CS-Images. The main advantage of these images is that they are free of distortions caused by sawing or dust and that annual ring borders are slightly emphasized. Pith estimation approaches treating CT-CS-Images are presented in Bhandarkar et al. (1996), Andreu and Rinhofer (2001), Longuetaud et al. (2004), Entacher et al. (2008).

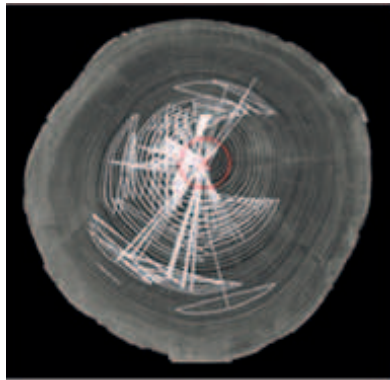
In Bhandarkar et al. (1996) a system to detect internal log defects using ct-image slices of a log is presented. Sobel edge detection and a subsequent threshold are used to extract the annual rings and their gradients. For each detected annual ring point the values inside of an accumulator array are raised in a certain range of the corresponding gradient vector. It is assumed that the maxima in the accumulator array is the location of the pith. The computational demand was reduced by only considering a sub-area around the geometric center of the image.

For enhancing the annual ring pattern in CT-CS-Images Andreu et al. (2002) used contextual Gabor filters. The proposed pith estimation algorithm utilizes the assumption that the orthogonal line of an annual ring cord through its bisect passes the pith. After preprocessing the annual rings are expressed as pixel chains. Each pair of pixels from a pixel chain defines

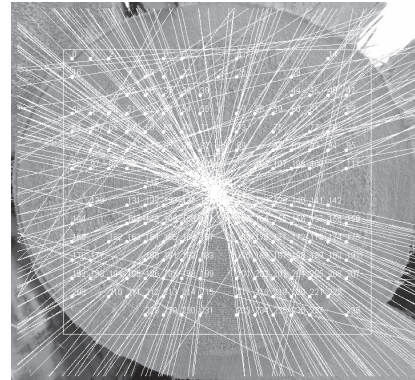
a chord. An accumulator array sums up the intersections of the orthogonal vectors and the maximum is assumed to hold the pith position.

Longuetaud et al. (2004) presented an algorithm to detect the pith in a set of ct-slices from a scanned log. Like Bhandarkar et al. (1996) gradients and an intersection image are used to determine the pith position for a single slice. Additional information of the pith location in the previous slice is used to speed up and to improve the accuracy of the algorithm. The algorithm in Boukadida et al. (2012) is a successor of this work and shows improved results by applying adaptive thresholds and an optional reversion of the CT slice order to improve the accuracy in case of branch forks. The authors performed experiments on 125 logs from 17 different tree species. It is shown that the proposed algorithm performs very accurate with an overall mean error of 1.69 mm.

Entacher et al. (2008) made a comparison between 6 different pith estimation methods. The main focus was on keeping the computational effort low. In addition to the pith estimation methods the influence of different preprocessing methods was evaluated. Except one method (Poincare (Poi) - well known from fingerprint recognition - see Maltoni et al. (2009)) all methods are annual ring analysis methods. The other methods use the circle equation (CE) or gradient estimation methods (GM). For CE and GM two different variations are presented respectively. The first variation for the circle equation - CEeg (equal gradients) uses the Kirsch operator to compute gradients for all pixels. Sets of adjacent pixels are used to determine annual ring arcs. For the second variation CErt (ring tracing) the entire image or a sliding window is cut at different positions and ring tracing is performed along the cut edge (indicated by white pixels). For both variations each pair of points $(x_i, x_y), (x_j, x_y)$ on an annual ring arc is used to determine the coordinates of the circle centre (x_0, y_0) . The centre points are used as votes for an accumulator array, where the maximum is assumed to represent the pith position. The two GM variations use a sliding window and ring tracing to detect annual ring arcs. One variation - GMi (intersection) determines the bisects of the previously localised annual ring arcs. The second variation - GMrl (radial length) additionally uses the radial lengths of the bisects and finally the centre point candidates are used to calculate a pith estimate. For pith estimation GMi intersects all gathered bisects and GMrl uses the point candidate as votes in an accumulator array. The fifth method - Curvature(Cur) uses the fact that the annual ring arc curvature increases towards the pith. Therefore CERl and two thresholds are used to choose annual ring arcs that are close to the pith. The estimated pith position is used to perform a local circle HT. The experiments show that CERt, GMi and especially CEeg are very accurate. Poi and Curv are not suitable for pith estimation.



(a) Intersection using the radial length of detected arcs. (Image source: (Entacher et al., 2008))



(b) Intersection using local orientations gathered by Fourier Spectrum analysis. (Image source: Schraml and Uhl (2013))

Figure 2.2: Intersection images

Pith estimation approaches for digital images (RGB CS-Images) are presented in Wu and Liew (2000); Hanning et al. (2003); Österberg et al. (2004); Norell and Borgefors (2008); Schraml and Uhl (2013).

While Wu and Liew (2000) basically applied the approach presented by Bhandarkar et al. (1996), in Hanning et al. (2003) two methods with the intent to fulfil the requirements of EN 1310 were presented. This European norm defines rules for visual ring width measurements on cut wood, where the pith position is a required feature. The main focus was on unpolished board end images because polishing or sanding of end faces would be too expensive in an industrial usage. One approach is based on finding annual ring structures from which gradients through their barycentre are computed. This is done by local quantization and clustering of neighbored pixels. In this case local connectivity components are defined as local long structures of adjacent pixels, similar to annual rings. In Fig. 2.3 a) the result of the local connectivity step is shown. The second approach uses the peak of the local Fourier spectrum as local orientation estimate of an annual ring section. The entire picture is subdivided into windows (e.g. 32x32 pixels). For each window or window position the local orientation of the annual ring section is determined by local Fourier Spectrum analysis. This is established by searching the peak in the corresponding Fourier Spectrum. For both methods the final pith estimate is computed by intersecting the gradients or local orientation estimates. This work was probably the first which uses local orientation estimation instead of annual ring analysis for pith estimation.

Österberg (2009) presented experiments using Fourier Spectrum analysis for well prepared and under perfect light conditions captured CS discs. Instead of moving a window over the

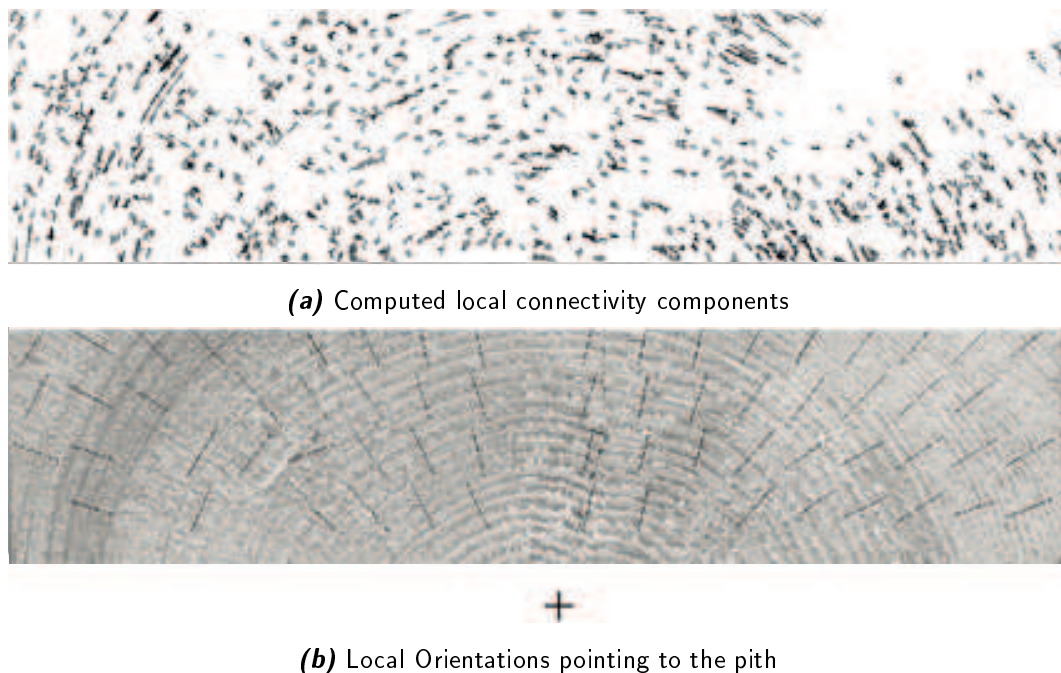


Figure 2.3: Pith estimation in images of rough log end boards. (Image source: Hanning et al. (2003))

entire image an interesting algorithm for pith estimation was introduced. The principle of this technique is that first two points around a reference point are chosen. Initially, the geometric center of the image is used as first reference point. Two further points are chosen, so that an angle of 90 degrees is formed. The distance from the starting point to the two other points is equal to the half-distance between the image border and the starting point. Then, two local orientation estimates are calculated for the annual ring sections around these points. The intersection of the two local orientations is used as next guess for the pith position. This one represents the new starting point for the next iteration. At each iteration the distance between the pith estimate and the other two points is reduced by a factor <1 . The procedure stops after a certain number of iterations or if the new reference point is close to the old one. The concept of this technique is based on the assumption that annual rings close to the pith are more circular. Optimally the pith estimate accuracy increases after performing several iterations.

The authors of Hanning et al. (2003); Österberg (2009) conclude that pith estimation using local Fourier Spectrum analysis could also be applied on images from rough log ends. So far two works focusing on the treatment of images of rough log ends have been presented by Norell and Borgefors (2008) and Schraml and Uhl (2013). In Norell and Borgefors (2008) two methods which compute local orientations by convolution of filter kernels in the spatial domain are introduced. Rough log end images from a sawmill yard were used for the experiments.

The first method fuses the output of three quadrature filters from which a local orientation estimate and a certainty value are computed. The second method uses the concept of linear symmetry and Laplacian pyramids. Both methods use a sliding window and for each pixel a local orientation estimate is computed. Subsequently, for 8×8 pixel blocks one estimate is chosen to represent the block orientation and an intersection image is created, smoothed and the maximum is used as estimate. For the quadrature filters a second iteration in a smaller region around the first estimate and a rotation filtering step is used to improve accuracy. In case of using linear symmetry the intersection image for pyramid level 2 is computed first. If the standard deviation is too high the intersection image is computed for level 1 as well. The intersection image with the lower standard deviation is used to estimate the pith. Finally, the validity of the pith estimate is determined by analyzing the standard deviation of a smoothed version of the intersection image.

Our work Schraml and Uhl (2013) provides a literature review and evaluates the performance of two pith estimation algorithms using four different Fourier spectrum analysis methods. One algorithm is similar to that proposed in Österberg et al. (2004) and the other one subdivides the image into blocks using a rectangular or circular grid (Figure 2.4).

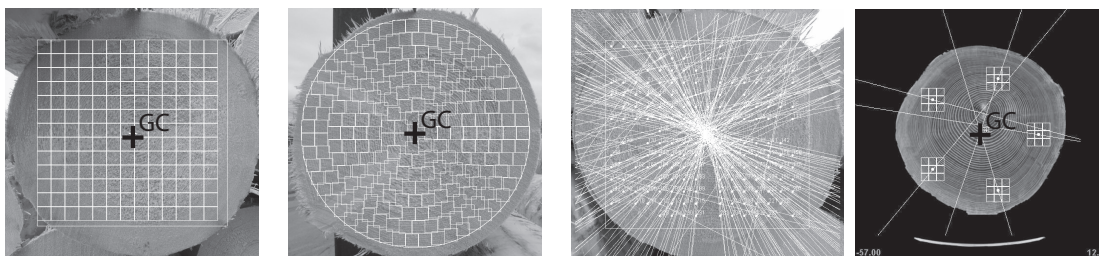


Figure 2.4: The first two images illustrate the rectangular and circular block selection procedure and in the third image the respective intersection image is shown. The last image illustrates the point based selection procedure including the computed local orientation estimates. (Image source: Schraml and Uhl (2013))

This led to different configurations which were applied to 109 rough spruce log end images and to the same CT-CS-Images as used in Entacher et al. (2008). The results for CT-CS-Images were compared to Entacher et al. (2008) and the results for rough log end images to those presented in Norell and Borgefors (2008). Results showed that principal component analysis method and peak analysis for local orientation estimation in the Fourier domain achieve the best results for both algorithms. The adopted algorithm proposed by Österberg et al. (2004) achieves good results for CT-CS-Images but is inapplicable to rough log end images. The grid based algorithm is well suited for pith estimation in rough log end images and achieves the best results using a rectangular grid. Generally, the work shows that the block size, the

distribution and the amount of blocks are crucial for the pith estimation accuracy.

Along with the described methods, a few other approaches are presented in Som et al. (1993), Som et al. (1995), Chalifour et al. (2001), Sliwa et al. (2003) and Flood et al. (2003). These methods are not examined in detail because these papers are not available to us. A structured review about these methods is presented in Longuetaud et al. (2004).

2.2.2 Annual ring analysis

Beneath the pith as the growth centre annual rings are the only constant features that are present in each CS. As described in Section 2.1.1, each year a tree produces a new annual ring around the existing annual rings of a tree stem. Depending on climatological and physical conditions the annual ring widths differ each year. Small annual ring widths indicate a low growth rate and high strength. Consequently, annual ring width measurement and annual ring counting are tasks to determine the strength of a log. Furthermore, these measures are used for log strength grading. The vast majority of literature contributes to the field of dendrochronology. In dendrochronology, the early-/ latewood proportion as well as the annual ring width are of interest (see Fig. 2.5). Compared to industrial annual ring width measurements, high resolution images are necessary to determine the exact early-/ latewood proportion as well as the exact singular annual ring widths.

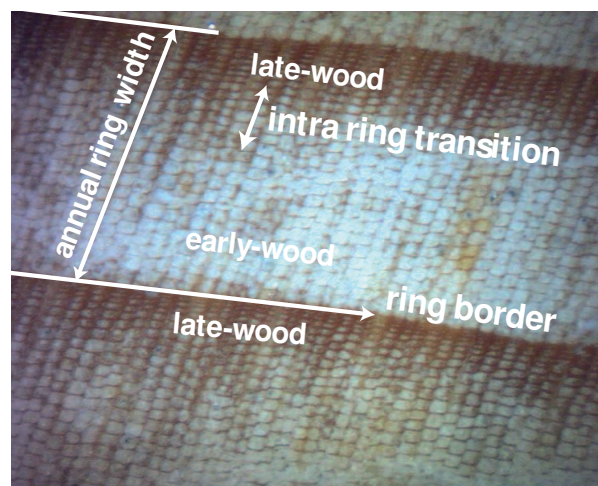


Figure 2.5: Microscopic view of an annual ring from a picea abies (spruce). The image depicts the smooth intra transition between early- and late-wood and the sharp transition between two annual rings from late- to early-wood. (Image adapted from: http://commons.wikimedia.org/wiki/File:Earlywood-latewood_PCAB.jpg)

2.2.2.1 Literature Overview

The focus in this thesis is on literature treating unprepared log end CS-Images and CS-Images from unprepared CS discs. For the sake of completion, the literature overview approaches treating CT-CS-Images or CS-Images from well prepared log end faces/ CS discs are described first.

Tree Ring Analysis in Dendrochronology A big part of literature focuses on image analysis to support dendrochronological tree ring analysis tasks. High resolution images of CS slices are analysed and almost always sanded and probably polished before they are captured. A major task in dendrochronology is to generate tree ring profiles for tree ring dating which is denoted as crossdating. For crossdating tree ring profiles are matched with other profiles. Another aspect is to analyse the climatological circumstances over the tree life time using its tree ring profile sometimes depicted as dendroecology. Consequently, dendrochronological tree ring analysis approaches analyse radial vectors from the pith outwards to the border and generate 1-dimensional tree ring profiles. All known approaches are semi-automatic and require that the pith is moved to the geometric image center or marked by an operator.

The first approach on tree ring analysis by McMillin (1982) is described at the beginning of this Chapter 2.2. Further approaches for annual ring detection and annual ring width measurement are presented in Rauschkolb (1994), Smith (1995), Conner (1999), Vaz et al. (2004), Laggoune et al. (2005).

In the master thesis of Rauschkolb (1994) approaches to identify and measure annual rings in high resolution images (400 dpi) of sanded log ends are introduced. The thesis focuses on detecting annual ring boundaries which arise between early- and late-wood. Basically, there are two boundaries that belong to a single annual ring. A slight border arises at the intra ring transition between early- and late-wood. After winter, the annual ring growth starts with fresh early wood and forms the real annual ring border. Then a strong and sharp crossover between dark coloured late-wood and light coloured early-wood is produced (see Fig. 2.5). As final algorithm the author introduced the "Hybrid Edge Detection from Center". For this algorithm the pith position has to be moved to the geometric image center. For each radius on a radial vector a set of 30 pixels is analysed. 15 pixels are taken from the left and right side respectively. The 30 pixel values of each radius along the radial vector are stored in a matrix. Each column represents a neighbour radial vector. Subsequently, the radial vectors in the columns of the matrix are analysed. For edge detection central differences between two

pixels on a radial vector are computed. Only pixel with a positive slope (transitions from dark to light) are marked as edge pixels. Finally, the average slope is computed and marked edge pixels smaller than the average are disregarded. Now the matrix is analysed and the edge pixels of each row are summed up. Finally a histogram is produced. The peaks are defined as being ring boundaries. This procedure is repeated four times for initially defined radial vectors with $\pi/2$ angular distance to each other.

Smith (1995) described an algorithm which requires perfect annual ring patterns without disturbances or interruptions. The algorithm starts from the outside towards the pith and detects ring boundaries by contour tracing. Subsequently, the area between two boundaries is calculated and assumed to be the annual ring area. As termination condition a flood fill procedure was introduced. This procedure relies on the fact that the innermost area is the smallest.

At the University of Arizona master theses regarding "TREES: computer assisted dendrochronology" are presented by Conner (1999), Giribalan (2000) and Engle (2000) (<http://www.ltrr.arizona.edu/pub/trees/>). The developed semi-automated system for dendrochronology of Conner is also addressed in Conner et al. (1998) and Conner et al. (2000). The system analyses an assembled set of images that are captured under a microscope from the pith outwards to the bark (see Fig. 2.6). For annual ring border detection, the Canny edge detector (Canny, 1986) was utilized. Non maxima suppression was performed by comparing the gradient magnitudes of the neighbours into the gradient direction. This ensures that edge borders are only one pixel wide. Additionally, the system uses the knowledge of the orientation of the captured annual ring section. Edges where the gradient is orthogonal to the annual ring section orientation are disregarded. At last, only transitions from late to early-wood (dark to light) are considered for the final edge image, so intra-ring transitions are disregarded as well. After linking the found edges, the ring widths are measured by counting and averaging pixel distances among them.

Several approaches to overcome problems with narrow ring widths are introduced in Vaz et al. (2004). As a solution, the image scale (represented by the annual ring width) is determined prior to annual ring detection. For this purpose, it is assumed that the gray value profile of an annual ring in radial direction can be modelled by a Gaussian profile. Gaussian kernels with different scales are applied to radial vectors. The extrema for each scale are used to determine annual ring centres of all annual rings lying on a radial vector. As intermediate step the signal of the radial vector is analysed and false maxima and minima are removed. Finally, transitions between early and late-wood are determined. First, the original signal of the radial vector is reconstructed with cubic polynomials and a cross-entropy similarity measure between both is

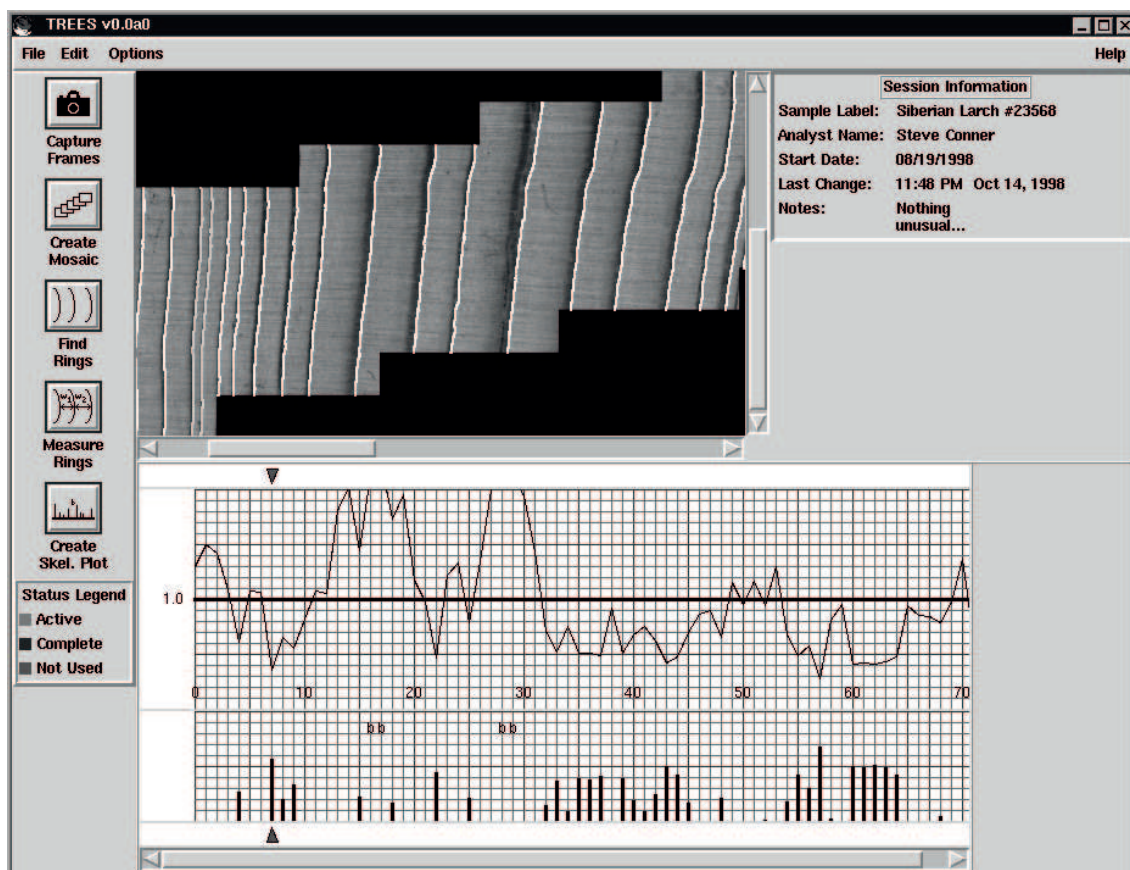


Figure 2.6: GUI of the TREES software for dendrochronology. (Image source: Conner (1999))

used to map the gray levels of a single annual ring into two classes. The border of the two classes defines the intra ring transition and the annual ring borders (see Fig. 2.7).

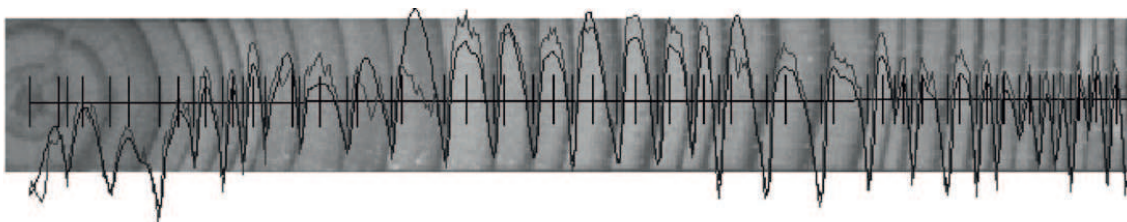


Figure 2.7: Estimation of intra- and annual ring borders. (Image source: Vaz et al. (2004))

Laggoune et al. (2005) paid attention to the image quality and proposed an edge detection filter adopted to noisy images. The test images were captured with a grayscale flat bed scanner (600 dpi). After edge detection thinning and thresholding is performed. Now the annual ring contours are searched analysing the neighbours into the gradient direction. Contours whose length are below a certain threshold are eliminated. At last, the found annual ring contours are used to reconstruct a 3D model.

Industrial Annual Ring Analysis Approaches Annual ring analysis approaches for CS-Images from rough log end ends/ CS discs are presented in Hanning et al. (2003), Cerda et al. (2007) and Norell (2009a), Norell (2010).

In the work of Hanning et al. (2003) an approach to determine the average annual ring width of rough log end boards is presented. With the intention to fulfil the requirements of DIN 4074 the pith position is required to determine the average annual ring width from the pith position to one of the border corners. The pith estimation approach is described in Section 2.2.1. Determining the annual ring width is performed by computing the main frequency of windows positioned along the line between the pith and the border edge. Some unacceptable outliers indicate that the method requires further investigation for an industrial usage.

An algorithm to approximate annual rings on a CS with closed polygons is described in Cerda et al. (2007). The pith position and the outer shape as polygon are required as input. First, the Canny edge detector is applied to the input image. Using the pith position and the intensity of each detected edge point, dark-to-light edges are determined for further processing. Now polygons of different scales (k) (each polygon can be represented as a function of the outer shape and the pith position) are computed (see Fig. 2.8). Each detected edge point is assigned to the closest polygon of a given scale. This results in an accumulator array where each assigned edge point represents a vote for a certain polygon with scale k . The polygons with local maxima in the accumulator array are assumed to represent an annual ring (see Fig. 2.8).

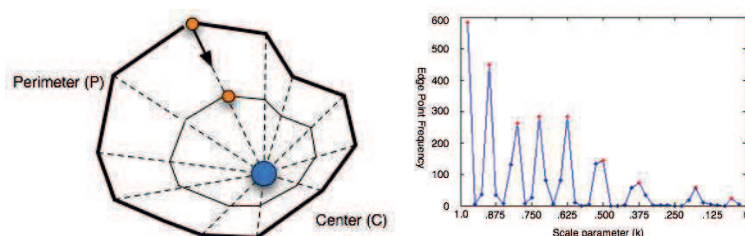


Figure 2.8: Polygons with different scale based on the outer shape and the pith position (left). Based on the accumulator array local maxima are chosen to represent annual rings (right). (Image source: Cerda et al. (2007))

The first approach for a full automated ring width measurement system in images from rough log ends was proposed by Norell (2009a). The system utilizes the pith estimation presented in Norell and Borgfors (2008). The log end images were captured in a Swedish sawmill and 20 images with clearly visible annual rings were used for the experiments. Additionally, a synthetic set of log end images was produced for evaluation (Synthetic Log End Images - Norell (2009b)). After preprocessing and pith estimation the algorithm determines a proper region for annual ring counting. For this purpose, the image is divided into N circle sectors using the

estimated pith position as center point. For all pixels at the CS, a local orientation estimate is computed. In each sector, the sum of errors between the computed local orientation and the pixel orientation relative to the pith is computed. Next, the contrast of the sector with the lowest error is enhanced. In this sector, annual rings are detected in a radial range between 1 and 9 centimetres from the pith using the grey weighted polar distance transform (GWPDT) presented in Norell et al. (2007) (see Fig. 2.9). Grey weighted polar distance transform can be

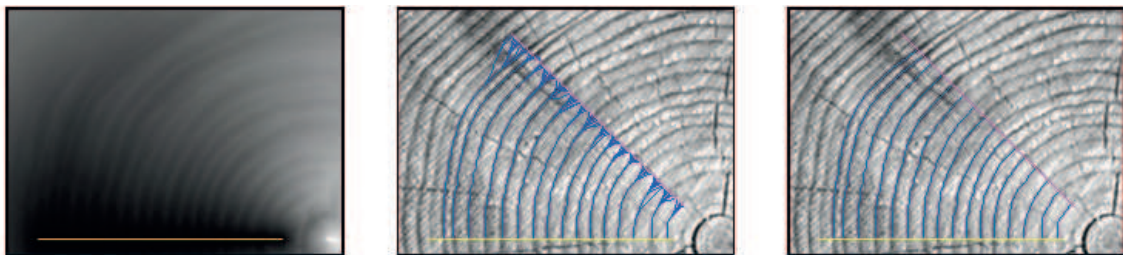


Figure 2.9: Illustration of the gray weighted polar distance transform. The left image shows the distance image computed with GWPDT. The image in the middle illustrates computed paths from the angular to the horizontal line. Finally in the right image the shortest paths between the two lines are selected. (Image source: (Norell et al., 2007))

used to compute circular and approximately circular paths in grayscale images. For the chosen sector two distance images are computed using the two sector borders as starting lines. Finally, the two distance images are analysed along a radial vector placed at the mean sector direction, which results in two one-dimensional vectors. Local minima in these vectors correspond to annual rings. Before counting the annual rings, elastic registration is used to best match the signals of the two one-dimensional vectors. After registration, the local minima of the registered signals are utilized to count the annual rings. The experiments on the synthetic images show that eccentric annual rings, small ring widths as well as disturbances result in considerable errors. The experiment on the real log end images are less meaningful because the test set was very small. One conclusion is that the proposed algorithm tends to count less rings than counted by visual inspection. Results for counting annual rings on 75 Scots pine logs are presented in Norell (2010). The approach is identical as the one proposed in Norell (2009a), except that marks from un-even sawing were removed by Fourier Spectrum filtering. The results showed that the proposed approach performs acceptable in a range from 12 to 20 rings. The author concluded that counting annual rings in a sawmill environment is a very difficult task mainly influenced by sawing disturbances.

Similar to Hanning et al. (2003), in Österberg (2009) local Fourier Spectrum analysis is used for pith estimation and several other algorithms (e.g. thickness fields, annual ring counting) are applied to images from well prepared CS discs. The pith estimation algorithm is described

in Section 2.2.1. For annual ring counting, a sliding window is moved along a predefined radial vector where the rings are to be counted. For each pixel on the line the local Fourier Spectrum is calculated using an appropriate window size. The dominating frequencies of the Fourier Spectrum of each pixel are determined and in combination with the line length the amount of annual rings is determined.

2.2.3 Further Literature on CS Analysis

Further literature on CS analysis mainly focuses on CT-CS-Images. A stack of CT-CS-Image slices from an entire wood log enables the non-invasive analysis of the internal log structure. The analysis of the internal log structure is required for two reasons. First, automated internal log defect detection systems promote the development and the standardisation of automated log grading systems. Second, internal log defects influence the physical properties and the visual appearance of the final wood products. The knowledge about internal log defects is used to improve the saw intake which increases the yield and the value (e.g. Berglund et al. (2014)).

Several wood properties and features visible on CT-CS-Images are labelled as wood defects. In case of analysing the internal log structure such defects are entitled as internal log defects (e.g. knots, resin pockets, cracks, spiral grain and compression or reaction wood). Beside the detection of internal log defects approaches for the detection of further wood properties not labelled as defects have been presented.

Subsequently, an overview on the most common literature treating log defect detection and the detection of further wood properties (bark detection and the detection of the hard- and sapwood boundary) is presented.

2.2.3.1 Log Defect Detection and Analysis

Except spiral grain all defects are detectable due to their specific gray values, geometric shapes and their location/orientation in CT-CS-Images. The majority of the related literature first determines defect regions in each CT-CS slice using different segmentation and clustering techniques. In case of CT-CS-Images it is assumed that different wood defects are represented by gray values in a certain grayscale range. By combining the information of all CT-CS-Image slices a 3D model of each detected defect is generated. Eventually, each 3D model is assigned to a certain wood defect using different approaches and techniques. The present literature

mostly differs in the procedure how the detected objects are assigned to a certain wood defect.

Spiral grain detection works in a different way. The detection of spiral grain can only be established by comparing a set of longitudinal neighboured annual ring structures extracted from the CT-CS-Image stack.

The first algorithm for defect detection in CT-CS-Images is described in Funt (1985) and Funt and Bryant (1987). This algorithm aims to segment and cluster similar gray-scale coloured regions and to classify the kind of defect based on 2D features of the previously segmented regions. Segmentation is based on histogram multi-thresholding. Each pixel is assigned to a certain class representing a set of possible defects. For example, knots are considered to be represented by the darkest pixels. In a further step the pixels of each class are clustered. Eventually, 2D information like size and orientation criterion's are used to validate if a cluster represents a certain defect. For example, knots have an elliptical shape and are longitudinal aligned into the direction of the pith position.

At the beginning of the 1990s different groups of researchers presented various approaches for internal log defect detection. Australian researchers presented CT-CS-Image defect detection approaches in Wells et al. (1991), Som et al. (1993), Som et al. (1995). As noted in the literature overview on pith estimation (see Section 2.2.1.1), these publications are not available to us and cannot be examined. Further information on these works can be found in the literature review on knot detection by Longuetaud et al. (2012).

Many publications on log defect detection are published by researchers from the Virginia Polytechnic Institute and State University. For example, in Zhu et al. (1996) a prototype for analysing CT-CS-Images of hardwood logs is presented. This prototype is the final result of a set of earlier published works (see literature review in Longuetaud et al. (2012)). It consists of a segmentation module and a scene analysis module. The segmentation module first applies the Unser filter to remove annual rings from the CT-CS-Image. In the next step, similar as in Funt and Bryant (1987) adaptive histogram multi-thresholding is utilized. According to the Ph.D.-thesis of Zhu (1993), the pixels are assigned to three different classes. For example, knot and bark pixels are in the same class and are separated by the scene analysis module. Morphological operations are applied to determine 2D regions representing wood defects. Finally, a 3D model is generated by clustering of the 2D areas of all slices together. For each detected object, geometric features and colour features are computed. Finally, the Dempster-Schafer theory of evidential reasoning is used to classify the kind of wood defect of each object. For this, basic knowledge about the shape, colour and location/ orientation of each wood defect is utilized.

Further publications published by researchers from the Virginia Polytechnic Institute and State University focus on artificial neuronal networks (ANNs) used to classify internal log defects (see Li et al. (1996), Schmoldt et al. (1997), Schmoldt et al. (1998) and Schmoldt et al. (2000)). A prototype system based on the noted previous works on ANNs is presented in Sarigul et al. (2003a) and Sarigul et al. (2003b). These publications provide a good overview on log defect detection using ANNs.

Further research on log defect detection has been published by researchers from the University of Georgia. In Bhandarkar et al. (1996) and Bhandarkar et al. (1999) the system CATALOG (Computer Axial Tomography for Analysis of LOGs) is described. The system uses 3D shape parameters to classify and 3D render internal log defects. In recent two publications, Bhandarkar et al. (2006) and Bhandarkar et al. (2008) presented a new approach based on Kalman filter tracking algorithms.

Further approaches are presented by Rojas et al. (2006), Wei et al. (2009), Baumgartner et al. (2010), Breinig et al. (2012), Longuetaud et al. (2012) and Cristhian A. Aguilera (2012).

In Rojas et al. (2006) two supervised classification algorithms (minimum distance classifier and maximum likelihood classifier) for wood defect detection are introduced and evaluated. The work of Wei et al. (2009) evaluates the applicability of a back propagation artificial network and the maximum likelihood classifier for wood defect detection in sugar maple and black spruce. In Baumgartner et al. (2010) the main focus lies on knot detection just in the heartwood region. For this purpose, the sapwood–hardwood boundary was detected in polar transformed CSs using the pith as pole.

Knot Detection A knot-detection (3DKnotDM) software package and exhaustive experiments and tests on the accuracy and timing performance are presented by Longuetaud et al. (2012). Additionally, this work includes a well-structured literature review on knot-detection in CT-CS-Images. Finally, in Cristhian A. Aguilera (2012) the idea of using active contours to detect internal log defects using a-priori information is introduced and evaluated.

Based on the results and insights presented in Longuetaud et al. (2012) further research on knot detection was presented in Krähenbühl et al. (2014); Roussel et al. (2014) with the aim to improve knot detection in wet areas like sapwood.

As knots are by far the most frequent internal log feature several publications within the CT-PRO project 2010–2013 focused on knot detection algorithms, their accuracy and how knot detection influences the performance of the sawing optimization (<https://www.sp.se/en/>

index/research/CT-Pro/Sidor/default.aspx)):

In Johansson et al. (2013) the knot detection approach by Grundberg and Grönlund (1992) was adopted to high-speed CT scanner CT-CS-Images and the algorithm was tested on Scots pine and Norway spruce logs by comparing the knot detection results to groundtruth data. Based on this algorithm, in Fredriksson et al. (2014b) the detected knots are projected from 3D to a 2D plane perpendicular to the log length axis with the aim to reduce the amount of data (Fig. 2.10). The centre of mass of the knot projection image together with the centre of a predefined sawing pattern are used to determine the log rotation for the saw intake. Simulation results indicated that the board quality increases compared to the industrial praxis of sawing logs horns down. In his PhD thesis Breinig (Breinig, 2015) focused on the accuracy

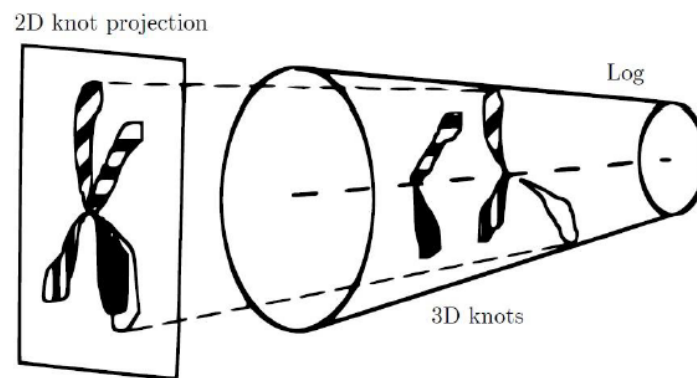


Figure 2.10: Projection of the detected knots from 3D to 2D. Based on the 2D knot image and a given saw pattern the best rotation for sawing is determined. (Image source: (Fredriksson et al., 2014b))

of knot detection and the impact of different knot detection errors on the performance of the sawing optimization. In Breinig et al. (2012) the accuracy of a knot detection algorithm was assessed by comparing the results to spatial measurements on the corresponding real log CSs. The impact of knot detection errors on the performance of the sawing optimization was investigated in Breinig et al. (2013) based on sawing simulations. Furthermore, in Breinig et al. (2014) an approach for appearance classification of wood board surfaces based on the knot-pattern is shown. Finally, in Breinig et al. (2015) for 57 CT scanned logs the cutting and the resulting board surfaces were simulated and virtually graded using the proposed algorithm. The results were compared to the real human graded board surfaces after cutting the logs. Results indicated that the obtained virtual grading results are largely consistent with the human perception and grading results.

2.2.3.1.1 Further Defects: Detection and Analysis So far, the listed literature treats the general task of internal log defect detection or specialises on knot detection and analysis.

A few other publications focused on the detection or analysis of cracks. Approaches for crack detection in CT-CS-Images are published by Bhandarkar et al. (2005), Li and Qi (2007) and Wehrhausen et al. (2012). In Bhandarkar et al. (2005) Sobel-like filters are used to detect annual rings and cracks which are aligned orthogonal to the annual ring structure. A recent approach presented by Wehrhausen et al. (2012) also uses directional filters and focuses on the evaluation of the approach. A novel approach based on fractal dimension is presented by Li and Qi (2007).

Another wood defect is compression wood or reaction wood. The only found work treating automated compression wood detection in CT-CS-Images or RGB CS-Images is presented by Nystrom and Hagman (1999). It seems that there is no further literature on compression/reaction wood detection.

Literature on spiral grain detection using ct-image slices of logs are presented in Sepúlveda (2001), Sepúlveda et al. (2002), Ekevad (2004) and Entacher et al. (2007). The approach presented by Sepúlveda (2001) manually analyses streaks in surfaces that are generated by cutting the CT-CS-Image stack concentrically around the pith. The streak inclination relative to the longitudinal axis corresponds to the spiral grain. In Sepúlveda et al. (2002) the authors tried to predict spiral grain based on variables extracted from CS-Images (e.g. knot volume and heart/sapwood relation). The results indicated that prediction of spiral grain should be possible.

Another algorithm to determine spiral grain is presented by Ekevad (2004). Principal directions of inertia of spheres that are distributed along the longitudinal axis of a log or wood board can be used to compute local fibre-directions which represent the local spiral grain angle.

Eventually, the applicability of motion estimation algorithms for spiral grain detection is evaluated in Entacher et al. (2007). For this purpose, the CT-CS-Image stack is interpreted as video data and three different motion estimation techniques are assessed. The results are too irregular and it is not clear if the detected movements are correlated to spiral grain in wood.

2.2.3.2 Further Wood Properties: Detection and Analysis

The group of wood properties that are not labelled as defects and which are relevant for CS analysis tasks is formed by the pith, annual rings, heart- and sapwood and the bark. Annual ring analysis and pith estimation were treated in Section 2.2.1.1 and Section 2.2.2, respectively. Subsequently, the most common literature treating detection and analysis of bark

and heart-/sapwood is quoted.

For heart- and sapwood detection, approaches based on heat sensitive infra-red images (Gjerdrum and Høibø (2004)) and CT-CS-Images (Longuetaud et al. (2007)) were published. In Gjerdrum and Høibø (2004) an approach to detect heartwood in Scots pine using heat infra-red images of log ends is introduced. Due to the different physical structure of heart- and sapwood their moisture contents differ which results in different temperatures. Consequently, heart- and sapwood can be clearly identified in heat infra-red images of log ends.

The heart-/sapwood boundary detection algorithm proposed by Longuetaud et al. (2007) uses the pith position and analyses the gray values of 360 radii. For each radii the first pixel exceeding a certain threshold is chosen as boundary point.

At last, bark detection is considered. Automated bark detection enables to determine the exact volume of a wood log without debarking it. For some wood species it is critical to remove the bark for longer periods - e.g when storing it on the sawmill yard. Basically, no research focuses on the particular task of bark detection. However, most of the approaches in the literature on log defect detection are able to detect and analyse the bark in CT-CS-Images. An industrial solution for bark detection is provided by Microtec (<http://www.microtec.eu/de>). A scanner entitled TOMOLOG automatically creates a 3D profile of the log with and without bark. In Baumgartner et al. (2007) results for automatic bark measurements using the TOMOLOG scanner are presented.

2.2.4 CS Segmentation

Generally, image segmentation is a fundamental image analysis task. Segmentation enables the detection of constituent regions or objects in an image. Algorithms for image segmentation can be subdivided into two categories: approaches based on discontinuity or approaches based on similarity of the pixel intensity values. Discontinuity approaches rely on boundary detection of an object or a region. Abrupt intensity value changes between neighbouring pixels indicate borders of objects or regions (e.g. edges or lines). Similarity approaches partition an image into regions based on similarity criteria (Gonzalez and Woods, 2001).

CT-CS-Images can be segmented using histogram thresholding techniques. Such an approach is not applicable for CS-Images of rough log ends. Subsequently, an exemplary comparison on segmentation using histogram thresholding techniques is presented. For this comparison, differently captured CSs are used. The results give information about the differences of CS

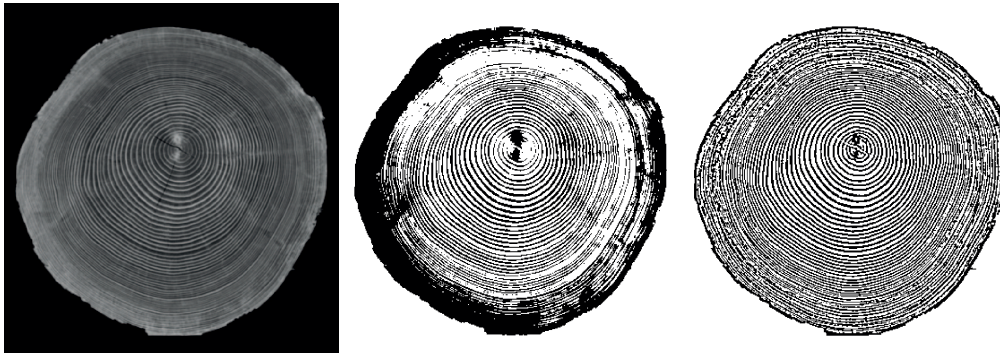


Figure 2.11: Two different thresholding techniques (p-tile and adaptive) applied to a CT-CS-Image (Image source: Schraml (2013))

segmentation in CT-CS-Images compared to CS-Images from rough log ends. Basically, CS segmentation can be performed for two reasons: First, segmentation is required to separate the CS in an CS-Image from the background. Second, annual rings are the main wood property of a CS. Consequently, the extraction and preservation of annual rings and structures are very important for further annual ring analysis tasks.

Thresholding methods are well suited for segmenting CSs in CT-CS-Images. In CT-CS-Images, annual rings are represented as white pixel chains and the background is dark coloured. Consequently, thresholding can be utilized for segmentation and to extract or emphasize annual ring structures and other wood features. In other words, the CSs features are separated as foreground pixels from the background pixels. The three pictures in Fig. 2.11 illustrate the results for two different thresholding techniques applied to a CT-CS-Image. One technique is a global thresholding technique and the second one is based on adaptive thresholding. The first picture in Fig. 2.11 depicts the original CT-CS-Image. The second picture shows the result for global p-tile thresholding with an assumed foreground amount of 50 %. In the third picture, the result for adaptive thresholding is shown. For adaptive thresholding, the mean values of 15x15 pixels blocks are used as local thresholds. Both thresholding methods indicate that thresholding is an appropriate technique for CT-CS-Image segmentation.

The same thresholding techniques using the same parameters are applied to the CS-Image of a sanded CS slice shown in the first picture of Fig. 2.12. The result for adaptive thresholding shows that this method is very sensitive to noise in the black background. However, both methods indicate that the CS can be separated from the background and annual ring structures can be extracted in studio-captured images of sanded CSs.

Finally, the thresholding results in Fig. 2.13 illustrate the arising difficulties using real-world images of rough log ends. In contrast to CT-CS-Images and studio captured CS-Images, the



Figure 2.12: Two different thresholding techniques (p-tile and adaptive) applied to a CS-Image of a sanded CS slice (Image source: Schraml (2013))



Figure 2.13: Two different thresholding techniques (p-tile and adaptive) applied to a CS-Image of a rough log end (Image source: Schraml (2013))

background of real world images is very heterogeneous and strongly varying in each image. Additionally, CS-Images of rough log ends are disturbed due to cutting. The results in Fig. 2.13 show that histogram thresholding is no appropriate technique to separate CSs from the background and to extract or separate annual ring structures in real world images of rough log ends.

Our work Schraml and Uhl (2014) is the first dealing with segmentation of the CS area in CS-Images of rough log ends. We proposed a similarity-based region growing procedure for CS segmentation. In the experimental evaluation different texture features (intensity histograms and Local Binary Patterns (LBP)) and histogram distances were utilized. Basically, the segmentation algorithm is subdivided into three consecutive stages: Cluster initialization, growing procedure and boundary estimation.

Cluster Initialization For cluster initialization the pith position is utilized and a predefined number of clusters which are equally distributed close around the pith are selected. Each cluster is initialised by computing three features which describe the contained texture.

Growing Procedure For the growing procedure the neighbourhood of each cluster is analysed and it is decided if a neighbourhood block is added to the cluster or not. The procedure continues until no more neighbourhood blocks can be added (Fig. 2.14). Finally, the clusters are merged and it is assumed that the merged cluster represents the area of the CS.

Boundary Estimation The CS boundary is computed in three consecutive steps. In the first step boundary blocks of the merged cluster are determined and selected with the aim to reduce the amount of blocks (Fig. 2.15a). Second, circle/ellipse fitting is performed (Fig. 2.15b). This step further reduces the amount of blocks and in the best case outliers are cut off. Finally, the alpha shape (Edelsbrunner et al., 1983) of all remaining blocks is computed (Fig. 2.15c) and is used as a final estimate of the CS boundary.

Our algorithm showed the best results for intensity histograms as texture features and the Earth Movers Distance (EMD) as histogram distance.

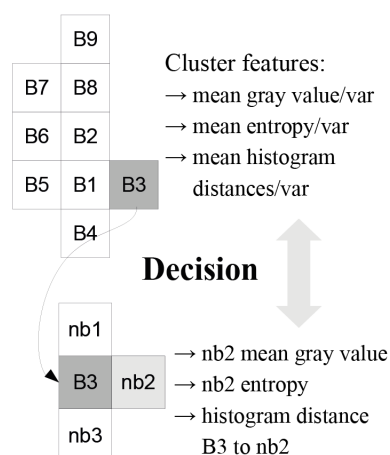


Figure 2.14: Illustration of the cluster growing procedure. (Image source: Schraml and Uhl (2014))

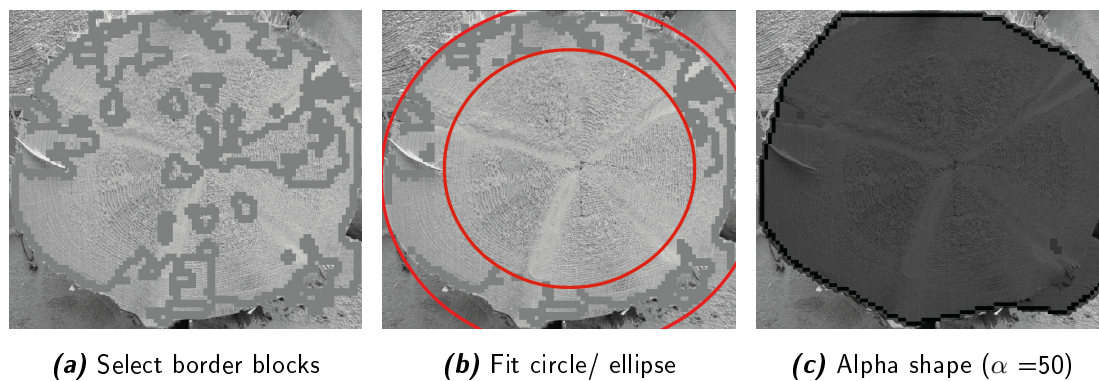


Figure 2.15: Cross-section (CS) boundary estimation (Image source: Schraml and Uhl (2014))

Chapter 3

Traceability of Wood Logs

3.1 Traceability Definition

There are various definitions for traceability. Some of these definitions originate from research and are therefore more or less related to a research topic. Others are defined by ISO quality standards and are adapted to the scope of an application. Most of the literature available focuses on part productions and on single companies (Kvarnström and Oghazi, 2008).

Like (Kvarnström and Oghazi, 2008, p.5) we use the definition from Töyrylä (1999) which suits the continuous processes: *"Traceability is the ability to preserve and access the identity and attributes of a physical supply chain's objects."* Kvarnström and Oghazi (2008) introduce the terms "traceability system" and "traceability methods". Thereby the ability of traceability is built up on a traceability system, which uses traceability methods to link process and object data.

3.2 Log Supply Chain - LSC

The above presented definition restricts traceability to the supply chain for predefined objects. Consequently it is necessary to define the process or time span in which traceability of wood logs as objects should be enabled. Päivinen and Lindner (2006) use the term Forest Wood Chain (FWC) to collect processes in which forest resources are converted into services and products. The author's focus is on the assessment of sustainability in Forest-Wood Chains. So Päivinen and Lindner (2006) are aware of the fact, that there are a lot of different FWCs.

In each of these FWCs logs are required as raw material. Logs have to be cut in the forest and transported to a sawmill, pulp mill or another processing company. This sub-chain can easily be defined as a supply chain called LSC. In general the LSC is restricted to the lifetime of a log. This lifetime starts when a single tree is felled and length cut into a number of logs. The lifetime ends when a log is further processed e.g. by cutting and therefore stops existing to be a single object. The term "LSC" indicates the objects and the time span for which we want to enable traceability. It mainly involves forest based and processing industries like sawmills or pulp mills.

3.3 Traceability Methods

The introduction classifies three groups of traceability methods: Manual Labels, Badge Labels, Transponders. These groups represent current methods used for traceability systems in the LSC. Industry and many small sized companies make use of these methods. It depends on the application of each method if it's possible to identify each object in the supply chain. For sustainability issues it would be sufficient to know the origin of each object. All methods rely on a marking/reading principle and require additional equipment.

3.3.1 Manual Labels

The simplest and oldest methods are conventional paint (Fig. 3.1b), hammer and chisel labels. While chisel labels are markings that are engraved with knives, conventional paint labels are simply applied with spray cans or chalk. Another method is the use of hammers with special stamps to create brands at the log end faces. Although these practices are very old and simple, forest smallholders prefer them. The major advantage of these methods is that they are very cheap and resistant to abrasion and damaging. Normally these methods are used to verify the origin of a log and not to identify it. Depending on the application these methods allow identification of each individual log. There are good solutions which show that these basic methods can be improved for industrial usage. The company Otmetka (www.otmetka.com) has developed a method where the harvester punches a set of hammer brands on the CS. This unique punching label is then used as an identity code and can be scanned automatically (Fig. 3.1a). Otmetka enhanced hammer brands to fulfil the requirement of identification of each log.



(a) Punching Label by Otmetka.
(Image source: www.otmetka.com)



(b) Marking with spray.
(Photo by Schraml)

Figure 3.1: Manual labels

3.3.2 Badge Labels

The second group of methods uses badge labels, consisting of paper, plastic or metal. These labels can be printed with different varieties of bar-codes, numbers or logos and provide the possibility to integrate additional information. Badges can be applied manually or automatically and are readable via scanning devices. Depending on how these labels are applied on the wood logs, major disadvantages are damages, fall offs and high prices compared to manual labels. In sawmills or pulp-mills metal badges and plastic labels can lead to problems in some processing steps. Therefore plastic badges consisting of a special plastic material are used. These are not detected by metal sensors and dissolve when they come in contact with paper base.



Figure 3.2: Plastic badges from Latschbacher. (Image source:www.signumat.com)

3.3.3 Transponders

This group of labels contains all kind of transponders which can be applied on wood logs. A major advantage is the fact, that transponders transponders can be scanned automatically without having visual contact. Disturbances (e.g. snow or dirtiness) do not influence the scanning quality and additional processing data can be transferred on the transponder. Therefore RFID is used as technology. Data readers can access data stored on a transponder. When a transponder enters the electromagnetic field of a data reader, data can be exchanged by radio

waves. RFID transponders can be active or passive and can be further distinguished by the frequency range they use. Active RFID transponders need a power supply like a battery. Passive ones are non-volatile and do not need any power supply to store data. Passive transponders receive the required submission energy from radio waves via the antenna of the transponder. Depending on the frequency range different reading ranges result. While Low Frequency (LF) transponders have a reading range of a few centimetres, High Frequency (HF) transponders have a reading range up to 1.5 metres. Ultra High Frequency (UHF) transponder reach reading ranges of several metres. Consequently, higher frequencies reach a better reading range and enable bulk reading, but they are more sensitive to dielectric material like metals or liquids (Kvarnström and Oja, 2008).



Figure 3.3: Different transponders:

- a)** Nail and Chip LF RFID Transponder. (Image source: Korten and Kaul (2008))
- b)** UHF RFID Transponder presented by Uusijärvi (2010)
- c)** RFID Transponder in batch format by Latschbacher. (Image source: www.signumat.com)
- d)** Lignin RFID Transponder by Fraunhofer (2010)

The two EU-projects Lineset and Indisputable Key propose RFID transponders in the LSC as traceability method. In the Lineset project the use of LF RFID transponders has been studied and pilot-tested. The image in Fig. 3.3 a) shows typical LF RFID tags. Because of higher reading ranges, the Indisputable Key project studied the use of UHF RFID transponders in which a special UHF RFID tag has been designed. These transponders promise higher reading ranges and rates as well as lower costs compared to LF RFID transponders. The most promising transponder with a reading range of 2 meter is shown in Fig. 3.3 b). This transponder is applied at the CS. In doing so mechanical damaging is low. Another UHF RFID

transponder is shown in Fig. 3.3 c) and is presented as preview by the company Latschbacher in Austria. It promises reading ranges up to 4 metres. It depends on the transponder material and the costs whether it is necessary to remove a transponder before a log is further processed. The Fraunhofer Institute presented a RFID Transponder which mainly consists of lignin. Lignin transponders have a low metal concentration and provide the possibility to save a single number (Fraunhofer, 2010). Bulk reading ability and no disruption of further processing steps make these transponders very interesting for future applications.

Chapter 4

Biometric Wood Log Traceability

The idea of using biometric characteristics for human recognition has been carried to the recognition of plants, vegetables, animals and industrial products. Hence, the concept of human biometrics was also carried to tree log recognition. By analogy to human recognition, it is assumed that wood logs are unique entities which can be recognized using biometric log characteristics.

This chapter first introduces theoretical background on biometric systems in Section 4.1 and second provides a structured review on research related to biometric log recognition in Section 4.2.

4.1 Biometric Systems

With the significant changes in society and economy human recognition became a major task in our life. Related to human recognition the term **Biometrics** stands for the study of behavioural or physiological characteristics to identify living people. Biometric systems are almost always computer aided systems for biometric recognition of humans. Currently used biometric systems use characteristics like fingerprints, iris, retina, handwriting, face, gait and many more to extract biometric features of living persons. Beneath biometric systems for human recognition - approaches treating recognition of vegetables, plants, animals or products were presented (Wayman et al., 2005).

These approaches are based on the theoretical background and concepts from human recognition to explore biometric systems for new fields of applications. Subsequently, an introduction

to biometric system characteristics (Section 4.1.1) and the performance evaluation of biometric systems (Section 4.1.2) is given.

4.1.1 System Characteristics and Classification Categories

In this section characteristics and classification categories of biometric systems are considered in detail. For this purpose categories and modes of biometric systems as described in Maltoni et al. (2009) are presented.

Verification vs. Identification mode Commonly, biometric systems are either classified as identification or as verification systems, whereat *recognition* is used as universal term regardless of the operation mode. Both modes require that humans become enrolled into the system (see Fig. 4.1). Depending on the used biometric characteristics specific sensors are used to capture/ digitize the related characteristics. Next, the biometric system extracts features from the captured characteristics. Out of these features a compact and comparable representation, called *template* is generated. Commonly, biometric applications store the template together with personal information (e.g. an ID or name) into a database or data carrier.

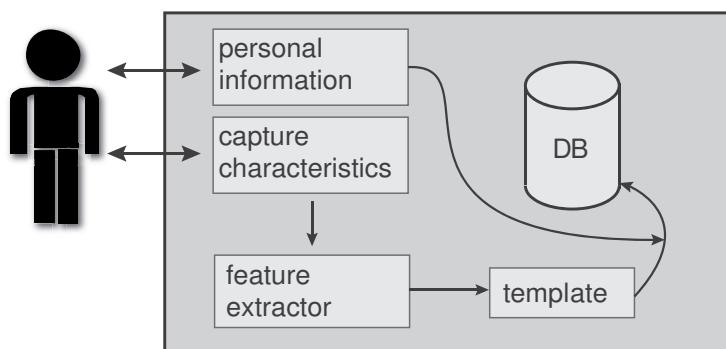


Figure 4.1: Biometric system - enrolment schemata

The two operation modes can be distinguished regarding the recognition procedure of the system:

- **Verification** systems are based on one-to-one comparison. A person requesting authentication by the system has to announce the claimed identity to the system using personal information (e.g. ID, PIN, magnetic cards, ...). The system then compares the biometric characteristics of the person to those from the pre-stored template of the

claimed person in the system database. Consequently, the system can accept or reject the claimed identity. The term **authentication** is likely used as synonym for verification, as verification confirms or negates the claimed identity of a person.

- **Identification** systems perform one-to-many comparisons. For each request of a person the system compares all pre-stored templates in the system database to the template generated from the biometric characteristics of the person. The system has to make a decision if the person is enrolled in the system. Consequently, a single template in the database has to be selected as the person's template. If there is no corresponding template available, the system fails and rejects the claim for identification.

Beside the basic classification into verification or identification systems a biometric system can operate in further modes:

- **online vs. offline**

Recognition can be performed immediately or with a long delay response. Online systems are almost always fully automatic, while off-line systems are likely to be supervised semi-automatic systems.

- **positive vs. negative recognition**

A system that operates in positive recognition mode tests if a person is already enrolled. Thereby the system checks if the claimed (explicit or implicit) identity is correct or not. Consequently, it prevents different users from using the same identity. In the negative recognition mode the system checks if the person is not enrolled in the system. It prevents a single user from using multiple identities. Positive recognition can be performed in identification or verification systems. Due to the fact that all templates have to be checked, negative recognition can only be established in an identification system.

Application Taxonomy: Additionally to these basic classifications biometric systems can be described using application-dependent categories (Wayman et al., 2005):

- overt vs. covert
- standard vs. non-standard environment
- habituated vs. non-habituated
- public vs. non-public
- attended vs. non-attended
- open vs. closed

Biometric characteristics quality: The development of a biometric system relies on the quality of the selected biometric characteristics. The quality of a biometric characteristic can be assessed considering a set of criteria (Maltoni et al., 2009):

- **universality** - is the characteristic available for each person?
- **distinctiveness** - is it possible to receive a strong variation between a set of individuals?
- **permanence** - is it invariant against change over time?
- **collectability** - can it be captured or digitized with sensors?
- **performance** - different measures that describe the accuracy, robustness and speed of the system using the characteristic (see Section 4.1.2)
- **acceptability** - is it tolerated by the individual to capture or digitize the characteristic?
- **circumvention** - is it possible to defraud the biometric system?

Compared to the other criteria, performance, acceptability and circumvention are criteria used to evaluate and describe the biometric system. The other criteria describe the quality of the biometric characteristic itself.

4.1.2 System Performance Evaluation

This section describes (error) measures that are used to assess the performance of biometric systems as described in Maltoni et al. (2009). Each time a biometric system compares two templates, a matching algorithm computes a matching score (s) normalized between 0 and 1. The closer to 1 the higher is the certainty that the templates are from the same person. The decision if two templates are said to be from the same person depends on a threshold (t). If the matching score between two templates is lower than the system's threshold, the two templates form a non-matching pair, otherwise they form a matching pair. Out of this, two biometric system errors are derived:

- **False match or false acceptance**
denotes a matching pair where the compared templates are not from the same person
- **False non-match or false rejection**
denotes a non-matching pair where the compared templates are from the same person

It has to be noted that the terms "false acceptance" and "false rejection" have different meanings in positive or negative recognition mode. Instead, false match and false non-match have the same mode-independent meaning. Nevertheless, in practical use the terms "false match" and "false non-match" are preferably used. The performance evaluation of a biometric system is based on the computation of the false match rate (FMR) and the false non-match rate (FNMR). These rates can be determined considering the impostor and genuine distribution of the system:

- **Impostor Distribution**

of the matching scores of each enrolled template of a single person to all templates of the other enrolled persons - can also be denoted as interclass variance.

- **Genuine Distribution**

of the matching scores between several templates generated from the biometric characteristics of a single person - can also be denoted as intraclass variance.

Figure 4.2 illustrates how the FMR and FNMR are determined for a certain threshold and given impostor and genuine distributions of a biometric system. For a positive recognition system the FMR describes the percentage of comparisons that would be accepted by the system although the templates are from different persons. The FNMR gives the percentage of comparisons that would be rejected although the templates are from the same person. Consequently, the

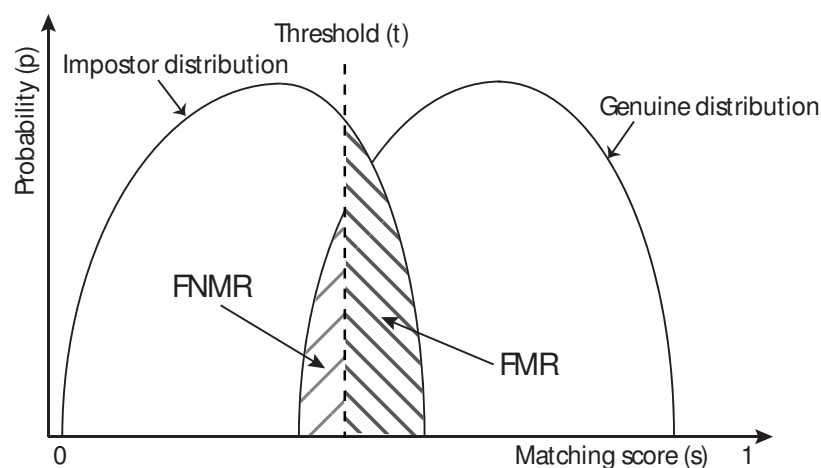


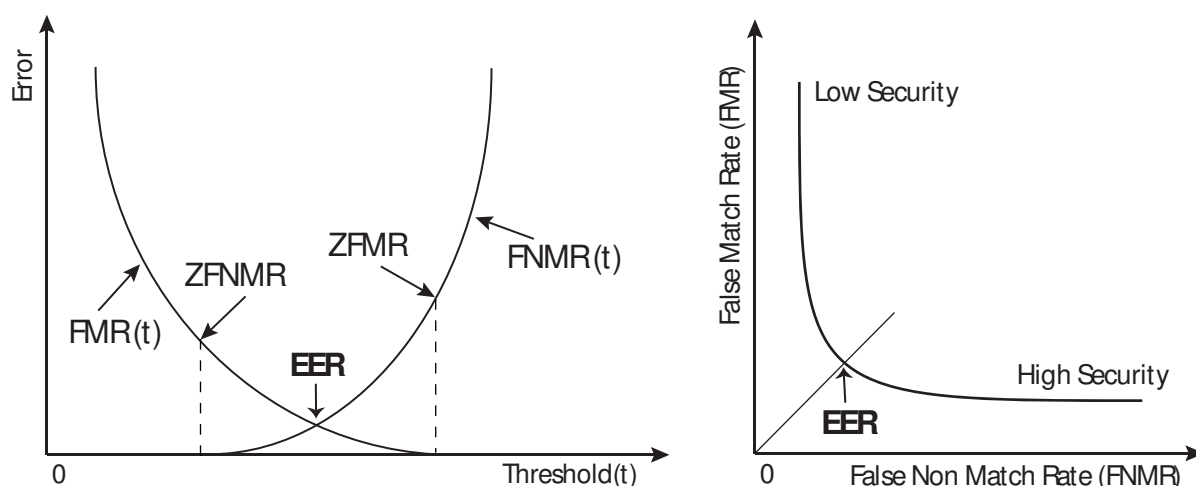
Figure 4.2: Biometric errors: FMR and FNMR for given impostor and genuine distributions at a certain threshold (t). (Template: Maltoni et al. (2009))

selection of the threshold influences the performance of the biometric system. For example, a high security application will choose a high threshold, taking into account that the system denies access for a higher percentage of actually authorized persons - increasing FNMR and decreasing FMR. Alternatively, tolerant systems use lower thresholds to ensure that a high

amount of authorized persons are accepted and so decreasing the FNMR. As described in Section 4.1.1, a biometric system operates either in verification or identification mode and the term recognition is used universally. In both modes the system has to decide if the template of an individual/ object is known to the system.

For verification performance evaluation the equal error rate (EER) is a general benchmark. The EER is defined as the error rate at the threshold where FMR and FNMR are equal. EER is likely used as measure for the comparison of different biometric systems. Because FMR and FNMR are depending on the threshold value they can be described as functions $FMR(t)$ and $FNMR(t)$ as illustrated in the plot in Fig. 4.3a. This plot offers further points of interests like the zero false match rate (ZFMR) and the zero false non-match rate (ZFNMR).

Another possibility to get an overview on the verification performance of a biometric system is to analyse its receiver operating characteristic (ROC). This curve visualizes the dependency of the FMR on the FNMR for changing system thresholds. Figure 4.3b depicts a sample illustration for a ROC curve and the resulting use cases using different thresholds. It is shown that low security applications (e.g. forensic applications) require a low FNMR and therefore take a higher FMR into account. High security applications have to ensure that they can only be accessed by authorized people and so they require a low FMR. On the other hand a lower FMR implies a higher FNMR and so the amount of actually authorized people that are not recognized by the system increases.



(a) Equal error rate estimation - Illustration of the $FMR(t)$ and $FNMR(t)$ curves and the corresponding points of interest.

(b) Illustration of a receiver operating characteristic and the corresponding use cases (ROC).

Figure 4.3: Biometric performance curves. (Templates: Maltoni et al. (2009))

The identification performance is evaluated by matching a set of probe templates to all templates enrolled in the database Jain et al. (2007). We refer to closed-set identification where it is assumed that all individuals/objects of the probe templates are enrolled in the system. The MSs between each probe template and all database templates are ordered according to the MS. The ordered MSs of each probe template are used to compute the probability that the correct template is ranked within the top k -ranked MSs. The probabilities for each rank are illustrated in a curve which is denoted as Cumulative Match Characteristic (CMC).

4.2 Research on Biometric Log Recognition

So far the research related to log recognition can be subdivided into four groups:

1. **Log Shape Recognition** In the works of Chiorescu and Grönlund (2003, 2004); Flodin et al. (2008a) the log shape is used as biometric characteristic and geometric properties are utilized as biometric features.
2. **Knot Recognition** The investigations in Flodin et al. (2007, 2008b) show that knots and their locations are suited as biometric characteristics and features, respectively.
3. **Log to Board Recognition** Equal as in the previous group knot positions are utilized in (Flodin et al., 2008a,b) to establish traceability between logs and the boards sawn from it. Furthermore, Peterson (2009) showed a preliminary study on log to board tracking using the pixel correlation between the log and board end face annual ring patterns.
4. **Log End Recognition** The group of research which directly relates to the topic of this work uses the log end of a log as biometric characteristic. Annual ring pattern and/or shape information are utilized as biometric features. Works treating log end biometrics were presented by Barrett (2008); Schraml et al. (2014b, 2015d,b,a).

In the subsequent sections a literature review on research in each group is presented. Additionally, Section 4.2.4 presents recent research dealing with wood board recognition.

4.2.1 Log Shape Recognition

In the works of Chiorescu and Grönlund (2003, 2004) measurement data from the outer shapes of logs are utilized as biometric features. The log shapes were captured with a two-axis log

scanner and a three-dimensional log scanner, respectively.

Basically, Chiorescu and Grönlund (2003) is the first work dealing with log biometrics. The authors had the intention to use existing environment to enable log traceability. For their experiments, the on-bark shape of 879.571 logs (spruce and pine) was scanned using a 2-axis scanner. Out of this data seven biometric features (length, diameter, bumpiness, taper, butt, bow and ovality) were computed and stored into a database. In a first step the whole dataset was used to find the most discriminative feature set, considering different combinations of features. Results show that the best feature combination consists of four features: diameter, length, taper and bumpiness. Using these features approximately 98% of the logs are recognized as unique individuals. The second step investigates the measurement accuracy of the utilized 2D-axis scanner. Hundred logs were measured five times at random rotational positions. The standard deviations for each feature are used to assess the measurement robustness. Based on the insights of the previous investigations a tree-based searching algorithm is introduced. The recognition rate for the proposed matching algorithm is evaluated by a simulation. Therefore a second test-set is created. This test-set is derived from the measured log features and incorporates measurement deviations caused by the scanner. The simulation indicates that the utilized 2-axis scanner is too inaccurate to accomplish a recognition rate over 34%. The authors assessed that the scanner measurement accuracy and the recognition algorithm have a major impact onto the recognition rate.

As a consequence of the previous insights Chiorescu and Grönlund (2004) used a three-dimensional scanner. This scanner is normally used for optimal positioning of the logs into the headrig and is able to create a complete three-dimensional shape model of a log. Out of this model 27 parameter for optimal sawing are calculated. Nine of them were selected as biometric features. They were chosen with regard to their measurement robustness (volume, length, area minimum diameter, middle diameter, log taper, top taper, bumpiness, relative taper and bow). As test set 772 debarked logs were divided into three diameter classes and each log was scanned three times. The first scan was performed after the log was debarked. Further two scans were performed after storing periods of two weeks and two months. For the recognition procedure two different algorithms were proposed and tested. The first algorithm is a further development of the search algorithm in Chiorescu and Grönlund (2003). It is an one-variable procedural search based on a robustness ranking of the features. The robustness was estimated regarding the measurement accuracy of the scanner during the repeated scanning of a set of logs. Compared to this, the second algorithm uses all features concurrently based on multivariate principal component analysis and a nearest neighbour search. Recognition rates ranged between 80% and 95% depending on the diameter, matching algorithm and the time

span between the scan cycles. Chiorescu and Grönlund (2004) advise that future work has to pay attention on the influence of bark on the recognition rate. In most Swedish sawmills, logs get debarked/ butt end reduced and scanned before they are processed by the headrig. It follows that the first scan at the log sorting station is done with bark and the second scan is done debarked and possibly butt-end reduced.

In the work of Flodin et al. (2008a) the authors take up the suggestion for future work in Chiorescu and Grönlund (2004). The authors present investigations on traceability from the log sorting station to the saw intake. Therefore, a special three dimensional scanner is used at the log sorting station. In bark suppression mode, the scanner is able to differentiate between clear wood and bark using the so-called tracheid effect of wood. For the experiments the logs were scanned at the log sorting station and before the saw intake. The test-set is divided into two diameter specific groups, each consisting of 50 logs. At the log sorting station, each log was scanned three times with bark suppression and once without bark suppression. The scan at the saw intake (each log got debarked and butt-end reduced) was done a month later. For each scanned log 11 biometric outer shape features were extracted. Further, the features were used to compute intra-measurement differences between the three bark-suppression log scans and the inter-differences between scans from the log sorting station and the saw intake. By analogy to the previous works the measurement differences are used to rank the features regarding to their robustness and reliability for a fingerprint approach. Like in Chiorescu and Grönlund (2004), the matching is based on multivariate principal components analysis. The recognition rate was computed comparing each log from the saw intake to all logs from the log sorting station of the respective diameter group. For small sized logs and bark suppression a recognition rate of 91.8% and without bark suppression 77.6% could be achieved. Large-sized logs were hardly influenced by the butt-end reducer and consequently a recognition rate of 63.6% - bark suppression and 54% - no suppression could be reached.

4.2.2 Log to Board Recognition

Two publications from Jens Flodin (Flodin et al. (2007), Flodin et al. (2008b)) focus on traceability between logs and cut boards. Each log was scanned with an x-ray and an optical log scanner. The log length as well as the knot positions and lengths were extracted as biometric features. After sawing, a surface scanner was used to determine the board lengths and knot positions plus lengths of each board. These biometric features were used to match each board to all logs of the test-set. Results show that this approach reaches a correct matching for approximately 90% of all boards.

Furthermore, in the master thesis of Peterson (2009) a feasibility study on using end-grain characteristics to enable traceability between sawn wood and their parent logs is presented. By using log end information his thesis is thematically related to log end recognition.

Sixty Douglas fir trees were cross cut at both ends which led to 120 CS slices. Each slice was captured in a studio - three times over a period of three days. On each CS reference points were used to capture three equally aligned CS-Images from each CS. The CS-Images were then manually cropped and subdivided into cants and boards simulating end grain images of sawn wood. As a matching score the ratio of the correlated pixels between two images is used. No features were extracted and no image processing was performed. In the experiments board images were matched against cant images and cant images against CS-Images. The matching was performed between images from different days. All matching configurations reached recognition rates between 83% to 98%. However, the detailed results are less meaningful due to the oversimplified approach and experimental settings.

4.2.3 Log End Recognition

As described in Section 4.1, various works showed that concepts of human biometrics can be transferred to other fields of applications. By comparing human fingerprints to the annual ring patterns of log ends one perceives their similarity. Log end faces show biometric information in terms of annual rings, pith position, shape and dimension. This raised the question if single wood logs can be identified using CS-Images of log ends as biometric characteristics.

Basically, the scheme of a biometric recognition system is set up on five components: Data Acquisition, Preprocessing, Feature Extraction, Template Generation and Template Matching. In case of log end biometrics, data acquisition is the capturing of digital CS-Images of log ends. In the preprocessing stage CS analysis is performed. In case of CS-Images the CS in the CS-Image is separated from the background (see Section 2.2.4). Furthermore, the pith position needs to be detected which is required as reference point for CS alignment (see Section 2.2.1). Finally, the annual ring pattern is enhanced. The preprocessed CS-Image is passed to the feature extraction component which extracts information of the annual ring pattern and shape of the CS. For template generation a compact and fast comparable representation of the extracted features is computed.

Template matching is the task of verification or identification of an individual or subject. For this purpose, the individual/ subject must be enrolled in the biometric system. In case of log

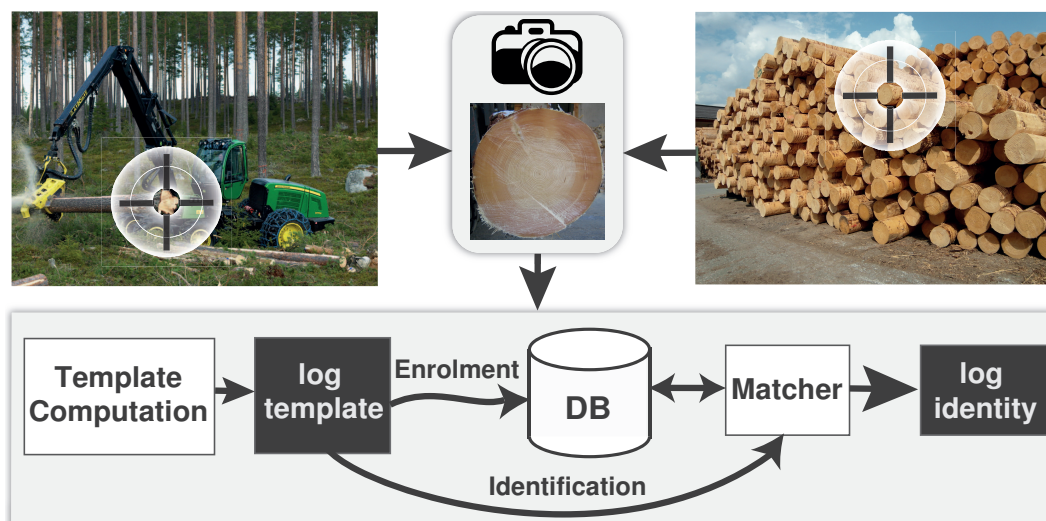


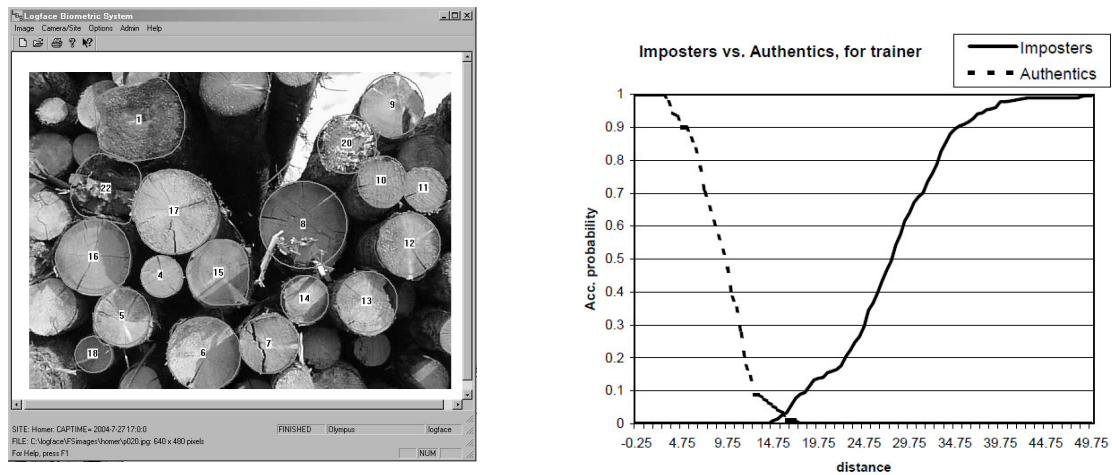
Figure 4.4: Exemplary enrolment and identification schemes for a biometric log recognition system (Image source: Schraml et al. (2015a))

recognition, the enrolment procedure could be performed during the harvesting procedure in the forest. An exemplary enrolment and identification scheme for wood logs is depicted in Fig. 4.4. For enrolment the end of a fresh cut log is captured using a digital camera mounted on a harvester. Subsequently, the first four steps of the biometric system chain are completed and the computed log template is stored to a database. Additionally, the harvester operator can assign further informational meta data to each log template in the database.

CS-Images for identification could be captured at the sorting station, at the sawmill yard or at any conveyor belt equipped with a capturing device. A captured CS Image is then processed by the biometric system and a log template is computed. This log template is matched to all available log templates in the database. Commonly, the best match is used to determine the identity of the log. Furthermore, additional meta data can be retrieved or appended from/ to the log record in the database.

4.2.3.1 Literature Review

The first work on log end biometrics was presented by Barrett (2008) as an effort to curb poaching of trees. In Fig. 4.5a the interface of the proposed biometric system is depicted. In the experimental evaluation CS-Images of the tree stump and the corresponding log ends are utilized. Both show up strong saw kerf patterns. As biometric features Pseudo-Zernike moments were computed. For establishing rotation invariance CS-Images segmented by an operator (Fig. 4.5a) are centred using the centre of mass. In the experimental evaluation



(a) Biometric System: The CSs are segmented by an operator.

(b) Genuine/ Impostor Score Distribution

Figure 4.5: Biometrics of cut tree faces (images source: Barrett (2008))

several hundred images from a few dozen samples of stump and log end were utilized. The images of each stump and log pair were captured at different distances and viewpoints. Additionally, the amount of imposter scores is increased by computing matching scores for a set of images captured from different log ends not included in the stump-log end set. The genuine and imposter distributions are depicted in Fig. 4.5b. The results are convincing and indicate that the combination of log end shape and saw pattern information represented by Zernike polynomials is suited for log to stump recognition.

As part of the FWF project TRP-254 entitled with *Traceability of logs by means of digital images (TreeBio)* we pushed the research in this field one step forward. In difference to Barrett (2008) our research focused on log tracking from forest to further processing companies (Fig. 4.4. My master thesis Schraml (2013) (sections from the theoretical part are used in this diploma thesis too) treats two tasks of a biometric log end recognition system: Pith Estimation and CS Segmentation. These tasks are treated in Section 2.2.1 and 2.2.4, respectively. So far, four publications derived from our research: Schraml et al. (2014b); Schraml and Uhl (2014); Schraml et al. (2015d,b). The testsets utilized in Schraml et al. (2015d,b) were captured in the context of this diploma thesis. In our first work Schraml et al. (2014b) longitudinal and temporal variances of CSs are analysed. These variances are related to the robustness and applicability of biometric log traceability using log end images. For this purpose, one single tree log was sliced into 35 CS slices using a bandsaw.

Each CS slice was captured four times in four time delayed sessions. Subsequently, for all CS-Images biometric templates were computed and matched to all other templates. Template computation relies on the fingerprint recognition approach proposed by Jain et al. (2000, 2001)

which was adopted and extended to work with CS-Images. This technique utilizes a Gabor-based descriptor which extracts local orientation and frequency information from the annual ring pattern. Rotation compensation is achieved by computing feature vectors for rotated versions of the input image (Fig. 4.6).

The computed intraclass matching scores were grouped into longitudinal and temporal matching scores. Longitudinal matching scores are computed between the CS-Images of different slices for each session. Temporal matching scores are computed by matching the four time delayed captured CS-Images of each CS slice.

Additionally, interclass matching scores were computed by comparing deliberately wrong rotated CS-Images to each other. The score distributions of the temporal, longitudinal and interclass matching scores are illustrated in Fig. 4.7a. The chart illustrates that the two intraclass SDs show a low overlap with the artificially computed interclass SD. A reasoning for these overlaps becomes obvious by analysing the subset structure of the temporal and longitudinal SD.

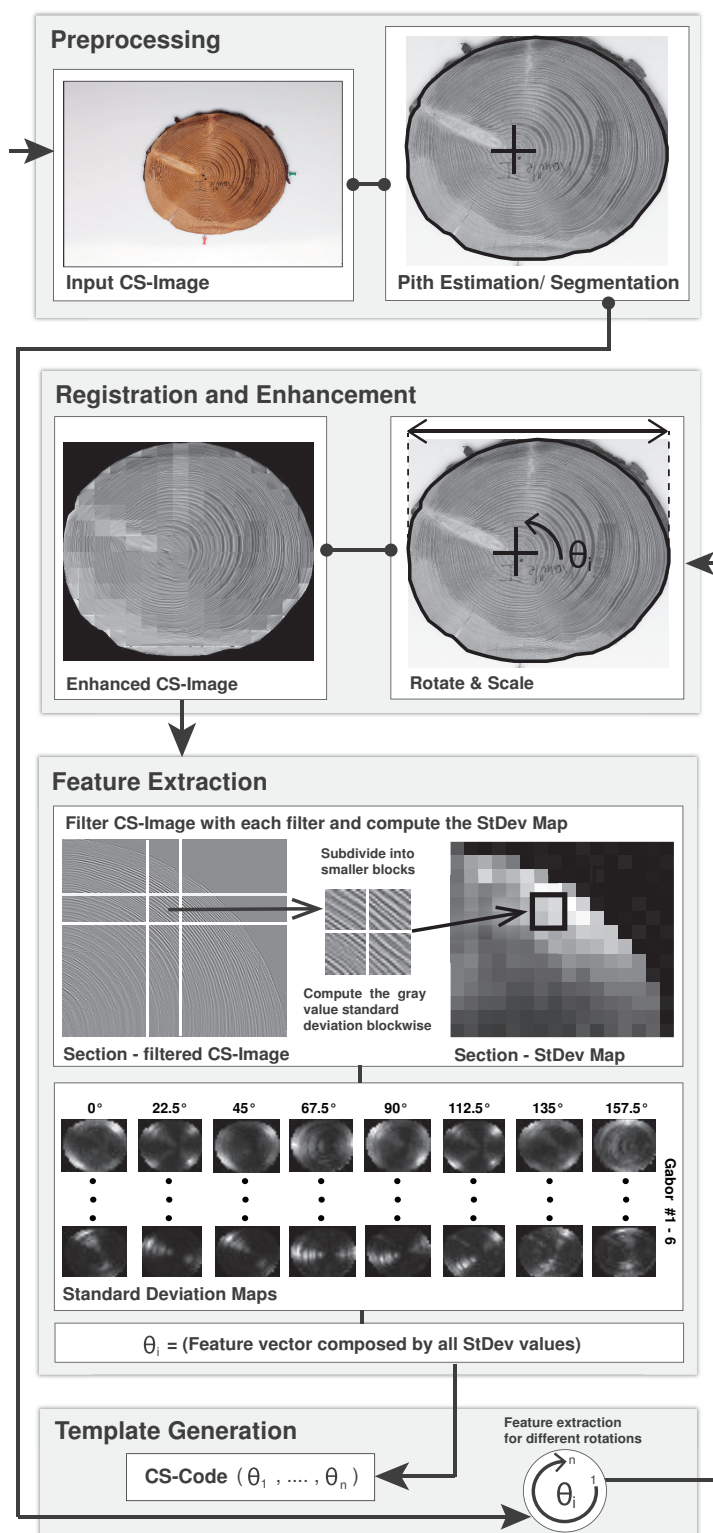


Figure 4.6: Log Template/ CS-Code computation illustration (Image source: Schraml et al. (2015a))

Results show that:

- With an increasing time span between two CS-Images of the same CS the matching score gets worse (see Fig. 4.7b) .
- Adjacent CS slices show good matching scores. An increasing slice distance between two CS slices deteriorates the matching score (Fig. 4.7c).

In our second work Schraml et al. (2015b) we shed light on the question if log end biometrics are suited to discriminate between a large set of tree logs. To address this question we explored the applicability of fingerprint and iris-recognition based methods to identify 150 different tree logs. The fingerprint-based method is the same as utilized in Schraml et al. (2014b), extended by two matching procedures which incorporate shape information in different ways. For the iris-based methods different feature extractors and matchers from the University of Salzburg Iris Toolkit (USIT) are utilized. Additionally, for both methods the impact of enhancement

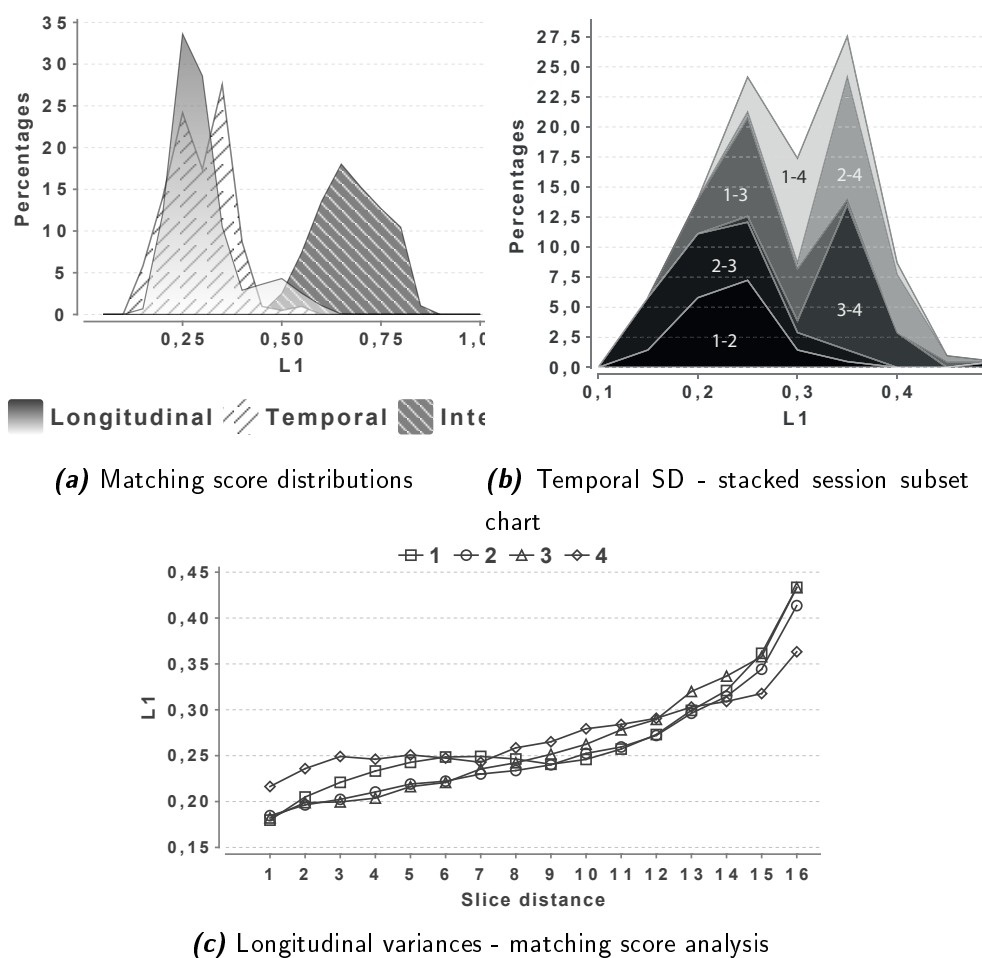


Figure 4.7: Temporal/longitudinal and interclass score distribution (SD) analysis (Images source: Schraml et al. (2014b))

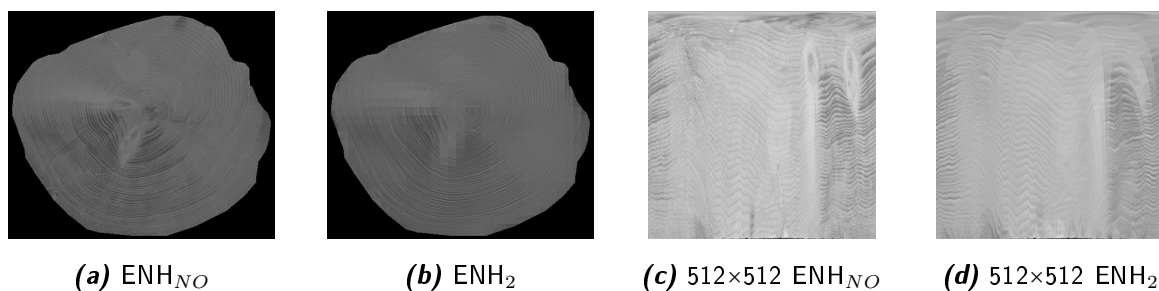


Figure 4.8: Illustration of the impact of enhancement for the two different techniques investigated in Schraml et al. (2015b). The illustrations in (c,d) show polar transformed CS-Images utilized by the iris-based methods.

is assessed. All experiments were performed without and with two different enhancement procedures. Exemplary preprocessed CS-Images utilized by the different methods are illustrated in Fig. 4.8. The results provide first valuable insights on the general applicability of log end biometrics to distinguish between a large set of tree logs. Results in Fig. 4.9 show that fingerprint and iris recognition based approaches can be successfully transferred to the field of wood log tracking. Based on the variety of 150 logs the results indicate that both approaches are suited for log identification. In the identification performance experiments the fingerprint based approach and all iris configurations which use Log-Gabor features (512×512 pixels polar transformation format) achieve 100% detection rate at Rank 1. We conclude that Gabor features are well suited to extract discriminative annual ring pattern features. All results show that shape information is important to increase the performance and the robustness of the biometric system. The best fingerprint-based approach utilized shape information in the matching procedure and the iris-based approaches rely on polar-transformation which is based on the CS boundary and pith position. Also the approach by Barrett (2008) relies to a high degree on shape information. Furthermore, all conducted experiments were based on groundtruth (GT) data of the CS boundary and pith position.

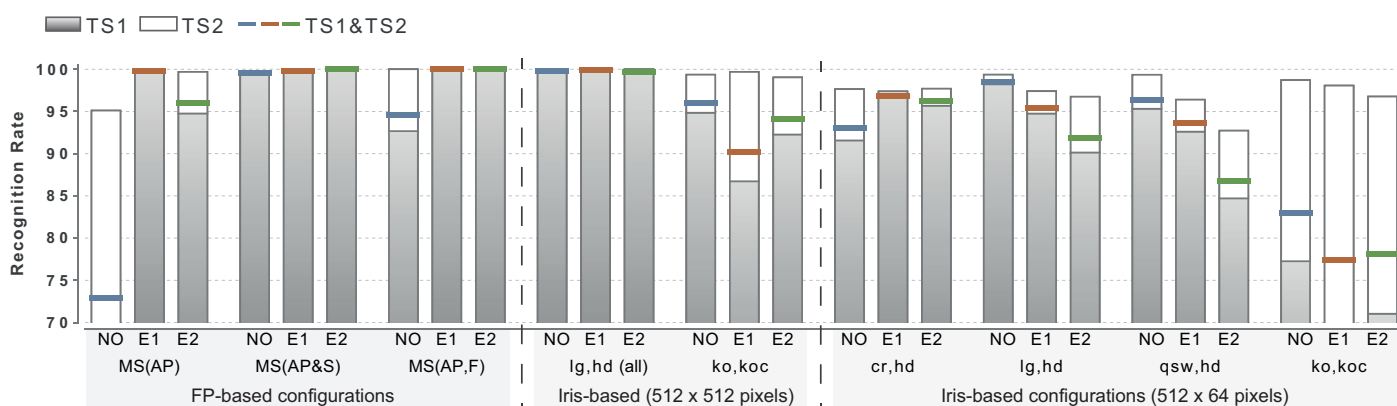


Figure 4.9: Identification performance evaluation - Rank 1 detection rates. (Image source: Schraml et al. (2015b))

Based on these observations, in Schraml et al. (2015d) we assessed the discriminative power of geometric log end features. For the experiments, again the acquired testsets of this diploma thesis were used and different geometric features (Fig. 4.10) were extracted based on the CS boundaries and pith positions. In assessing the verification performance for groundtruth data we investigated the basic discriminative power of these features. In case of groundtruth data for the CS border and pith position the verification performance evaluation showed that radial distances from the pith and centroid center to the CS boundary and Zernike moments (Z) show a high discriminative power. Score level fusion of these features leads to an EER of 0.54%. The validation of these features for automated segmentation Schraml and Uhl (2014) and pith estimation Schraml and Uhl (2013) showed that Zernike moments achieve the highest reliability. Compared to Zernike moments the EERs for centroid distances and pith distances are strongly influenced by automated segmentation and pith estimation.

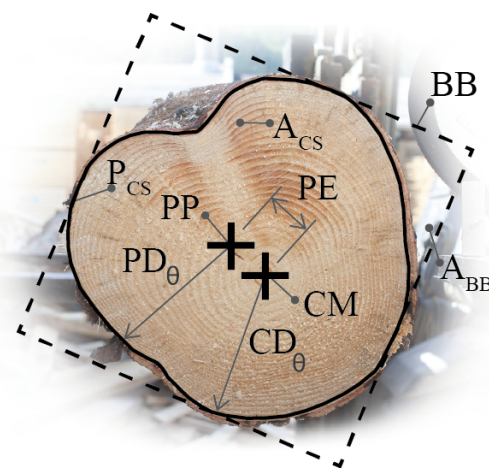


Figure 4.10: Geometric feature extraction illustration.

Finally, in Schraml et al. (2015a) additionally to the single log used in Schraml et al. (2014b) further two logs are used to explore the robustness of log end biometrics in an industrial application. From each log 16 CS slices were cut down and the rough and sanded CS surfaces of each CS slice were captured with a digital camera. Consequently, the captured CS-images enable to consider a third group of CS variations, denoted as CS surface variations. Surface variations arise if different cutting tools are utilized for the first cut in the forest and the clearance cut in the further processing company (e.g. chain-saw and circular saw). In the experiments the impact of longitudinal and surface variations on the intraclass variability and the separability between the intra- and interclass matching scores are investigated. Furthermore, the identification performance for different real world like scenarios is evaluated. For template computation the fingerprint-based approach and the improved enhancement procedure of Schraml et al. (2015b) is utilized. Three different template matching procedures enable to present results for annual ring pattern features, shape features and the fusion of both. All results show that feature fusion increases the robustness significantly and it turned out that CS surface variations are not crucial for the verification performance. Based on the identification performance experiments we conclude that biometric log recognition is qualified to overcome

the issue of cutting log ends in the sawmill up to 7.5 centimetres in thickness, even if the second cut in the sawmill is performed with another cutting tool. The analysis of the longitudinal CS variations for different slice distances points out that knots are disturbing factors. Surprisingly, the results indicate that knots do not introduce any propagative effects to the annual ring pattern and the CS shape.

4.2.4 Wood Board Recognition

Besides the recognition of logs or log to board recognition, efforts were taken to establish wood board recognition. In the context of the PhD thesis of Pahlberg (2014) three publications treat tracking of sawn boards based on digital surface images: Pahlberg and Hagman (2012); Pahlberg et al. (2015a,b).

Basically, it is assumed that knots on wood boards are suited for board recognition. In Pahlberg and Hagman (2012); Pahlberg et al. (2015a) a corner/blob detector is utilized to detect keypoints = knots on the surface of each wood board. For each keypoint a feature descriptor is computed. The feature descriptors then compose the biometric template of the corresponding board. As feature descriptors Block and Speeded-up Robust Features (SURF, Bay et al. (2008)) were utilized. Block features compute the normalized intensity information in a 25x25 pixel region around each keypoint. For the Block features two different keypoint detectors were utilized: In Pahlberg and Hagman (2012) the Features from Accelerated Segment Test (FAST, Rosten and Drummond (2006)) and in Pahlberg et al. (2015a) the Harris corner detector (Harris and Stephens, 1988) was utilized because of robustness considerations. In case of SURF features blobs are detected at different scales. For each detected blob a feature vector with 64 values is computed. SURF was configured to cover regions between 9x9 to 147x147mm. In the second paper Pahlberg et al. (2015a) the blob keypoint detector sensitivity was decreased to increase the amount of keypoint detections. Furthermore, the fusion of both methods was evaluated. In Fig. 4.11 for one board the Block and SURF feature descriptors are visualized on the original board and for an distorted version of the board which was used for matching the features. Results in Pahlberg and Hagman (2012); Pahlberg et al. (2015a) showed that the fusion of both descriptors increases the accuracy. In case of boards with more than 20 knots 100% accuracy was obtained for high and low-quality wood board surface images. For boards with a minimal number of >10 knots the accuracy decreases to 90%.

In the last paper (Pahlberg et al., 2015b) for every keypoint (=knot) a descriptor is created by computing the distances and angles to the k closet neighbours. Hence, the descriptor is

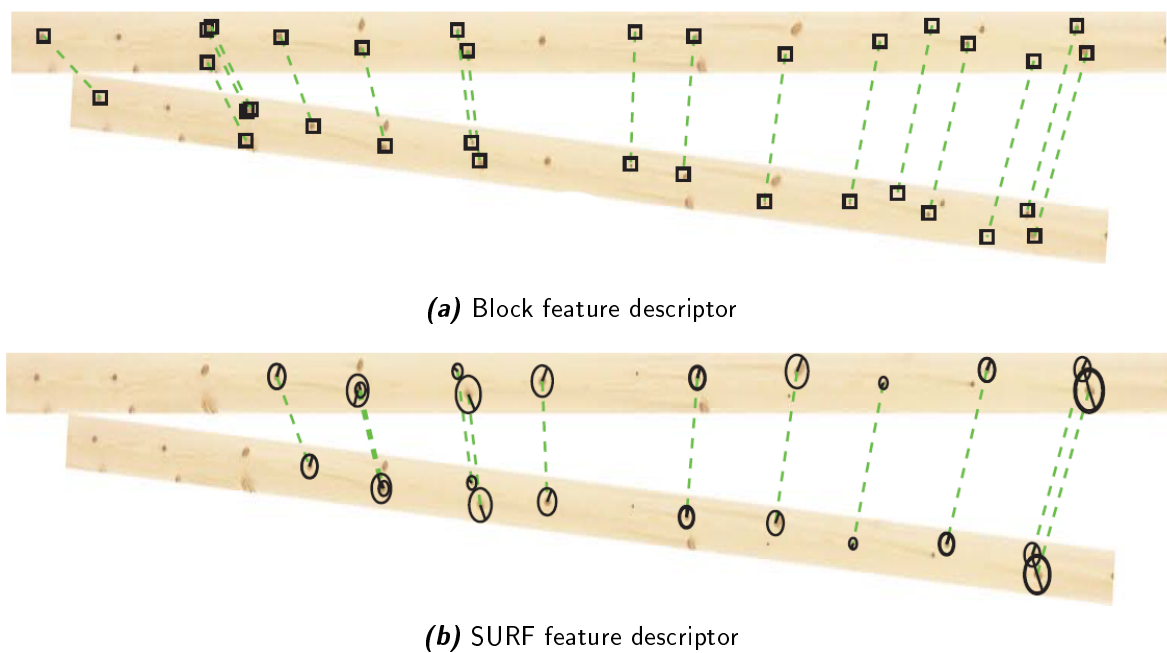


Figure 4.11: Wood board recognition based on knot detection and feature extraction (Image source: Pahlberg and Hagman (2012))

denoted as k -plet descriptor. The k -plets for each keypoint are normalized and stored in a matrix. For matching the k -plets of two boards the sum of squared (SSD) is computed between each k -plet pair. Pairs which show a low similarity $< \lambda$ are removed. In their investigations the authors searched for the best k and λ values. The authors investigated the performance with different error levels regarding the knot position detection accuracy. For an error level of 5mm, 100% recognition rate was achieved. Results show that with an increasing error level the recognition performance decreases significantly.

Part II

Log End Image Analysis Project

Chapter 5

Project Report

This chapter presents a report for the project conducted by the three pupils of the higher technical college in Kuchl. Our research on log end biometrics within the FWF TRP-254 project forms the basis for this project. For this purpose, Section 5.1 shines a light on the necessity for databases in biometric performance evaluation and in Section 5.1.1 the requirements for the acquisition of log end image databases are worked out. These requirements lead to the definition of the project goals described in Section 5.2. In Section 5.3 the project implementation is outlined. At the beginning, legal and formal requirements for the project start are outlined. Subsequently, the workpackage structure defined by the pupils is shown. In the subsequent sections (5.4,5.5,5.6) detailed reports for each workpackage are provided. This includes a very detailed description of the CS annotation tool, especially developed for this project, in Section 5.5.2. Finally, Chapter 6 concludes this thesis and summarizes the contributions of this project.

5.1 Databases for Performance Evaluation

Naturally, performance evaluation demands a database suited to compute the errors a biometric system produces. The basics of biometric performance evaluation were already introduced in Section 4.1. During the last decade several databases were published for different human biometric traits. Such databases enable that performance evaluations and results for different approaches get comparable. Nowadays, for scientific investigations in the field of human biometrics one or more of these databases have to be used in the experimental evaluation.

One major issue when exploring new fields of applications is the lack of testset data. Thus, one of the first tasks is to acquire testset data. Depending on the field of application this can be quite challenging, different requirements need to be considered and domain specific problems have to be addressed. In the next section problems and requirements for acquiring an appropriate database for log end biometrics are discussed and summarized.

5.1.1 Log End Image Database Requirements

Depending on the application a biometric system has to deal with a certain amount of individuals. Just think of human biometrics: While a door or smart-phone fingerprint scanner just needs to grant access to a few individuals, an international criminal fingerprint recognition system probably needs to handle millions of individuals.

However, biometric research is commonly conducted using databases containing a sufficient number of individuals. Such databases enable to investigate the uniqueness and permanence of the utilized biometric characteristic. Uniqueness means that the biometric characteristic and the computed templates for different individuals should vary strongly. Permanence is the requirement that they do not change over time. Related to those requirements there are two basic issues which a biometric system must handle:

Intraclass variability and Interclass similarity Interclass similarity is the problem that different individuals eventually show up similar biometric characteristics. Intraclass variability is an issue due to internal and external caused variations between a set of templates of the same individual. External variations occur due to irregularities in the template generation procedure, e.g. different sensors or capturing environments. Furthermore, the visual appearance of the biometric characteristic is affected or modified by external influences, e.g. abrasion of fingerprints. Internal variations are eventually caused by an intrinsic modification or change of the biometric characteristic itself, e.g. temporal variations caused by the ageing process.

As a consequence, two simple requirements for data acquisition in the project were defined. The first one enables to assess the interclass similarity between different logs:

Database Requirement 1 (Interclass Similarity - Variation of Individuals) *A database for investigating log end biometrics has to be composed by CS-Images of as many different logs as possible.*

The second requirement enables to assess the intraclass similarity. In case of log ends external and internal caused variations/ modifications of CSs of a single log have an impact on the intraclass variability:

Database Requirement 2 (Intraclass Variability - Variations of each individual) *Biometric system performance evaluation requires manifold data of the biometric characteristic of each individual. For each log in the database several image of it's log end need to be captured.*

5.2 Project Goals

Based on the basic need for a database the project goals were extended to provide a scope which unifies practical and a theoretical aspects. From the beginning on Erwin Tremml, my counterpart from the HTL Kuchl, was very endeavoured to set up a project together. Based on his idea, the second goal of the project was to investigate dependencies between wood properties visible on the CS and other quality relevant log measurements. Particular attention was given to investigate if any measurements show a significant correlation to the presence of reaction wood on the CS. Consequently, two goals formed the basis for the collaboration and for the pupils which processed the project:

Project Goal 1 (Database Acquisition) *Acquire a database which fulfils Database Requirement 1 and 2.*

Project Goal 2 (Analysis of log end face properties) *Investigate potential correlations between wood properties visible on log end faces and log measurements provided by a 3D log scanner.*

In declaring the project goals it turned out that a software tool is required which enables to annotate wood properties on log end faces (documentation see Section 5.5.2). A valuable side effect of such a tool is that annotated CS-Images contain groundtruth information which is useful for assessing the performance of automated CS analysis approaches. Furthermore, ground truth data can be used for template computation in the preprocessing stage. This is very valuable in case of log end biometrics to circumvent errors caused by pith estimation and CS segmentation errors.

5.3 Project Implementation

The implementation of a project as a part of the higher school certificate examination is regulated by the Austrian school education law §34(3) SchUG in conjunction with the exam regulations for higher vocational schools §22(1) BGBl. II Nr. 70.

For the official approval of the project by the HTL Kuchl, the pupils had to compose a project application in German (see Appendix .1). Together with the two advisor's and two formal representatives of the school the pupils signed this application and agreed to submit their diploma thesis until the 16th of May, 2014. In addition, a project agreement between the director of the HTL Kuchl and the FWF TRP-254 project head Alexander Petutschnigg was signed.

The application contains a short description of the project, summarizes the project baseline and specifies project and non-project goals. Furthermore, the pupils subdivided the project into six workpackages (WPs), each including a set of tasks. For each task the overall aim and the responsibilities were defined. Based on this, the pupils scheduled the project timeline (see Appendix .2).

5.3.1 Workpackages

Six WPs were processed by the pupils:

- | | |
|-----------------------|-------------------------|
| 1. Project Management | 4. Literature Research |
| 2. Data Aquisition | 5. Statistical Analysis |
| 3. Data Annotation | 6. Diploma Thesis |

On behalf of the official project partner (University of Applied Sciences Salzburg/ project leader of the FWF TRP-254) I acted as contact person for the pupils. Therefore, I was involved in the data acquisition, data annotation and statistical analysis WPs. The other WPs were carried out by the pupils with support from their advisor's. For the documentation of the project progress the pupils wrote monthly reports (Appendix .4) and protocols of our meetings (Appendix .3).

Subsequently, a review on the Data Acquisition and Data Annotation WPs is presented.

5.4 Database Acquisition

This WP constitutes the practical part of the project which was intended to be completed until the end of the summer holidays for those final projects. Consequently, the pupils have all data they need and enough time to process the theoretical part of the project and to draft their thesis.

The data acquisition WP represents the practical project part. The pupils were minor employed to honour their work and to enable a basic insurance. Thanks to Mr. Entacher and Trembl two sawmills supported the project and provided logs and technicians to accomplish data acquisition. Hence, two appointments were fixed to capture two datasets, one at each sawmill.

Basic Setup All log end images were captured using a Canon EOS DMark (35mm). Instead of using a common tripod the pupils hand-crafted a special mounting device. This device enables to fix a certain distance between the log end face and the camera sensor for all logs (Fig. 5.1).



Figure 5.1: Dataset Acquisition: The pupils handcrafted a mounting device and did all the work. Each log end was cross-cut before capturing.

5.4.1 Testset Entacher

The first log end capturing session (09.07.2013) was supported by the sawmill Entacher in Grossarl. Together with the two advisor's (Entacher, Trembl) and me we all met at the sawmill yard in the morning. While Mr. Entacher and Trembl organized a set of logs and a small truck the pupils and me explored how to fix the acquisition setup with respect to fulfil the database requirements 1 and 2 formulated in Section 5.1.1. Subsequently, the pupils captured tree by

tree. Michael Geistlinger operated a small truck and transported each log from the log pile to the place where the images were captured. Subsequently, Michael Schober chopped the log end with a chain saw which was assembled with a full chisel chain to avoid strong cutting disturbances and to emphasize the annual ring pattern. After cutting Michael Geistlinger moved the log end face to the height of the mounting device which was placed to fix the camera/log end distance. Finally, Alexander Sampl took the pictures of each log.

Altogether, log end images from 50 different logs were taken. One log end of each log was captured four times with and four times without flash. Furthermore, eight logs were chopped again and were captured once again, with and without flash.



Figure 5.2: Testset Entacher: Each row shows four CS-Images of a single log. The first two CS-Images illustrate the difference of capturing the log end with and without flash. The latter two images are taken after the log end was cross-cut, with and without flash.

5.4.2 Testset Mayr-Melnhof

The second capturing session was done in the sawmill Mayr-Melnhof (MM) in St. Georgen im Attergau by the pupils. The sawmill showed a great support and 141 logs were especially taken out of the log processing chain. To investigate a possible relationship between reaction wood on the log end face and other log properties, bended logs were chosen. Bended logs tend to show up reaction wood on their end faces.

Initially, each log was labelled with a number on the end face using a spray. Subsequently, each log was measured with the 3D-scanning device installed at the sawmill. The device provides measurements regarding taper, ovality and bending of each log. All numbered and measured logs were aligned at the sawmill yard.

For image capturing each log was processed in the following way: First, the numbered log end

was chop cut using the chain saw using the full chisel chain. Second, the cut end face was damped using a sponge to emphasize the reaction wood areas (Fig. 5.3). Third, the camera mounting device was positioned and each log was captured three times without flash. Finally, the cut slice with the reference number was captured. The captured CS-Images of each log were labelled according to the reference number.



Figure 5.3: Testset Mayr-Melnhof: CS-Images from 8 different logs

By finishing the data acquisition at the Entacher and the MM sawmill, the pupils fulfilled Project Goal 1 (see Section 5.2).

5.5 Database Annotation

This WP is required because the captured CS-Images need to be annotated for the analysis of possible relationships between CS wood properties as defined for Project Goal 2 (see Section 5.2). Hence, the annotated CS databases serve as basis for the statistical analysis WP.

Initially, the pupils sorted and labelled all captured CS-Images. For labelling the CS-Images of both datasets were named according to the following convention:

[Testset Name]_[Log ID]_[Number of CS-Image] | e.g. Entacher_1_1, MM_1_1

The IDs for the Entacher dataset logs were defined by the capturing order. For the MM dataset the same IDs as marked on the log ends were utilized. Unluckily, it turned out that for the 141 logs of the MM dataset the captured data for the logs with ID 104 to 122 (=19 logs) were lost for any reason. Thus, the MM dataset is composed by CS-Images of 141-19 = 122 logs.

Annotation of each CS-Image was done using an especially developed tool. Subsequently, the annotated wood properties and their features are outlined, followed by a detailed description of the developed annotation tool.

5.5.1 Annotated CS Properties

We decided to annotate a set of wood properties which are valuable for two different purposes:

First, the CS border and the pith position are required for image registration by the biometric log end recognition system. In case of automated pith estimation and CS segmentation there are always errors which deteriorate the biometric system performance. By using groundtruth data those errors are omitted. Furthermore, groundtruth data can be utilized to compete the performance of automated segmentation and pith estimation procedures against.

Second, further four properties are annotated to explore possible relationships between them and to investigate relationships between log end face properties and the 3D laser scanner measurement data. Furthermore, the annotated data enables to assess the performance of automated CS feature detection methods - e.g. for knots, cracks, resin pockets and reaction wood.

5.5.2 Annotation Software/ CrossSection Editor

In this section the development and the functionalities of the CS annotation software, denoted as CrossSection Editor (CS-Editor) are introduced. The tool is written in Java and thus works platform independent. For the graphical user interface (GUI) of the tool Java Swing is utilized. The wood properties are marked by defining region of interests (ROIs). For this purpose, the ROI functionalities provided by ImageJ are utilized. Basically, the tool enables to mark the following properties represented by a certain type of ImageJ ROI:

- Pith Position - Point ROI
- CS border - Polygon ROI
- Knots - Polygon ROIs
- Cracks - Polygon ROIS
- Resin Pockets - Polygon ROIs
- Reaction Wood - Polygon ROI and Line ROI

The CS-Editor enables that for each log end image of a testset all properties can be marked

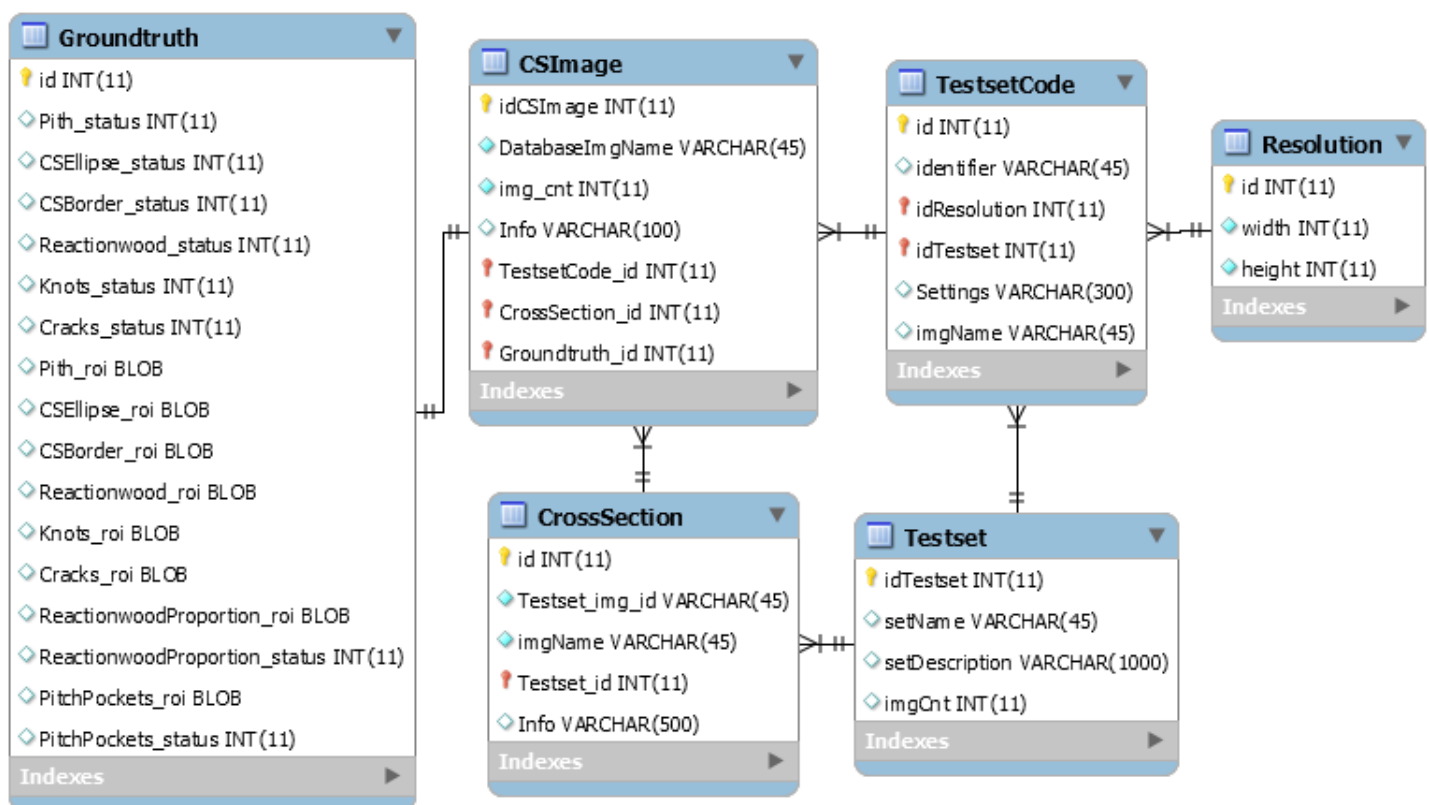


Figure 5.4: Database Scheme for the CS-Editor

and stored in a MySQL Database. For this purpose, information of each testset and each single CS-Image of a log needs to be available in the database.

5.5.2.1 Database

The database scheme utilized to map all relevant information is depicted in Fig. 5.4. The database scheme is designed to record the annotated data and meta information for each captured CS-Image. The pivotal table is the CS-Image table which contains references to the groundtruth data and meta data.

Meta information for each CS-Image is composed by information related to the testset, the subset structure of the testset and the corresponding CS of a log which was captured. Testset information is stored in the *Testset* table. Basically, a testset entry contains the name of the testset, a short description and the number of logs contained in the testset. The two entries in the *Testset* table for the Entacher and MM datasets are shown in the top left table depicted in Fig. 5.5. As described in Section 5.4.1 and Section 5.4.2 the Entacher and MM datasets contain CS-Images from 50 and 122 different logs, respectively. For each log and

the corresponding CS an entry in the *CrossSection* table is created as exemplary illustrated for 11 logs of the Entacher dataset in the middle right table depicted in Fig. 5.5. In order to map specific CS-Image capturing scenarios to each CS-Image, different testset codes in the *TestsetCode* table are specified. A testset code is assigned to a single testset by the foreign key *idTestset* and is composed by title, image resolution and a description for the testset code scenario. All testset codes for both datasets are shown in the top right table of Fig. 5.5. For each captured CS-Image an entry in the CS-Image table is created by

1. specifying a name for the CS-Image,
2. assigning a serial image number to each CS-Image of a CS,
3. may assigning a specific textual info,
4. specifying the TestsetCode ID for the session in which the CS-Image was taken (*TestsetCode_id*),
5. specifying the CrossSection ID from which the CS-Image descends from,
6. and finally specifying the ID for the corresponding entry in the Groundtruth table.

Each entry in the *Groundtruth* table is associated to one single CS-Image and contains status and data fields for each markable CS property. The status fields are restricted to hold Integer values which are used in a twofold way.

Initially, the status fields are used as markers and they are set to -2. A marker value of -2 expresses that no information for the related wood property is available so far. Depending on the wood property the status fields can be changed to values from -1 to N. Properties like the pith and the CS-border which always exist are standard wood properties. They should be annotated in each CS-Image by the annotator. Thus, the status is changed to -1 if the corresponding property has been annotated, otherwise it remains -2.

In case of wood properties which are not present in each CS-Image, the status fields can be changed to -1 which means that the corresponding wood property is not shown in the CS-Image. In case of wood properties that may occur each singular instance of a property can be annotated separately (e.g. knots). For this reason, the status field is set to the amount of marked instances. As noted, each wood property can be marked using a certain ROI type. The ROIs of each wood property are serialized in JAVA and stored as BLOB in the respective ROI field of the groundtruth table. For both testsets all required records in the database tables were created manually using a script. In case that a new dataset is captured, new entries in the database tables have to be added manually.

Testsets (in Table Testset)

idTestset	setName	setDescription	imgCnt
1	Entacher	Testet wurde im Juli 2013 im Sägewerk Entacher aufgenommen. Die Bilder wurden von 50 unterschiedlichen Baumstämmen aufgenommen. Von einem Ende jedes Baumstammes wurden jeweils 4 Fotos mit Blitz und 4 Fotos ohne Blitz aufgenommen. Von den ersten 8 Stämmen wurde zusätzlich noch eine Scheibe abgeschnitten und 1 Foto mit und ohne Blitz gemacht.	50
2	MM	Diese Holzstammenden wurden im Juli 2013 im Sägewerk von Mayr-Melnhof aufgenommen und stammen von Stämmen mit starker Krümmung. Von jedem Holzstammende gibt es 3 Bilder und eines als Referenz für die 3D Vermessung	141

Different Subsets (in Table TestsetCode)

id	identifier	idResolution	idTestset	Settings
1	ENT-OB	1	1	Entacher - Stammende mit Blitz ab fotografiert
2	ENT-MB	1	1	Entacher - Stammende mit Blitz ab fotografiert
3	ENT-NSOB	1	1	Entacher - Stammende - neuer Schnitt ohne Blitz ab...
4	ENT-NSMB	1	1	Entacher Stammende - neuer Schnitt mit Blitz abfot...
5	MM-OB	1	2	MM - Stammende ohne Blitz ab fotografiert
6	MM-REF	1	2	Referenzfoto Mayr Melnhof

List of logs/cross-sections (in Table CrossSection)

id	Testset_img_id	imgName	Testset_id	Info
1	1	Entacher_CS#1	1	NULL
2	2	Entacher_CS#2	1	NULL
3	3	Entacher_CS#3	1	NULL
4	4	Entacher_CS#4	1	NULL
5	5	Entacher_CS#5	1	NULL
6	6	Entacher_CS#6	1	NULL
7	7	Entacher_CS#7	1	NULL
8	8	Entacher_CS#8	1	NULL
9	9	Entacher_CS#9	1	NULL
10	10	Entacher_CS#10	1	NULL

CS-Images of each log/cross-section (in Table CS-Image)

idCSImage	DatabaseImgName	img_cnt	Info	TestsetCode_id	CrossSection_id	Groundtruth_id
1	Entacher_1_1	1	NULL	1	1	1
2	Entacher_1_2	2	NULL	1	1	2
3	Entacher_1_3	3	NULL	1	1	3
4	Entacher_1_4	4	NULL	1	1	4
5	Entacher_1_1_f	5	NULL	2	1	5
6	Entacher_1_2_f	6	NULL	2	1	6
7	Entacher_1_3_f	7	NULL	2	1	7
8	Entacher_1_4_f	8	NULL	2	1	8
10	Entacher_1_cut	10	NULL	3	1	10
11	Entacher_1_cut_f	11	NULL	4	1	11

Groundtruth Information for each CS-Image of a log/cross-section (in Table Groundtruth)

id	Pith_status	CSEllipse_status	CSBorder_roi	Reactionwood_roi	Knots_roi	Cracks_roi	ReactionwoodProportion_roi	ReactionwoodProportion_status	PitchPockets_roi	PitchPockets_status
1	1	-1	[BLOB - 252 B]	[BLOB - 414 B]	[BLOB - 22 B]	[BLOB - 200 B]	[BLOB - 725 B]	3	[BLOB - 222 B]	1

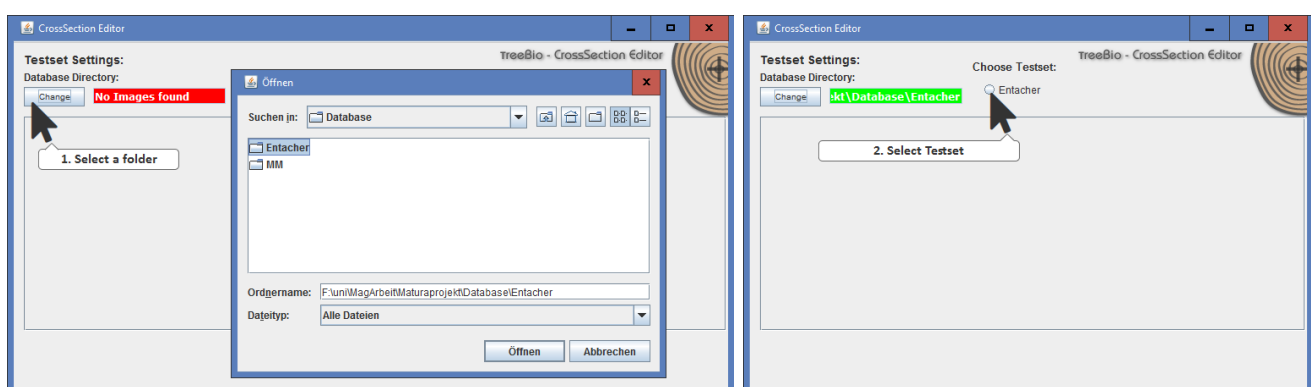
Figure 5.5: CS-Editor - MySQL Database Tables: Exemplary entries illustrating the mapping of the data which is stored for each CS-Image in the database.

5.5.2.2 CS-Editor Workflow and Features

At startup the CS-Editor searches for CS-Images of all testsets which are available in the predefined standard CS-Image database folder. In order that CS-Images are detected the files have to be named in the same way as in the CS-Image database table. Each testset for which CS-Images were found is made available for selection in the menu bar. If no CS-Images were found the user can select another directory which is subsequently used to search for CS-Images (Fig. 5.6a). When the user selects a testset (Fig. 5.6b) the CS-Editor fetches the Groundtruth record for each CS-Image of the testset which is available in the directory. Subsequently, an overview for all CS-Images and wood properties is shown in the main frame of the CS-Editor (Fig. 5.7). If the CS-Image name in the first column (Image List) has a red background the image file is not available in the chosen directory; otherwise a green background is shown (Fig. 5.8). For each available CS-Image the fetched groundtruth table record is utilized to provide information about the corresponding wood properties in a set of columns in the main frame (Property Options).

Annotation Procedure The property option columns (Fig. 5.7) in the main frame enables to edit a certain wood property. As noted, some wood properties are mandatory and others are not.

For the mandatory properties (Pith, Ellipse, CS border) the corresponding cell of the CS-Image provides background-colour and textual information which indicate if the property has already been annotated. If the property has already been annotated it is layered green and the textual information indicates that the annotation can be modified. To open the annotation dialogue



(a) CrossSection Editor at startup: Select directory.

(b) Each detected testset is selectable.

Figure 5.6: CS-Editor startup



Figure 5.7: Overview of all CS-Images and wood properties for the selected testset.

Slices_RGB_Session4_Kanüle1_02	Edit PP	Select	Edit	Yes/No
Slices_IR715_Session4_Kanüle1_02				

Figure 5.8: Display for two CS-Images of the same CS of a testset. For the green layered image name the corresponding image file is available in the selected database directory. The corresponding image file of the red layered image name was not found.

and to start the annotation procedure a single-click on the button in the corresponding property cell is required.

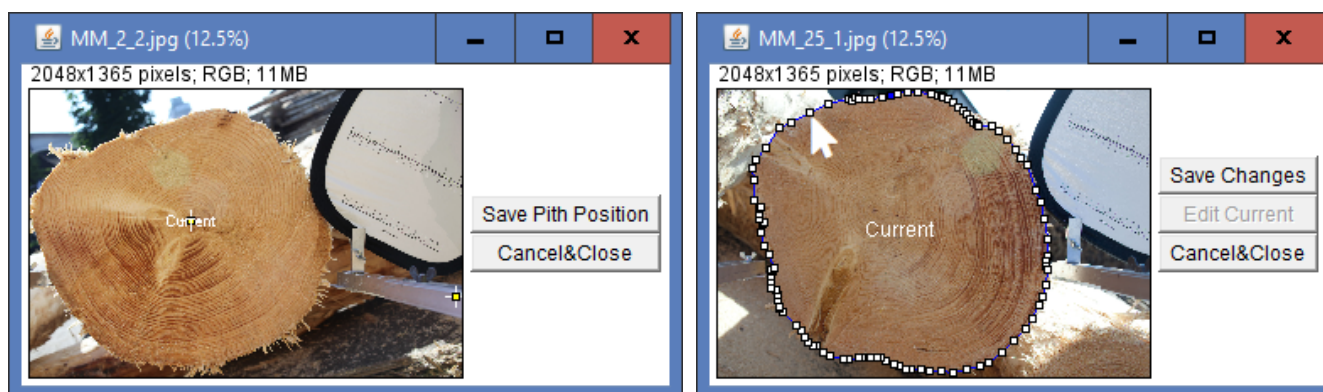
In case of the non-mandatory properties a two-fold annotation procedure needs to be performed. For this purpose two different cells are used to annotate each property. The first column is used to specify if a CS-Image shows this property. Initially, the non-mandatory properties are layered with a dark-yellow colour and the textual information asks the user to provide information regarding the presence of the property. By single-clicking the button in the corresponding cell, the user can specify if the property exists or not. If the user confirms that a specific property exists, the state of the second column switches and provides the same functionality as the cells for the mandatory fields. Just a single-click is required to start the annotation procedure.

Basically, all annotation dialogues share some basic features. Each dialogue provides a button for saving and closing. Editing is different for features which occur once and for features where several instances of a property may occur. In case of the mandatory properties all are single instance properties. Hence, if the dialogue has been opened in edit mode a third button provides an option to modify the currently annotated instance of this property. On

the other hand, all non-mandatory properties may show no or multiple instances on a CS. For this purpose, the ROI Manager of ImageJ is utilized. When the annotation dialogue opens additionally the ROI Manager is shown. The ROI Manager provides an add, delete and edit option to annotate multiple instances of a specific property.

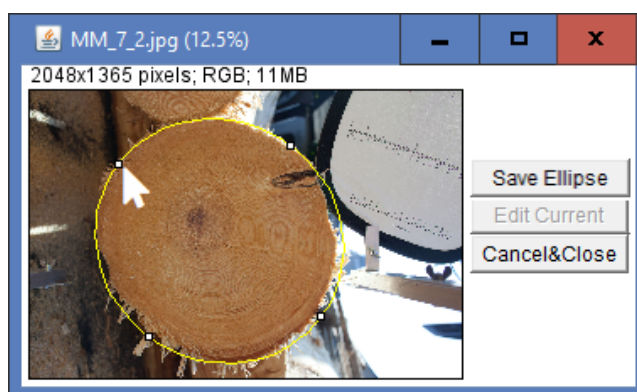
Furthermore, all dialogues enable zooming using the plus and minus key of the keyboard. Therefore, the cursor should be placed at the center point of the desired zoom region and by pressing + or - the image is enlarged or shrunk with the cursor position as center point. Thus, it is easy to navigate around and to zoom in/out to a certain ROI. Subsequently, short descriptions for the annotation procedures of each wood property are provided.

Pith For annotating the pith position the user just has to click on the pith position in the CS-Image in the dialogue using the mouse cursor (Fig. 5.9a). This places a pith position marker. The marker can be moved or reset to another position.



(a) Pith = set point at the pith position.

(b) CS border = polygon points along the CS area border.



(c) Ellipse = ellipse which embraces the CS area.

Figure 5.9: Mandatory CS properties

Ellipse The ellipse is placed in the CS-Image window by one click. By clicking and holding the mouse button the left x-axis point is set. Then the ellipse can be shrunk or enlarged by dragging the right x-axis point of the ellipse. After releasing the mouse button the ellipse is fixed. After fixing, four anchor points enable to improve the position and form of the ellipse (Fig. 5.9c).

CS border For the CS border the points of a polygon have to be specified. The start point of the polygon is defined by the first click. Subsequently, further points should be added according to the complexness of the CS border shape until the start point is reached again. Finally, the polygon needs to be closed by clicking on the start point. The final polygon can be modified by dragging the anchor points (Fig. 5.9b).

Reaction Wood Proportion The reaction proportion is determined according to the Austrian grading rules (ÖHHU). Therefore, the reaction proportion is determined in relation to the log diameter. Thus, the log diameter needs to be specified by an arrow that crosses the pith position and intersects the largest possible share of reaction wood (Fig. 5.10 - Arrow). Initially, the user has to specify an arrow which defines the log diameter. The log diameter arrow is marked by a click at the start and the end point in the CS-Image. Subsequently, the user has to confirm the log diameter arrow using the "Save arrow" button. By doing this, the ROI Manager is opened and the arrow is added to the ROI Manager list. All subsequent ROI lines, added over the ROI Manager, should be placed on this arrow at sections where the arrow crosses a reaction wood area. For adding a new line, the line needs to be drawn first. By clicking the "Add" button from the ROI Manager the new line is added to the ROI Manager. Each ROI line can be modified by selecting it in the ROI Manager and dragging the anchor points. The reaction wood proportion is defined as the ratio between the length of the log diameter arrow and the total length of all placed reaction wood lines.

Reaction Wood Areas Like for the CS border each reaction wood area should be annotated by a single polygon. For this purpose, the user draws a polygon embracing a certain reaction wood area (Fig. 5.11). The reaction wood polygon can be added using the add option in the ROI Manager. Subsequently, a new area can be annotated by a polygon. Each added reaction wood polygon can be added/deleted by selecting it in the ROI Manager. Finally, the status of the ROI Manager needs to be saved using the "Save RM-Status" button. This quits the annotation procedure.

Knots, Cracks and Resin Pockets The annotation procedures for knots (Fig. 5.12), cracks (Fig. 5.13) and resin pockets (Fig. 5.14) are the same as for reaction wood areas. The

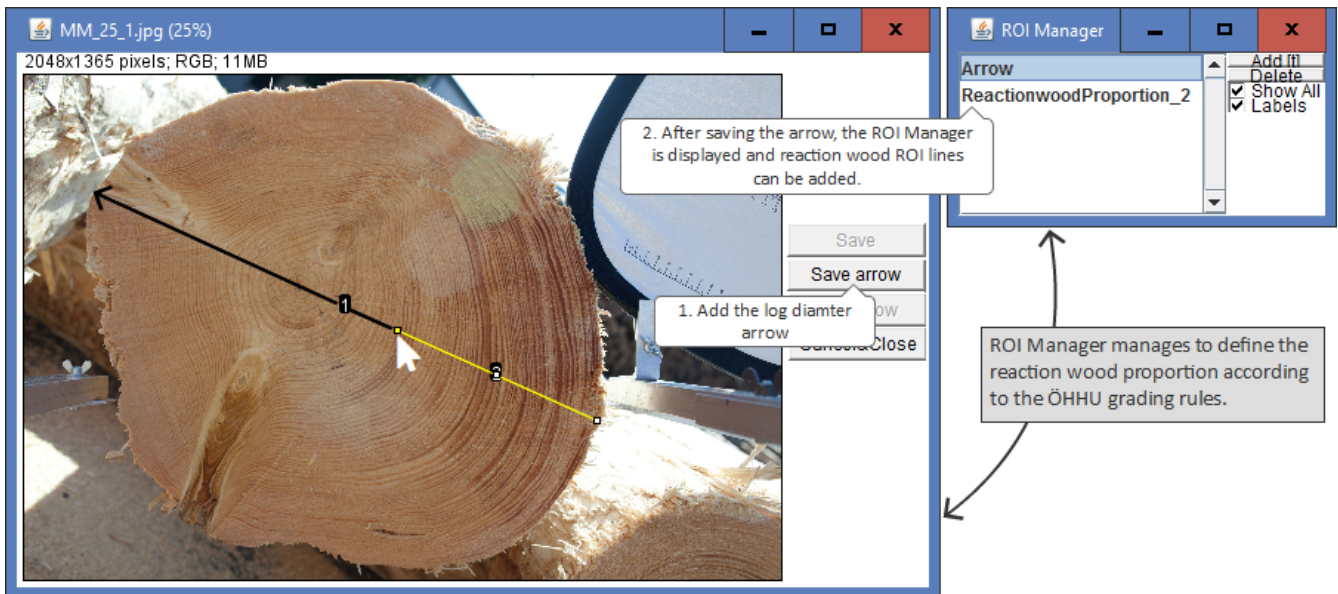


Figure 5.10: Reaction Wood: Specifying the reaction wood amount according to the ÖHHU.

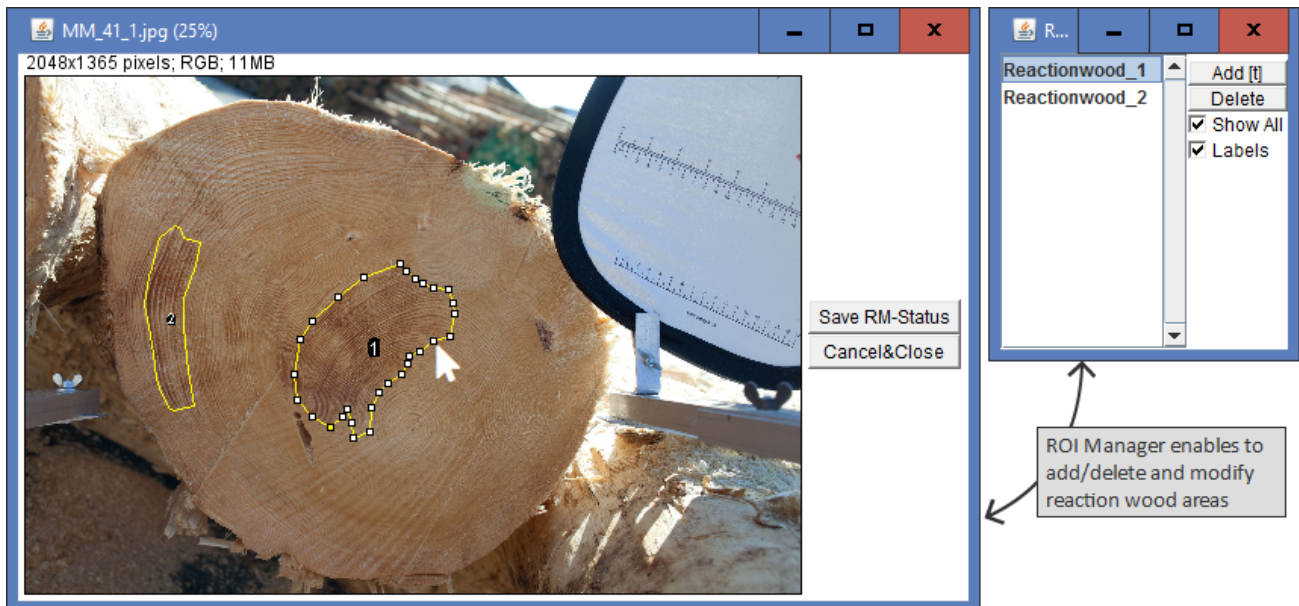


Figure 5.11: Reaction Wood Areas: Each reaction wood area is specified by a single polygon.

area of each property instance is annotated with a polygon which is added to the ROI Manager.



Figure 5.12: Knots: Each knot is specified by a single polygon embracing the knot area.

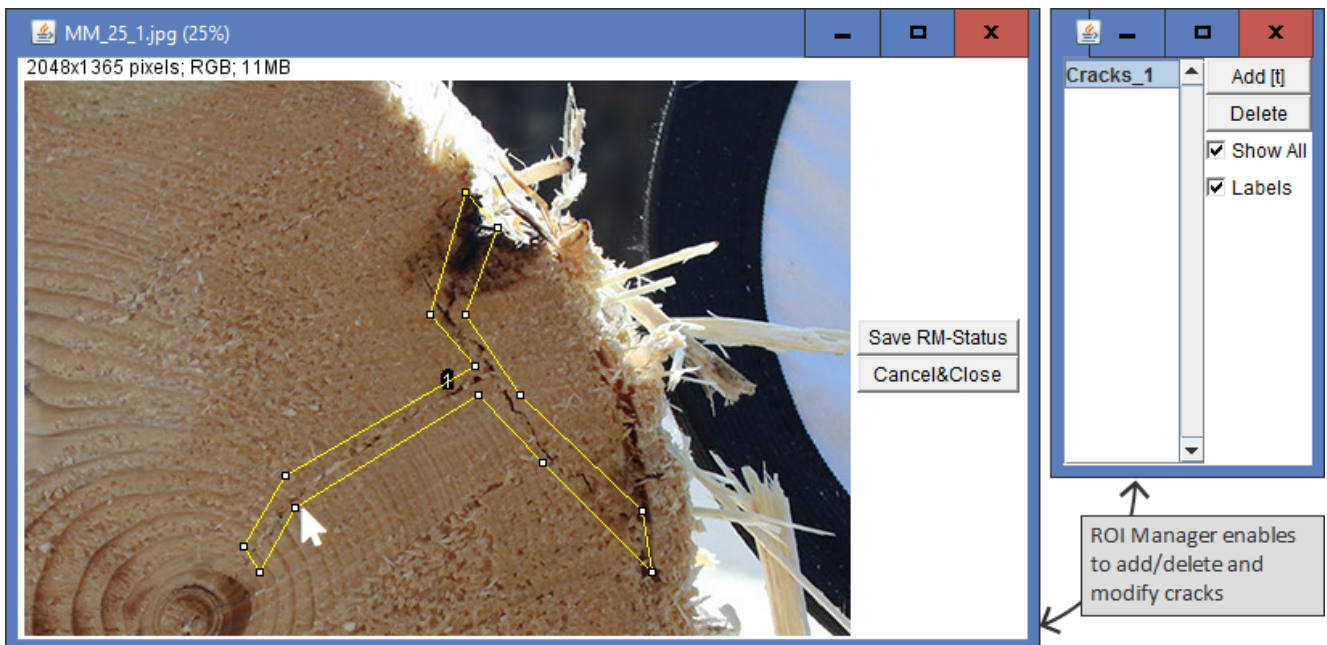


Figure 5.13: Cracks: Each crack is specified by a single polygon embracing the knot area.

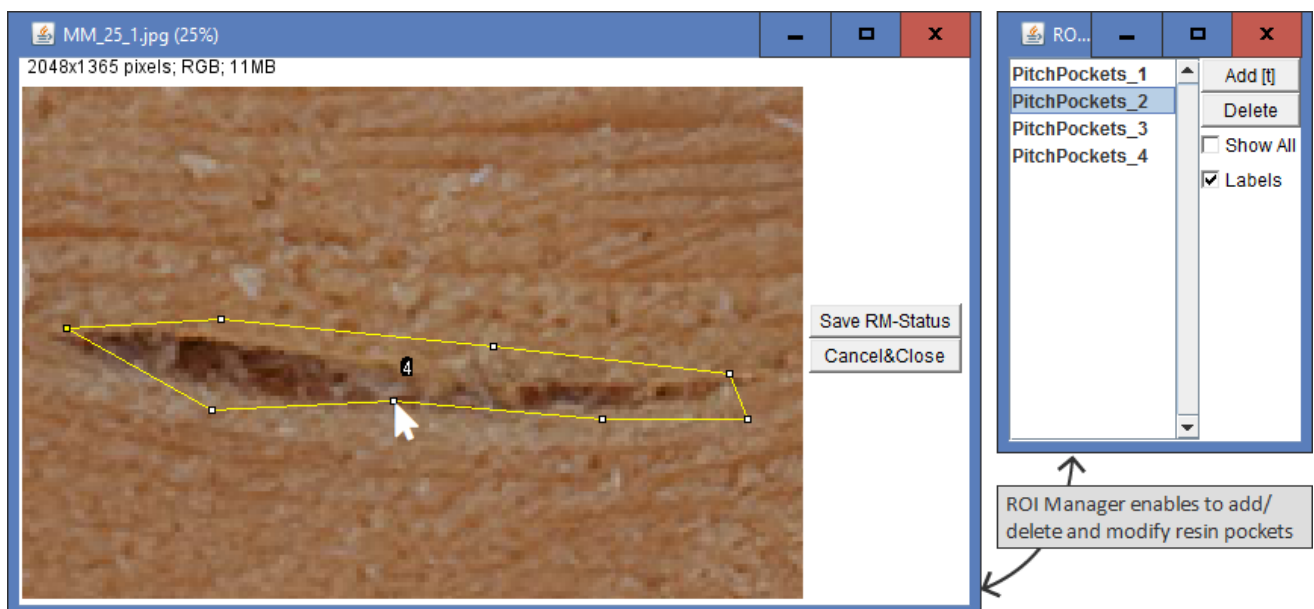


Figure 5.14: Resin Pockets: Each resin pocket is specified by a single polygon embracing the area of the resin pocket.

Workflow Features To improve and support the annotation workflow three features were implemented (see Fig. 5.15):

1. A double click on the CS-Image name in the first column opens the CS-Image and visualizes all annotated properties.
2. The pictures of a single CS for both datasets were captured with nearly no positional variations. Thus, a copy function is valuable to copy the annotated properties of one CS-Image of a CS to the other CS-Images. Two Drag&Drop functions are available. The first option enables to copy all annotations from one to another CS-Image by dragging the image name cell to the target image name cell. After releasing the mouse button the user is asked to confirm the copy action. Already annotated features for the target image are overwritten. The second function needs to be enabled using the "Single D&D" checkbox. Subsequently, particular annotated properties can be copied between CS-Images. For this purpose, the corresponding property cell of the origin CS-Image needs to be dragged from to the respective wood property cell of the target CS-Image. The user is again asked to confirm the copy action.
3. Because there are still variations between different CS-Images of a CS the locations of the copied wood property annotations need to be adjusted. To enable this adjustment for all wood properties together in a single procedure a move feature is provided. Therefore, a reference property for the movement action must be chosen. After selecting the reference property and pressing the "Move Rois" button a dialog is shown (Fig. 5.15). In this dialogue the reference property is shown which should be moved to the correct position. After confirming the action in the dialogue the movement is applied to all other annotated wood properties.

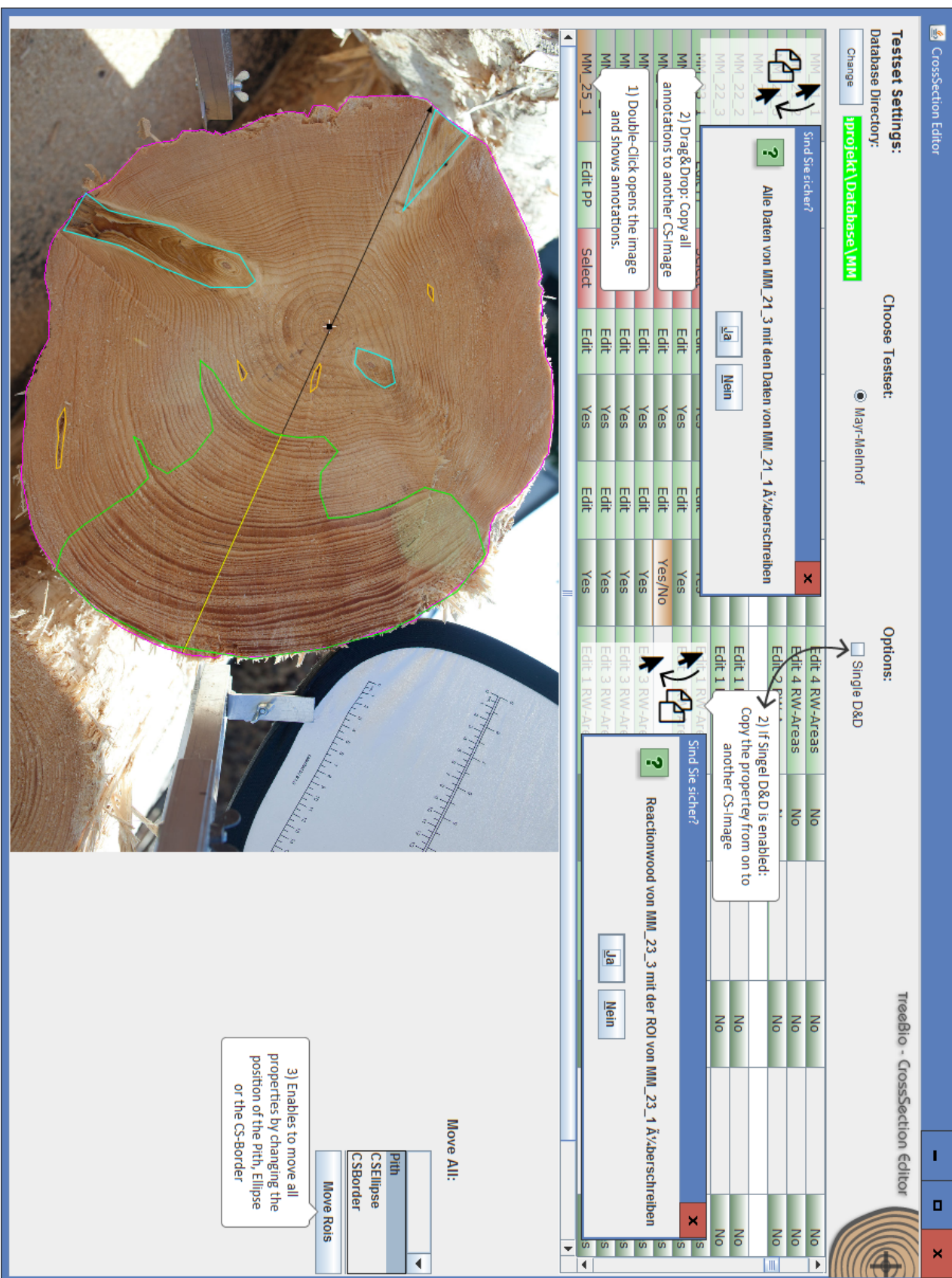


Figure 5.15: The CS-Editor interface provides three extra features to improve and support the workflow.

5.6 Statistical Analysis

In this work package the pupils investigated possible relationships within wood properties on log end faces and to other log properties provided by a 3D log scanner as formulated for Project Goal 2 in Section 5.2.

For the statistical analysis we had to define relevant property measurements which can be computed from the annotated properties. We selected eight measurements which are denoted as log end face measurements - see Table 5.1. These log end face measurements were computed

1. CS-Area = Area of the CS [Pixel].
2. RW-Area = Summed area of all annotated reaction wood areas [Pixel].
3. R-Area = Summed area of all annotated resin pockets [Pixel].
4. K-Area = Summed area of all annotated knots [Pixel].
5. λ -Ellipse = Axis ratio of the CS shape ellipse.
6. E (Eccentricity) = distance between the pith position and the CS ellipse centre [Pixel].
7. D = Diameter, marked for the measurement of the reaction wood proportion according to the grading rules [Pixel].
8. RW-Length = Summed lengths of the reaction wood areas intersected by the diameter arrow [Pixel].

Table 5.1: Log End Face Measurements

for each single CS-Image using the annotated data and were stored in an Excel file. For the MM dataset the pupils assigned the 3D-scanner protocol entries to each log using the protocol image which shows the ID label sprayed on the log end face (Fig. 5.16). The 3D-scanner protocol (just available for the MM dataset) provides a large list of log shape measurements that can be used for the statistical analysis. The utilized measurements are listed in Table 5.1.

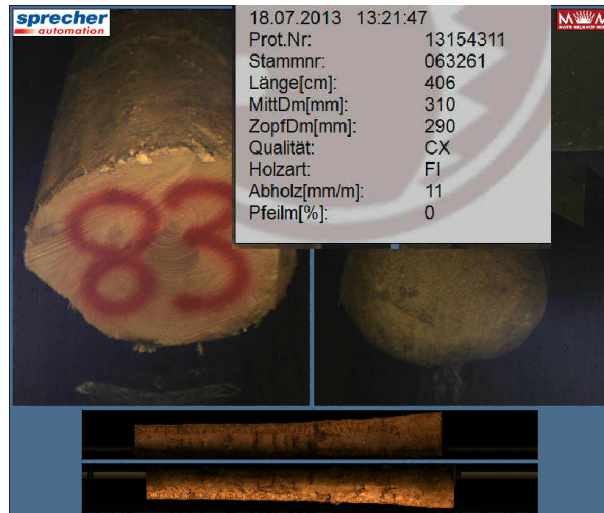


Figure 5.16: Protocol Image for log ID 83 of the MM dataset produced by the Sprecher 3D-log scanner

1. O-Top = Ovality measured at the top of the tree log.
2. O-Mean = Mean ovality of all ovality measurements.
3. O-L1021 = Ovality measured according to the ÖNORM L1021.
4. Curvature = Curvature of the log.
5. Taper = Taper of the log.

Table 5.2: 3D-Scanner Log Shape Measurements

5.6.1 Results

The statistical analysis was carried out by the pupils supported by their advisor's. Subsequently the main results of the statistical analysis presented by the pupils, in their diploma thesis Geistlinger et al. (2014), are summarized. The pupils subdivided their statistical analysis into a correlation and a regression analysis.

5.6.1.1 Correlation Analysis

One major question in the project was to investigate if there is any relationship between the reaction wood measurements on the log end face and the ovality log shape measurements provided by the 3D log scanner. The correlation plots are shown in Fig. 5.17. For a better

overview all correlation plots depicting the correlation between the ovality and reaction wood measurements are coloured with a green background. The yellow coloured plots show the correlation just for reaction wood measurements from the log end face or the ovality measurements from the 3D log scanner. Results show that there is no remarkable correlation between

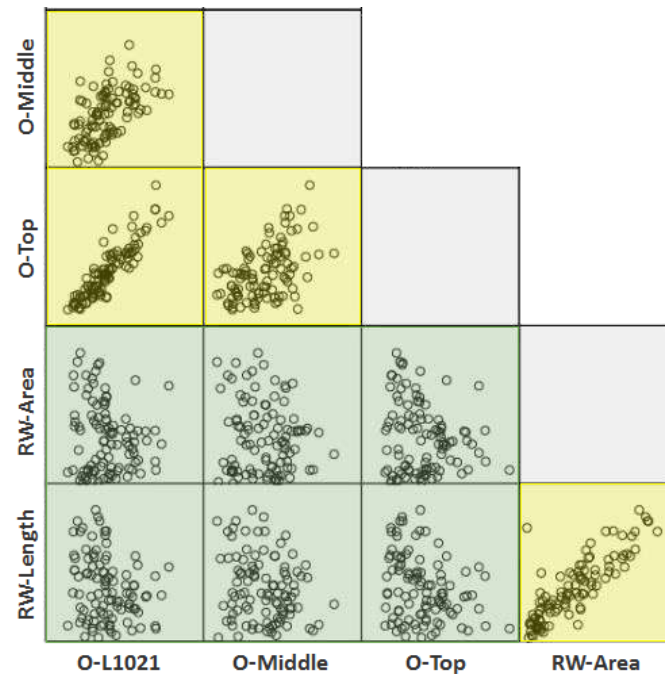


Figure 5.17: Correlation of ovality measured by the 3D log scanner and the two log end face reaction wood measurements (Image source: Geistlinger et al. (2014)[p.45, modified])

reaction wood measured on the log end face and ovality measured by the 3D log scanner (green background). On the other hand, the results show that there is some correlation within the different reactionwood and ovality measurements (yellow background). This leads to the conclusion that ovality measured by the 3D-log scanner is not suited as a predictor for the reaction wood content of a log.

Furthermore, correlations between reaction wood or ovality and other measurements were assessed. The corresponding correlation coefficients (R^2) are depicted in Table 5.3. The first two rows in Table 5.3 show the correlation coefficients between reaction wood (RW-Length, RW-Area) and the eccentricity (E) log end face measurements. The correlation for RW-Length/E accounts $R^2 = 0.44$ and for RW-Area/E a value of $R^2 = 0.160$ was observed. These values show that there is at least a kind of correlation between the eccentricity and the presence of reaction wood on log end faces.

The correlation for RW-Length/Curvature ($R^2 = 0.159$) is in the same range and shows that there exists a minimal correlation between reaction wood on the log end face and the curvature

Measurement 1	Measurement 2	R ²
RW-Length	E	0.244
RW-Area	E	0.160
RW-Length	Curvature	0.159
RW-Length	RW-Area	0.715
O-L2012	E	0.00005
O-Top	O-Middle	0.279

Table 5.3: Correlation coefficients for selected measurements

of the log. To be able to make an exact statement more data is required and the structure of the data should be more balanced. The MM testset basically consists of logs which show a strong curvature and for a meaningful evaluation also logs with a low curvature are required.

Next, the correlation between the two log end face reaction wood measurements was assessed which shows a correlation of $R^2=0.715$. Compared to all other results, these measurements are highly correlated. It can be stated that the simplified reaction wood measurement method according to the Austrian grading rules is well suited.

The pupils also assessed if the 3D log scanner ovality measurement (O-L2012) correlates with E. These two measures show clearly no correlation which confirms the results of the reaction wood/ovality results.

Finally, the pupils assessed the correlation between the O-Top/O-Middle ovality measurements of the 3D-log scanner which achieves a R^2 of 0.279. This correlation is also not that high and shows that the ovality is not constant along the log length axis.

5.6.1.2 Regression Analysis

In the final step a regression analysis was performed. For different configurations one dependent and a set of independent variables were defined. In the regression analysis for each configuration the best independent variables subset was determined.

RW-Length/Curvature Analysis For this configuration the RW-Length was set as dependent variable and different curvature measurements (not introduced in this thesis) from the 3D log scanner measurements were set as independent variables. Except the middle curvature (given in %) all other curvature measurements were sorted out by SPSS using gradual

selection. Therefore, a correlation coefficient of $R^2=0.399$ is achieved which is quite high compared to the correlation analysis results.

5.6.1.2.1 RW-Length Regression Analysis Again the RW-Length was used as dependent variable. As independent variables all available measurements were utilized. In the gradual selection E, λ -Ellipse and O-Top were selected and together they achieve a correlation coefficient R^2 of 0.773.

Chapter 6

Conclusions

The aim of this diploma thesis was to acquire testset data for the TreeBio project (FWF TRP-254). For this reason a graduate project at the higher technical college Kuchl was initialized and accompanied. Three pupils successfully processed the project. Within the project the pupils completed a practical and a theoretical part. In the practical part two different CS-Image datasets were captured at two different sawmills. In total 172 different logs were captured and all CS-Images were annotated by the pupils. For the practical part of the project the pupils used the annotated data and log shape measurements from a 3D log scanner to perform a statistical analysis. In this analysis relationships for the annotated properties and the log shape measurements were investigated. Results showed no strong correlation between log end face measurements and the 3D laser scanner measurements. However, the results showed that the reaction wood measurement procedure defined by the Austrian grading rules produces reliable results and correlates with the reaction wood area measurements.

As a practical component of this diploma thesis an annotation tool was developed which enables to annotate CS properties in CS-Images. Meta-information and the annotated groundtruth information for each CS-Image is stored in a database. Within the TreeBio project the annotated datasets were already used for the experimental evaluation in two publications Schraml et al. (2015b,d). Furthermore, the annotation tool was used to annotate further testsets which were already utilized in Schraml et al. (2014b, 2015a).

Part III

Appendix

.1 Project Application HTL Kuchl

	Holztechnikum Kuchl	
	Abteilung: Betriebsmanagement - Holzwirtschaft	

DIPLOMARBEIT

5BHBMMH – Reife- und Diplomprüfung 2013/2014

Thema/Projekttitle	„TreeBio – Fotografie von Holzstammenden“
Aufgabenstellung (Kurzfassung)	<p>Ziel des Projekts ist die Untersuchung eines möglichen Zusammenhangs zwischen messbaren Größen eines Stammes (z.B. Ovalität oder Krümmung) und Reaktionsholzbildung.</p> <p>Weiters soll geeignetes Datenmaterial für wissenschaftliche Untersuchungen zur Stammverfolgung gewonnen werden.</p> <p style="text-align: right;">Ergänzende Ausführungen siehe Seiten 3 bis 5.</p>
Kandidaten / Kandidatinnen	Betreuer / Betreuerin
Michael Geistlinger	Dr. Karl Entacher
Alexander Sampl	DI Erwin Tremel
Michael Schober	
Externe Kooperationspartner	
Firma / Institution: <ul style="list-style-type: none"> - Fachhochschule Salzburg GmbH, Campus Kuchl, Markt 136, A-5431 Kuchl - Universität Salzburg, Department of Computer Sciences, Jakob Haringer Str. 2, 5020 Salzburg - Firma Mayr-Melnhof Holz, 4890 Frankenmarkt - Sägewerk Entacher GmbH & CO KG, 5611 Großarl 	
Betreuer / Kontaktperson: Prof. Dr. Alexander Petutschnigg	
Schriftliche Kooperationsvereinbarung liegt vor: Siehe Anhang 1	
Budget: siehe Punkt 6	
Bedeckung durch: siehe Punkt 6	
Geplante Verwertung der Ergebnisse:	
Die Ergebnisse werden zu wissenschaftlichen Zwecken verwendet und den kooperierenden Institutionen zur Verfügung gestellt.	

 hfi bildung mit zukunft	Holztechnikum Kuchl Betriebsmanagement - Holzwirtschaft	 hfi holz technikum Kuchl
Abteilung:	Betriebsmanagement - Holzwirtschaft	

Erklärung

Die unterfertigten Kandidaten / Kandidatinnen haben gemäß § 34 (3) SchUG in Verbindung mit § 22 (1) ZI. 3 lit. b der Verordnung über die abschließenden Prüfungen in den berufsbildenden mittleren und höheren Schulen, BGBl. II Nr. 70 vom 24.02.2000 (Prüfungsordnung BMHS), die Ausarbeitung einer Diplomarbeit mit der umseitig angeführten Aufgabenstellung gewählt.

Die Kandidaten / Kandidatinnen nehmen zur Kenntnis, dass die Diplomarbeit in eigenständiger Weise und außerhalb des Unterrichtes zu bearbeiten und anzufertigen ist, wobei Ergebnisse des Unterrichtes mit einbezogen werden können.

Die Abgabe der vollständigen Diplomarbeit hat bis spätestens

16. Mai 2014, 12.00 Uhr

beim zuständigen Betreuer zu erfolgen.

Die Kandidaten / Kandidatinnen nehmen weiters zur Kenntnis, dass gemäß § 9 (6) der Prüfungsordnung BMHS nur der Schulleiter bis spätestens Ende des vorletzten Semesters den Abbruch einer Diplomarbeit anordnen kann, wenn diese aus nicht beim Prüfungskandidaten (bei den Prüfungskandidaten) gelegenen Gründen nicht fertiggestellt werden kann.

Kandidaten / Kandidatinnen	Unterschrift
Michael Geislinger	
Alexander Sampl	
Michael Schober	


Dr. Erwin Troim
Betreuer


Prof. Dr. Johann Brtner
Abteilungsleiter

Genehmigung:

Kuchl, am 25. Mai 2013


Dr. Karl Ertacher
Betreuer


Prof. Dr. Herfried Kogler
Direktor


HR Dr. Robert Vasek
Landeschulinspektor

 hfi bildung mit zukunft	Holztechnikum Kuchl Betriebsmanagement - Holzwirtschaft	 hfi holz technikum Kuchl
Abteilung:	Betriebsmanagement - Holzwirtschaft	

1. Kurzbeschreibung des Partnerbetriebes

Mit 16 Bachelor- und 9 Masterstudiengängen sowie einem postgradualen Lehrgang ist die Fachhochschule Salzburg ein leistungsstarker Bildungsanbieter im Hochschulbereich. Gegründet Mitte der Neunziger Jahre hat sich die FH Salzburg in den Bereichen Ingenieurwissenschaften, Sozial- & Wirtschaftswissenschaften, Design, Medien & Kunst sowie Gesundheitswissenschaften einen hervorragenden Ruf in der europäischen Hochschul- und Forschungslandschaft erworben.

Der für dieses Projekt zentrale Kooperationspartner ist der Studiengang Holztechnik und Holzbau (HTB), der dem Diplomstudiengang HTW nachfolgende Bachelorstudiengang. Dieses Projekt wird im Rahmen eines FWF Forschungsprojekts in Zusammenarbeit mit der Universität Salzburg, Department of Computer Sciences durchgeführt.

2. Ist-Situation im Betrieb (Projektausgangssituation)

Ob Zusammenhänge zwischen Holzanmalen, die am Stammmerschnitt erkennbar sind und messbare Größen eines Stammes vorhanden sind wurde in dieser Form noch nicht genauer untersucht. Die Ausgangssituation besteht deshalb darin grundlegende Rahmenbedingungen festzulegen in welcher Form diese Untersuchung stattfinden soll. Es wurde eine Datenaufnahme im Sägewerk Meyr Melnhof in Frankenmarkt sowie im Sägewerk Entacher in Großarl geplant. Hier sollen die Daten in Form von digitalen Bildern der Holzstammenden aufgenommen werden und danach mittels einer 3D-Vermessung die Ovalität des Stammes erhoben werden. Anschließend sollen entsprechende Fotos analysiert werden um numerische Daten zu erhalten. Mittels dieser Daten können danach Zusammenhänge etwaiger Größen erarbeitet werden.

3. Ziele / Nichtziele

3.1. Ziele

- Erfassung von Daten und Informationen zur Thematik
- Erkennung von Holzmerkmalen in digitalen Bildern von Stammenden
- Erarbeiten von möglichen Zusammenhängen zwischen Buchs und anderen messbaren Größen eines Stammes
- Präsentation der Ergebnisse im Sägewerk Meyr-Melnhof und im Sägewerk Entacher
- Zur Verfügung stellen und bearbeiten der Daten für die FH Salzburg und die Universität Salzburg zu wissenschaftlichen Zwecken

3.2. Nichtziele

- Untersuchungen auf weitere Holzanomalien in Bezug auf messbare Größen eines Stammes
- Programmierung der automatischen Erkennung von Merkmalen
- Eigenständige Publikation der Ergebnisse

 hfi bildung mit zukunft	Holztechnikum Kuchl Betriebsmanagement - Holzwirtschaft	 Holztechnikum Kuchl 63111 10100
Abteilung: Betriebsmanagement - Holzwirtschaft		

4. Arbeitspakete mit Kurzbeschreibung der Tätigkeiten

Arbeitspaket 1 „Projektmanagement“

Aufgabenstellung	Zielsetzung/Ergebnis	Verantwortlichkeit
Antrag erstellen	Ausarbeiten des Projektantrages, Genehmigung der Diplomarbeit	Geistlinger, Sampl, Schöber
Ablaufplan erstellen	Erstellung des Projektlaufplans, Vollständige zeitliche Einteilung	Geistlinger
Projektdatner verwalten	Verwalten aller Dokumente (Monatsberichte, Besprechungsprotokolle,...), Übersichtlichkeit der Daten	Sampl
Präsentationen erstellen	Erstellen und Vorbereiten der Projektpäsentationen; Präsentation des Projekts	Geistlinger, Sampl, Schöber

Arbeitspaket 2 „Datenaufnahme“

Aufgabenstellung	Zielsetzung/Ergebnis	Verantwortlichkeit
Fotografie von Holzstammenden	Fotografie von Holzstammenden um eine große Grundgesamtheit für weitere Untersuchungen zu erreichen.	Geistlinger, Sampl, Schöber

Arbeitspaket 3 „Literaturstudie“

Aufgabenstellung	Zielsetzung/Ergebnis	Verantwortlichkeit
Einhessen in die Literatur	Einhessen in Fachliteratur	Geistlinger, Sampl, Schöber
Zusammenfassung der Literatur	Zusammenfassen der erarbeiteten Literatur.	Schöber

Arbeitspaket 4 „Analyse der ermittelten Daten“

Aufgabenstellung	Zielsetzung/Ergebnis	Verantwortlichkeit
Markierung des Mittelpunktes	Alle Mittelpunkte auf den erfassten Fotos zu markieren.	Sampl
Markierung des Stammurisses	Den Stammuriss auf dem erfassten Foto zu markieren.	Schöber
Markierung des Buchses It. OHU	Den Buchs auf den Fotos zu erkennen und It. der OHU zu erfassen.	Geistlinger
Markierung des Buchsumrisses	Markierung des Buchsumrisses auf den Fotos.	Geistlinger
Markierung der Äste	Mögliche Äste an allen Bildern zu erfassen.	Sampl
Markierung von Rissen	Alle Risse auf den erfassten Fotos markieren.	Schöber
Markierung von Harzgalien	Markierung von möglichen Harzgalien auf allen Bildern.	Sampl

 hfi bildung mit zukunft	Holztechnikum Kuchl Betriebsmanagement - Holzwirtschaft	 Holztechnikum Kuchl 63111 10100
Abteilung: Betriebsmanagement - Holzwirtschaft		

Arbeitspaket 5 „Statistische Analyse der Ergebnisse“

Aufgabenstellung	Zielsetzung/Ergebnis	Verantwortlichkeit
Vorbereitung der Daten	Die aus dem AP1 erfassten Daten auf die weiterführende Analyse vorbereiten.	Schöber
Beschreibende Statistik	Mittels beschreibender Statistik die aus AP2 genommen werden.	Sampl
Graphische Aufarbeitung und Analyse	Die ermittelten Daten graphisch aufarbeiten und analysieren.	Geistlinger
Korrelationsanalyse	Berechnung einer Korrelation zweier Daten (z.B. Buchsanstell und Ovalität).	Geistlinger, Sampl, Schöber
Regressionsanalyse	Ermittlung einer möglichen Regression der Ergebnisse.	Schöber
Interpretation der Ergebnisse	Ermittelte Ergebnisse interpretieren.	Geistlinger
Überarbeitung und Nacharbeit	Mögliche Über- und Nacharbeitung der Ziele.	Schöber

Arbeitspaket 6 „Verfassen der Diplomarbeit“

Aufgabenstellung	Zielsetzung/Ergebnis	Verantwortlichkeit
Diplomarbeit verfassen	Dokumentation des Projektlaufs und der Projektergebnisse.	Geistlinger, Sampl, Schöber
Präsentation erstellen	Vorbereiten und Erstellen der Abschlusspräsentation.	Geistlinger, Sampl, Schöber

5. Projektlaufplan

Siehe Anlage 4

6. Projektkosten

Nr.	Kostenstelle	Kosten [€]	Kostenträger
1.	Fahrtkosten	300,00	Projektteam
2.	Materialkosten (Motorsägekette, Aluminium für den Distanzhalter....)	180,00	FH Salzburg
3.	Druckkosten	200,00	FH Salzburg
4.	Kamera	0,00	Von FHS gestellt.

Das Projektteam wird während des Zeitraums der Diplomarbeit geringfügig bei der FH Salzburg beschäftigt. Somit können die vom Projektteam zu tragenden Kosten übernommen werden.

7. Dokumentation des Projekts (Projektcontrolling)

- Monatsberichte bis zum 10. des jeweiligen Monats per E-Mail an die Betreuer und Ansprechpartner im Partnerbetrieb.
- Projektmappe (Papier und elektronischer Ordner) mit Dokumentation aller projektrelevanter Tätigkeiten und Ergebnisse incl. Besprechungsprotokollen und Stundenaufzeichnungen je Teammitglied.
- Zwischenpräsentationen und Endpräsentation.
- Projektabgabe in Form der Diplomarbeit.

 HfL Bildung mit Zukunft	Holztechnikum Kuchl	 holz technikum kuchl an der HTS Salzburg
Abteilung: Betriebsmanagement - Holzwirtschaft		

8. Anhänge

Anhang 1 - Vereinbarung

Zwischen dem Auftraggeber FH Salzburg, vertreten durch **Prof. Dr. Alexander Petutschnigg** und dem **Holztechnikum Kuchl**, vertreten durch den **Direktor DI Helmuth Kogler** über eine Zusammenarbeit in der Form einer Diplomarbeit bzw. Abschlussarbeit im Zeitraum vom 09.09.2013 bis 16.05.2014.
Vom **Holztechnikum Kuchl** werden in diesem Zeitraum die nachfolgend angeführten Themenbereiche als Diplomarbeit bzw. Abschlussarbeit bearbeitet:

- Erfassung von Daten und Informationen zur Thematik,
- Verarbeiten der ermittelten Informationen in Bezug auf Markierung des Stammmaterials und des Mittelpunktes, Buchsanteil lt. ÖHfU, Buchstäche am Stammquerschnitt und die Markierung von anderen Holzanomalien wie Risse und Astle.
- Erarbeiten von möglichen Zusammenhängen zwischen Buchs und anderen messbaren Größen eines Stammes.

Am Projekt teilnehmende SchülerInnen:

Michael Geistlinger
Alexander Sampl
Michael Schober

Der Auftraggeber verpflichtet sich,

- für die beteiligten Schüler und Schülerinnen einen räumlich und zeitlich abgegrenzten Bereich festzulegen, innerhalb dessen der Auftraggeber die Schadenhaftung übernehmen kann,
- für Schäden in der Firma, die durch Projektkanalen verursacht und die nicht durch grobsträfliches Verhalten entstanden sind, die volle Haftung zu übernehmen,
- bei dieser Festlegung die körperliche und geistige Reife des Schülers, bzw. der Schülerin zu beachten,
- die beteiligten Schüler und Schülerinnen vor allenfalls vorhandenen Gefahren ausdrücklich zu warnen,
- einen Besuch (Kilometergeld) der Betreuungslerner zu finanzieren. Eventuell darüber hinaus anfallende Kosten werden nach Absprache ebenfalls vom Auftraggeber übernommen.

Der Auftragnehmer verpflichtet sich,

- die beteiligten Schüler und SchülerInnen darauf hinzuweisen, dass bei Tätigkeiten in Betrieben grundsätzlich nicht einzeln sondern zumindest paarweise agiert werden darf,
- dafür zu sorgen, dass der betreuende Lehrer bzw. Lehrerin oder ein Vertreter bzw. eine Vertreterin der Schule im betreffenden Zeitraum erreichbar ist,
- Lehrer und Schüler auf die mit dem außerschulischen Projekt verbundenen Pflichten hinzuweisen.

TreabIO

Seite 6 von 10

 HfL Bildung mit Zukunft	Holztechnikum Kuchl	 holz technikum kuchl an der HTS Salzburg
Abteilung: Betriebsmanagement - Holzwirtschaft		

Zur Beachtung:

Die Abwicklung des Diplomarbeitprojektes ist Bestandteil der Ausbildung am Holztechnikum Kuchl. Aus diesem Grunde kann das Holztechnikum Kuchl keine Garantie bzw. Produkthaftungsansprüche aus dem Projekt übernehmen. Sowohl Auftragnehmer, als auch Auftraggeber behalten sich das Recht vor, ein Projekt abzubrechen.

Kuchl, am 24.5.13

Unterschrift des Direktors des Holztechnikums Kuchl



Kuchl, am 10.10.13



Unterschrift und Stempel der Firma

TreabIO

Seite 7 von 10

.3 Project Meeting Report Example



Sitzungsprotokoll

Projekttitel: Diplomprojekt - TreeBio - Fotografie von Holzstammenden

Thema der Sitzung: Ferialpraxis, Details bezüglich erste Fotoaufnahmen im Sägewerk Entacher

Ort: Holztechnikum Kuchl

Datum: 04.07.2013

Beginn: 14.00 Uhr Ende: 14.45 Uhr Dauer: 45 min

Anwesende Teilnehmer: Rudi Schraml, Erwin Tremel, Karl Entacher, Michael Geistlinger,
Michael Schober, Alexander Sampl

Fehlende Teilnehmer (entschuldigt, nicht entschuldigt): -

Verfasser des Protokolls: Michael Geistlinger

Inhalte und Ergebnisse der Sitzung:

In der 2. Besprechung wurden folgende Themen behandelt und abgeklärt:

- Der Termin für den Beginn der Ferialpraxis wurde auf den 09.07.2013 im Sägewerk Entacher - Großarl festgesetzt.
- Außerdem wurden einige Einzelheiten in Bezug auf die Methodik besprochen.
- Pro Stammende müssen jeweils 4 Bilder vor dem Besprühen und 4 Bilder nach dem Besprühen gemacht werden, außerdem jeweils 1 Bild mit Blitz.
- Mit 35er und 50er Objektiv wird fotografiert.
- Stärkeklassen: 2b/3a/3b.
- Alle Stammscheiben werden mitgenommen um evtl. gescannt zu werden.
- Außerdem wurde eine Empfehlung ausgesprochen neben der Recherche an der Universität für Bodenkultur in Wien, den Unterlagen von Herrn Rudi Schraml und der Internetrecherche auch die Diplomarbeit (FH-Salzburg ca. 2005) von Karin Hauer zu lesen, die ein ähnliches Themengebiet behandelt.

WELCHE weiteren Aktionen werden von WEM bis WANN gesetzt?

Treffpunkt: Sägewerk Entacher in Großarl am Dienstag um ca. 10.00 Uhr

Bis dahin müssen der Abstandhalter und alle etwaigen Vorkehrungen (Objektiv, Blitz, Farbkarte => Schraml; Abstandhalter, Sprühung, sonstige Utensilien => Geistlinger, Sampl, Schober) abgeschlossen sein.



Material: Dose/Blaukreide, Fotoapparat mit Zubehör, Wasser, Behälter, Maßband, Motorsäge, Abstandshalter.

Sonstiges.

- Reisepass/Personalausweis scannen Betreuer zukommen lassen.
- Eine Woche vor Datenaufnahme bei Mayr Melnhof muss Herrn Tremel Bescheid gegeben werden, sodass eine ausreichende Anzahl an Stämmen mit gesuchten Holzanomalien vorhanden ist. (06506541765 Tremel)

Termin, Ort für die nächste Sitzung:

09.07.2013 Sägewerk Entacher – Großarl

Datenaufnahme der Stammenden.

Verteiler:

Karl Entacher, Erwin Tremel, Rudi Schraml, Michael Geistlinger, Alexander Sampl, Michael Schober

.4 Project Progress Report Example



HTL für Betriebsmanagement - Holzwirtschaft

MONATSBERICHT

Monat: November 2013

Projekttitel: TreeBIO – Fotografie von Holzstammenden

Projektteilnehmer: Michael Geistlinger
Alexander Sampl
Michael Schober

Verteiler: Karl Entacher, Erwin Tremml, Rudolf Schraml

1. Projekt Kurzbeschreibung:

Ob Zusammenhänge zwischen Holzanomalien, die am Stammquerschnitt erkennbar sind und messbare Größen eines Stammes vorhanden sind wurde in dieser Form noch nicht genauer untersucht. Unsere Ausgangssituation besteht darin grundlegende Rahmenbedingungen festzulegen in welcher Form diese Untersuchung stattfinden soll. Es wurde eine Datenaufnahme im Sägewerk Mayr Melnhof in Frankenmarkt und im Sägewerk Entacher in Großarl geplant. Hier sollen die Daten in Form von Fotos der Holzstammenden aufgenommen werden und danach mittels einer 3D-Vermessung die Kubatur des Stammes erhoben werden. Anschließend sollen entsprechende Fotos so analysiert werden um numerische Daten zu erhalten. Mittels dieser Daten können danach Zusammenhänge etwaiger Größen erarbeitet werden.

2. Projektziele:

- Erfassung von Daten und Informationen zur Thematik
- Erarbeiten von möglichen Zusammenhängen zwischen Buchs und anderen messbaren Größen eines Stammes.
- Präsentation der Ergebnisse im Sägewerk Mayr-Melnhof und im Sägewerk Entacher.
- Zur Verfügung stellen der Daten an die FH Salzburg zu wissenschaftlichen Zwecken.

5. Aktivitäten des vergangenen Monats

Im vergangenen Monat wurde unter anderem das oben angeführte Programm auf unsere Ansprüche abgestimmt und überarbeitet.

Des Weiteren konnte das Arbeitspaket 3 vollständig ausgeführt werden. Hierbei wurde eine umfassende Literaturrecherche an der Universität für Bodenkultur in Wien durchgeführt und einschlägige Literatur in Bezug auf Reaktionsholz ermittelt und gleichzeitig erfasst.

Außerdem konnte mit der Analyse der ermittelten Daten (AP4) begonnen werden.

6. Geplante Aktivitäten für das kommende Monat

Das Ziel des kommenden Monats liegt darin, das komplette „AP4 Datenanalyse“ umgehend fertigzustellen. Dies bedeutet von allen fotografierten Holzstammenden die oben genannten Analysen durchzuführen

Des Weiteren sollte bei baldiger Fertigstellung des 4. Arbeitspaketes sofort mit der Vorbereitung der Daten für die statistische Analyse begonnen werden.

Anhang 1:

Bibliography

- Andreu, J.-P. and Rinnhofer, A. (2001). Automatic detection of pith and annual rings on industrial computed tomography log images. In *Procs. of the 9th International Conference on Scanning Technology and Process Optimization for the Wood Industry*, pages 37–47, Washington, USA.
- Andreu, J. P., Rinnhofer, A., and Petutschnigg, A. (2002). Enhancement of annual rings on industrial CT images of logs. In *Proceedings of the 16th International Conference on Pattern Recognition (ICPR'02)*, pages 261–264, Washington, USA. IEEE Computer Society.
- Barrett, W. (2008). Biometrics of cut tree faces. In Sobh, T., editor, *Advances in Computer and Information Sciences and Engineering*, pages 562–565. Springer Netherlands.
- Baumgartner, R., Brüchert, F., and Sauter, U. (2010). Knots in CT scans of scots pine logs. In *Proceedings of the Final Conference on The Future of Quality Control for Wood & Wood Products (COST Action E53)*, Edingburgh, UK.
- Baumgartner, R., Brüchert, F., Staudenmaier, J., and Sauter, U. (2007). Bark measurements with x-ray technology. In *Proceedings of the Conference on Quality Control for Wood and Wood Products (COST E 53)*, pages 13–16, Warsaw, PL.
- Bay, H., Ess, A., Tuytelaars, T., and Van Gool, L. (2008). Speeded-up robust features (surf). *Comput. Vis. Image Underst.*, 110:346–359.
- Berglund, A., Broman, O., Grönlund, A., and Fredriksson, M. (2013). Improved log rotation using information from a computed tomography scanner. *Computers and Electronics in Agriculture*, 90:152 – 158.
- Berglund, A., Johansson, E., and Skog, J. (2014). Value optimized log rotation for strength graded boards using computed tomography. *Holz als Roh- und Werkstoff*, 72(5):635–642.

- Bhandarkar, S., Faust, T., and Tang, M. (1996). A system for detection of internal log defects by computer analysis of axial CT images. In *Proceedings of the 3rd Workshop on Applications of Computer Vision (WACV '96)*, pages 258–263.
- Bhandarkar, S., Luo, X., Daniels, R., and Tollner, E. (2008). Automated planning and optimization of lumber production using machine vision and computed tomography. *IEEE Transactions on Automation Science and Engineering*, 5(4):677–695.
- Bhandarkar, S. M., Faust, T. D., and Tang, M. (1999). Catalog: a system for detection and rendering of internal log defects using computer tomography. *Machine Vision and Applications*, 11(4):171–190.
- Bhandarkar, S. M., Luo, X., Daniels, R., and Tollner, E. W. (2005). Detection of cracks in computer tomography images of logs. *Pattern Recognition Letters*, 26(14):2282–2294.
- Bhandarkar, S. M., Luo, X., Daniels, R., and Tollner, E. W. (2006). A novel feature-based tracking approach to the detection, localization, and 3-D reconstruction of internal defects in hardwood logs using computer tomography. *Pattern Analysis Applications*, 9(2):155–175.
- Boukadida, H., Longuetaud, F., Colin, F., Freyburger, C., Constant, T., Leban, J. M., and Mothe, F. (2012). Pithextract: A robust algorithm for pith detection in computer tomography images of wood - application to 125 logs from 17 tree species. *Computers and Electronics in Agriculture*, 85:90–98.
- Breinig, L. (2015). *CT log scanning for sawing optimization with regard to the aesthetic quality of wood*. PhD thesis, University of Freiburg.
- Breinig, L., Berglund, A., Grönlund, A., Brüchert, F., and Sauter, U. H. (2013). Effect of knot detection errors when using a computed tomography log scanner for sawing control. *Forest Products Journal*, 63(7-8):263–274.
- Breinig, L., Broman, O., Brüchert, F., and Becker, G. (2015). Optimization potential for perception-oriented appearance classification by simulated sawing of computed tomography-scanned logs of norway spruce. *Wood Material Science and Engineering*, 10(4):319–334.
- Breinig, L., Brüchert, F., Baumgartner, R., and Sauter, U. H. (2012). Measurement of knot width in CT images of Norway spruce (*picea abies* [L.] karst.)-evaluating the accuracy of an image analysis method. *Computers and Electronics in Agriculture*, 85:149–156.

- Breinig, L., Leonhart, R., Broman, O., Manuel, A., Brüchert, F., and Becker, G. (2014). Classification of wood surfaces according to visual appearance by multivariate analysis of wood feature data. *Journal of Wood Science*, 61(2):89–112.
- Canny, J. (1986). A computational approach to edge detection. *IEEE Transactions on Pattern Analysis and Machine Vision*, 8(6):679–698.
- Cerda, M., Hitschfeld-Kahler, N., and Mery, D. (2007). Robust tree-ring detection. In Mery, D. and Rueda, L., editors, *Procs. of Advances in Image and Video Technology*, volume 4872 of *LNCS*, pages 575–585. Springer Berlin / Heidelberg.
- Chalifour, A., Nouboud, F., Deprost, B., and Okana, S. (2001). Automatic detection of tree-rings on wood disc images. In *Proceedings of the 5th International Conference on Quality Control by Artificial Vision*, pages 348–352.
- Chiorescu, S. and Grönlund, A. (2003). The fingerprint approach: using data generated by a 2-axis log scanner to accomplish traceability in the sawmill's log yard. *Forest Products Journal*, 53:78–86.
- Chiorescu, S. and Grönlund, A. (2004). The fingerprint method: Using over-bark and under-bark log measurement data generated by three-dimensional log scanners in combination with radiofrequency identification tags to achieve traceability in the log yard at the sawmill. *Scandinavian Journal of Forest Research*, 19(4):374–383.
- Conner, W. (1999). A computer vision based tree ring analysis and dating system. Master's thesis, University of Arizona, Department of Electrical & Computer Engineering.
- Conner, W., Schowengerdt, R., Munro, M., and Hughes, M. (1998). Design of a computer vision based tree ring dating system. In *Proceedings of IEEE Southwest Symposium on Image Analysis and Interpretation*, pages 256–261.
- Conner, W. S., Schowengerdt, R. A., Munro, M., and Hughes, M. K. (2000). Engineering design of an image acquisition and analysis system for dendrochronology. *Optical Engineering*, 39(2):453–463.
- Cristhian A. Aguilera, Mario A. Ramos, A. D. S. (2012). *Simulated Annealing - Advances, Applications and Hybridizations*, chapter Simulated Annealing: A Novel Application of Image Processing in the Wood Area, pages 91–104. INTECHOPEN.
- Edelsbrunner, H., Kirkpatrick, D., and Seidel, R. (1983). On the shape of a set of points in the plane. *Information Theory, IEEE Transactions on*, 29(4):551–559.

- Ekevad, M. (2004). Method to compute fiber directions in wood from computed tomography images. *Journal of Wood Science*, 50(1):41–46.
- Engle, J. B. (2000). A computer-assisted tree-ring chronology composition system. Master's thesis, University of Arizona, Department of Electrical & Computer Engineering.
- Entacher, K., Hegenbart, S., Kerschbaumer, J., Lenz, C., Planitzer, D., Seidel, M., Uhl, A., and Weiglmaier, R. (2008). Pith detection on CT-cross-section images of logs: An experimental comparison. In *Proceedings of the 3rd International Symposium on Communications, Control and Signal Processing*, pages 478–483, St.Julians, MT.
- Entacher, K., Lenz, C., Seidel, M., Uhl, A., and Weiglmaier, R. (2007). Applicability of motion estimation algorithms for an automatic detection of spiral grain in CT cross-section images of logs. In *CAIP*, pages 36–44.
- Fellner, J., Teischinger, A., and Zschokke, W. (2006). *Holzspektrum*. proHolz Austria.
- Flodin, J., Oja, J., and Grönlund, A. (2007). Fingerprint traceability of sawn products using x-ray log scanning and sawn timber surface scanning. In *Proceedings of Quality control for wood and wood products: COST Action E 53 the first conference*.
- Flodin, J., Oja, J., and Grönlund, A. (2008a). Fingerprint traceability of logs using the outer shape and the tracheid effect. *Forest Products Journal*, 58(4):21–27.
- Flodin, J., Oja, J., and Grönlund, J. (2008b). Fingerprint traceability of sawn products using industrial measurement systems for x-ray log scanning and sawn timber surface scanning. *Forest Products Journal*, 58:11.
- Flood, K., Danielsson, P.-E., and Seger, A. M. (2003). On 3D segmentation of knots in 3D-volume data acquired from x-ray linear cone-beam scanning. In Rinnhofer, A., editor, *Proceedings of the 5th International Conference on Image Processing and Scanning of Wood*, pages 151–159.
- Fraunhofer (2010). Rundholz mit Antenne. <http://www.fraunhofer.de/de/presse/presseinformationen/2010/08/rundholz-mit-antenne.html>. [last accessed: 28.07.2011].
- Fredriksson, M., Broman, O., Persson, F., Axelsson, A., and Ah Shenga, P. (2014a). Rotational position of curved saw logs and warp of the sawn timber. *Wood Material Science and Engineering*, 9(1):31–39.

- Fredriksson, M., Johansson, E., and Berglund, A. (2014b). Rotating pinus sylvestris sawlogs by projecting knots from computed tomography images onto a plane. *BioResources*, 9(1):816–827.
- Funt, B. (1985). A computer vision system that analyzes CT-scans of sawlogs. In *Proceedings of IEEE Conference on Computer Vision and Pattern Recognition*, pages 175–177, San Francisco, USA.
- Funt, B. and Bryant, E. (1987). Detection of internal log defects by automatic interpretation of computer tomography images. *Forest Products Journal*, 37(1):56–62.
- Geistlinger, M., Schober, M., and Sampl, A. (2014). Treetree - bildanalyse von holzstammenden. Master's thesis, Higher Technical College HTL Kuchl, Salzburg, Austria.
- Giribalan, G. (2000). An interactive image analysis system for dendrochronology. Master's thesis, University of Arizona, Department of Electrical & Computer Engineering.
- Giudiceandrea, F., Ursella, E., and Vicario, E. (2011). A high speed ct scanner for the sawmill industry. In *Proceedings of the 17th International Nondestructive Testing and Evaluation of Wood Symposium*, Sopron, HU.
- Giudiceandrea, F., Ursella, E., and Vicario, E. (2012). From research to market: a high speed ct scanner for the sawmill industry. In *Proceedings XXXI Scuola Annuale di Bioingegneria*, Brixen, ITA.
- Gjerdrum, P. and Høibø, O. (2004). Heartwood detection in scots pine by means of heat-sensitive infrared images. *Holz als Roh- und Werkstoff*, 62(2):131–136.
- Gonzalez, R. C. and Woods, R. E. (2001). *Digital Image Processing*. Addison-Wesley, Boston, MA, USA, 2nd edition.
- Grundberg, S. and Grönlund, A. (1992). Log scanning : extraction of knot geometry in CT-volumes. In *Proceedings of the Seminar/Workshop on Scanning Technology and Image Processing on Wood*.
- Hanning, T., Kickingereeder, R., and Casasent, D. (2003). Determining the average annual ring width on the front side of lumber. In Osten, W., Kujawinska, M., and Creath, K., editors, *Proceedings of SPIE: Optical Measurement Systems for Industrial Inspection*, volume 5144, pages 707–716, Munich, Germany.
- Harris, C. and Stephens, M. (1988). A combined corner and edge detector. In *In Proceedings of the Fourth Alvey Vision Conference*, pages 147–151.

- Jain, A., Ross, A., and Prabhakar, S. (2001). Fingerprint matching using minutiae and texture features. In *Procs. of the International Conference on Image Processing (ICIP'01)*, volume 3, pages 282–285, Thessaloniki, GR.
- Jain, A. K., Flynn, P., and Ross, A. A. (2007). *Handbook of Biometrics*. Springer-Verlag New York, Inc., Secaucus, NJ, USA.
- Jain, A. K., Prabhakar, S., Hong, L., and Pankanti, S. (2000). Filterbank-based fingerprint matching. *IEEE Transactions on Image Processing*, 9(5):846–859.
- Johansson, E., Johansson, D., Skog, J., and Fredriksson, M. (2013). Automated knot detection for high speed computed tomography on pinus sylvestris l. and picea abies (l.) karst. using ellipse fitting in concentric surfaces. *Computers and Electronics in Agriculture*, 96:238 – 245.
- Korten, S. and Kaul, C. (2008). Application of RFID (Radio frequency identification) in the timber supply chain. *Croatian Journal of Forest Engineering*, 29(1).
- Krähenbühl, A., Kerautret, B., Debled-Rennesson, I., Mothe, F., and Longuetaud, F. (2014). Knot segmentation in 3d ct images of wet wood. *Pattern Recognition*, 47:3852–3869.
- Kvarnström, B. and Oghazi, P. (2008). Methods for traceability in continuous processes- experience from an iron ore refinement process. *Minerals Engineering*, 21(10):720–730.
- Kvarnström, B. and Oja, J. (2008). *Applications of RFID to Improve Traceability in Continuous Processes*, chapter Sustainable Radio Frequency Identification Solutions, page 19. InTech.
- Laggoune, H., Sarifuddin, and Guesdon, V. (2005). Tree ring analysis. In *Procs. of the Canadian Conference on Electrical and Computer Engineering*, pages 1574–1577.
- Li, L. and Qi, D. (2007). Detection of cracks in computer tomography images of logs based on fractal dimension. In *Proceedings of the IEEE International Conference on Automation and Logistics*, pages 2259–2264.
- Li, P., Abbott, A., and Schmoltdt, D. (1996). Automated analysis of CT images for the inspection of hardwood logs. In *Proceedings of the IEEE International Conference on Neural Networks*, volume 3, pages 1744–1749.
- Longuetaud, F., Leban, J.-M., Mothe, F., Kerrien, E., and Berger, M.-O. (2004). Automatic detection of pith on CT images of spruce logs. *Computers and Electronics in Agriculture*, 44(2):107–119.

- Longuetaud, F., Mothe, F., Kerautret, B., Krähenbühl, A., Hory, L., Leban, J. M., and Debled-Rennesson, I. (2012). Automatic knot detection and measurements from x-ray CT images of wood: A review and validation of an improved algorithm on softwood samples. *Computers and Electronics in Agriculture*, 85:77–89.
- Longuetaud, F., Mothe, F., and Leban, J.-M. (2007). Automatic detection of the heartwood/sapwood boundary within Norway spruce (*picea abies* (L.) karst.) logs by means of CT images. *Computers in Electronics and Agriculture*, 58(2):100–111.
- Maltoni, D., Maio, D., Jain, A. K., and Prabhakar, S. (2009). *Handbook of fingerprint recognition*. Springer New York.
- McMillin, C. W. (1982). Application of automatic image analysis in wood science. *Wood Science*, 14:97–105.
- Norell, K. (2009a). An automatic method for counting annual rings in noisy sawmill images. In *Proceedings of the Conference on Image Analysis and Processing (ICIAP)*, number 5716 in LNCS, pages 307–316. Springer Berlin / Heidelberg.
- Norell, K. (2009b). Creating synthetic log end face images. In *Proceedings of 6th International Symposium on Image and Signal Processing and Analysis (ISPA'09)*, pages 353–358.
- Norell, K. (2010). Counting annual rings on *pinus sylvestris* end faces in sawmill industry. *Computers and Electronics in Agriculture*, 75(2):231–237.
- Norell, K. and Borgefors, G. (2008). Estimation of pith position in untreated log ends in sawmill environments. *Computers and Electronics in Agriculture*, 63(2):155–167.
- Norell, K., Lindblad, J., and Svensson, S. (2007). Grey weighted polar distance transform for outlining circular and approximately circular objects. In *Procs. of 14th International Conference on Image Analysis and Processing (ICIAP'07)*, pages 647–652.
- Nystrom, J. and Hagman, O. (1999). Methods for detecting compression wood in green and dry conditions. In *Proceedings of the Conference on Polarization and Color Techniques in Industrial Inspection (SPIE)*, pages 287–294, Bellingham, Wash.
- Österberg, P. (2009). *Wood Quality and Geometry Measurements Based on Cross Section Images*. PhD thesis, Tampere University of Technology, Department of Automation Science and Engineering.

- Österberg, P., Ihalainen, H., and Ritala, R. (2004). Method for analyzing and classifying wood quality through local 2D-spectrum of digital log end images. In *Proceedings of International Conference on Advanced Optical Diagnostics in Fluids*, Tokyo, JP.
- Pahlberg, T. (2014). *Wood Fingerprints: Recognition of Sawn Wood Products*. PhD thesis.
- Pahlberg, T. and Hagman, O. (2012). *Feature recognition and fingerprint sensing for guiding a wood patching robot*, pages 724–733. New Zealand Timber Design Society.
- Pahlberg, T., Hagman, O., and Thurley, M. (2015a). Recognition of boards using wood fingerprints based on a fusion of feature detection methods. *Computers and Electronics in Agriculture*, 111:164–173.
- Pahlberg, T., Johansson, E., Hagman, O., and Thurley, M. (2015b). Wood fingerprint recognition using knot neighborhood k-plet descriptors. *Wood Science and Technology*, 49(1):7–20.
- Päivinen, R. and Lindner, M. (2006). Assessment of sustainability of forest-wood chains. Technical report, EFI Technical Report 23.
- Peterson, G. (2009). The potential of using log biometrics to track sawmill flow. Master's thesis, Oregon State University.
- ProHolz (2007). Dendrochronologie. <http://www.proholz.at/zuschnitt/27/dendrochronologie/>. [last accessed: 28.07.2011].
- Rauschkolb, M. R. (1994). Algorithms for automatic tree ring identification and measurement. Master's thesis, Mississippi State University.
- Rojas, G., Condal, A., Beauregard, R., Verret, D., and Hernández, R. E. (2006). Identification of internal defect of sugar maple logs from CT images using supervised classification methods. *Holz als Roh- und Werkstoff*, 64(4):295–303.
- Rosten, E. and Drummond, T. (2006). Machine learning for high-speed corner detection. In *European Conference on Computer Vision*, volume 1, pages 430–443.
- Roussel, J.-R., Mothe, F., Krähenbühl, A., Kerautret, B., Debled-Rennesson, I., and Longueaud, F. (2014). Automatic knot segmentation in CT images of wet softwood logs using a tangential approach. *Computers and Electronics in Agriculture*, 104:46–56.
- Sarigul, E., Abbott, A., and Schmoltdt, D. (2003a). Progress in analysis of computed tomography (CT) images of hardwood logs for defect detection. In *Proceedings of the Tenth*

International Conference on Scanning Technology and Process Optimization in the Wood Industry (ScanTech'03), pages 19–30.

- Sarigul, E., Abbott, A., and Schmoldt, D. (2003b). Rule-driven defect detection in CT images of hardwood logs. *Computers and Electronics in Agriculture*, 41:101–119.
- Schmoldt, D., Daniel, L., He, J., and Lynn, A. (1998). A comparison of several artificial neural network classifiers for CT images of hardwood logs. In *Proceedings of Machine Visions Applications in Industrial Inspection VI*, volume 3306, pages 34–43, SPIE.
- Schmoldt, D., He, J., and Abbott, A. (2000). Automated labeling of log features in CT imagery of multiple hardwood species. *Wood and Fiber Science*, 32(3):287–300.
- Schmoldt, D., Li, P., and Abbott, A. (1997). Machine vision using artificial neural networks with local 3D neighborhoods. *Computers and Electronics in Agriculture*, 16(3):255–271.
- Schraml, R. (2013). Treebio - preliminary study on traceability of tree logs using digital log end images. Master's thesis, Department of Scientific Computing, University of Salzburg, Austria.
- Schraml, R., Charwat-Pessler, J., Petutschnigg, A., and Uhl, A. (2014a). Robustness of biometric wood log traceability using digital log end images. Technical Report 2014-08, Department of Computer Sciences, University of Salzburg, Austria, <http://www.cosy.sbg.ac.at/tr>.
- Schraml, R., Charwat-Pessler, J., Petutschnigg, A., and Uhl, A. (2015a). Towards the applicability of biometric wood log traceability using digital log end images. *Computers and Electronics in Agriculture*, 119:112–122.
- Schraml, R., Charwat-Pessler, J., and Uhl, A. (2014b). Temporal and longitudinal variances in wood log cross-section image analysis. In *IEEE International Conference on Image Processing (ICIP'14)*, Paris, FR.
- Schraml, R., Hofbauer, H., Petutschnigg, A., and Uhl, A. (2015b). Tree log identification based on digital cross-section images of log ends using fingerprint and iris recognition methods. In *Proceedings of the 16th International Conference on Computer Analysis of Images and Patterns (CAIP'15)*, LNCS, pages 752–765. Springer Verlag.
- Schraml, R., Hofbauer, H., and Uhl, A. (2015c). Tree log identification based on digital cross-section images of log ends using fingerprint and iris recognition methods. Technical

- Report 2015-01, Department of Computer Sciences, University of Salzburg, Austria, <http://www.cosy.sbg.ac.at/tr>.
- Schraml, R., Petutschnigg, A., and Uhl, A. (2015d). Validation and reliability of the discriminative power of geometric wood log end features. In *Proceedings of the IEEE International Conference on Image Processing (ICIP'15)*.
- Schraml, R. and Uhl, A. (2013). Pith estimation on rough log end images using local fourier spectrum analysis. In *Proceedings of the 14th Conference on Computer Graphics and Imaging (CGIM'13)*, Innsbruck, AUT.
- Schraml, R. and Uhl, A. (2014). Similarity based cross-section segmentation in rough log end images. In Iliadis, L. et al., editors, *Proceedings of the 10th Artificial Intelligence Applications and Innovations Conference (AIAI'14)*, volume 436 of *Springer IFIP AICT*, pages 614–621, Rhodes, GR.
- Sepúlveda, P. (2001). Measurement of spiral grain with computed tomography. *Journal of Wood Science*, 47(4):289–293.
- Sepúlveda, P., Oja, J., and Grönlund, A. (2002). Predicting spiral grain by computed tomography of Norway spruce. *Journal of Wood Science*, 48(6):479–483.
- Sliwa, T., Brunet, P., Voisin, Y., C., O. M., Stolz, C., and A. Diou, A. (2003). Détection automatique des stries de croissance des arbres par transformée en ondelettes (automatic detection of growth rings of trees by wavelet transforms). In *Proceedings of the 16th International Conference on Vision Interface*, Halifax, CAN.
- Smith, W. R. (1995). A prototype and algorithms for tree ring area measurement. In *Proceedings of the 33rd annual on Southeast regional conference*, ACM-SE 33, pages 254–259, New York, USA. ACM.
- Som, S., Davis, J., Wells, P., and Svalbe, I. (1993). Morphology methods for processing tomographic images of wood. In *Digital Image Computing: Techniques and Applications (DICTA'93)*, volume 2, pages 564–571, Sydney, AU.
- Som, S., Svalbe, I., Davis, J., Grant, J., Gold, E., Tsui, K., and Wells, P. (1995). Internal scanning of logs for grade evaluation and defect location. In *Digital Image Computing: Techniques and Applications (DICTA'95)*, pages 408–413, Brisbane AU.
- Töyrylä, I. (1999). *Realising the Potential of Traceability – A Case Study Research on Usage and Impacts of Product Traceability*. PhD thesis, Helsinki University of Technology.

- Tzoulis, I. and Andreopoulou, Z. (2013). Emerging traceability technologies as a tool for quality wood trade. *Procedia Technology*, 8(0):606–611.
- Uusijärvi, R. (2010). Forest RFID transponder and reader design - indisputable key project. Technical report, IST - ICT for Networked Businesses - Extended products and services. [last accessed: 22.03.2012].
- Vaz, C., Carvalho, P., Duarte, F., and Dourado, A. (2004). A vision-based system for automatic growing ring detection and measurement. *Comput. Ind. Eng.*, 46(2):347–354.
- Wayman, J., Jain, A., and Maltoni, D. (2005). *Biometric Systems*. Springer Berlin / Heidelberg.
- Wehrhausen, M., Norvin, N., Bruchert, F., and Sauter, U. (2012). Crack detection in computer tomographic scans of softwood tree discs. *Forest Products Journal*, 62(6):434–442.
- Wei, Q., Chui, Y., Leblon, B., and Zhang, S. (2009). Identification of selected internal wood characteristics in computed tomography images of black spruce: a comparison study. *Journal of Wood Science*, 55(3):175–180.
- Wells, P., Som, S., and Davis, J. (1991). Automated feature extraction from tomographic images of wood. In *Digital Image Computing: Techniques and Applications (DICTA'91)*, volume 2, pages 564–571, Melbourne, AU.
- Wiedenhoef, A. (2010). *Wood Handbook - Wood as an Engineering Material*, chapter Structure and Function of Wood. Forest Products Laboratory. Wood handbook U.S. Department of Agriculture.
- Wu, J. and Liew, D. (2000). A computer vision method for detection of external log cracks and pith in log cross-section images. In *Procs. of the World Automation Congress: International Symposium on Intelligent Automation and Control (ISIAC'00)*, Hawaii, USA.
- Zhu, D. (1993). *A feasibility study on using ct image analysis for hardwood log inspection*. PhD thesis, Virginia Polytechnic Institute and State University. AA19323799.
- Zhu, D., Connors, R., Schmoltdt, D., and Araman, P. (1996). A prototype vision system for analyzing CT imagery of hardwood logs. *IEEE Transactions on Systems, Man, and Cybernetics, Part B: Cybernetics*, 26(4):522–532.